UNIVERSITAT POLITÈCNICA
DE CATALUNYA
BARCELONATECH

Design of the BELEN detector for wide energy range with flat and high detection efficiency

Author:
Albert RIEGO

Supervisor:
Dr. Guillem CORTES

BARCELONA, GENER 2016

Programa de doctorat: Enginyeria Nuclear i de les Radiacions Ionitzants

Tesi presentada per obtenir el títol de Doctor per la Universitat Politècnica de Catalunya

UNIVERSITAT POLITÈCNICA DE CATALUNYA
BARCELONATECH
Escola de Doctorat

Acta de qualificació de tesi doctoral

Curs acadèmic:

Nom i cognoms

Programa de doctorat

Unitat estructural responsable del programa

Resolució del Tribunal

Reunit el Tribunal designat a l'efecte, el doctorand / la doctoranda exposa el tema de la seva tesi doctoral titulada

_____

_____.

Acabada la lectura i després de donar resposta a les qüestions formulades pels membres titulars del tribunal, aquest atorga la qualificació:

☐ NO APTE ☐ APROVAT ☐ NOTABLE ☐ EXCEL·LENT

(Nom, cognoms i signatura)	(Nom, cognoms i signatura)	
President/a	Secretari/ària	
(Nom, cognoms i signatura)	(Nom, cognoms i signatura)	(Nom, cognoms i signatura)
Vocal	Vocal	Vocal

_____, _____ d'/de _____ de _____

El resultat de l'escrutini dels vots emesos pels membres titulars del tribunal, efectuat per l'Escola de Doctorat, a instància de la Comissió de Doctorat de la UPC, atorga la MENCIÓ CUM LAUDE:

☐ SÍ ☐ NO

(Nom, cognoms i signatura)	(Nom, cognoms i signatura)
President de la Comissió Permanent de l'Escola de Doctorat	Secretari de la Comissió Permanent de l'Escola de Doctorat

Barcelona, _____ d'/de _____ de _____

Design of the BELEN detector for wide energy range with flat and high detection efficiency

Author:
Albert RIEGO

Supervisor:
Dr. Guillem CORTES

BARCELONA, GENER 2016

Programa de doctorat: Enginyeria Nuclear i de les Radiacions Ionitzants

Tesi presentada per obtenir el títol de Doctor per la Universitat Politècnica de Catalunya

Abstract

The BEta-deLayEd Neutron detector (BELEN) is being developed for experiments at the future FAIR facility within the DESPEC (DEcay SPECtroscopy) collaboration. The detector consist on a set of ^{3}He tubes embedded in a polyethylene matrix. Different prototypes of the detector have been employed at JYL and GSI facilities for the study of β-delayed neutron emitters and in particular the determination of the neutron emission probability P_{n}. The detector concept is a modular one, which allows an easy adaptation to different experimental environments and the optimization of the detector efficiency. The design of these detectors, has served to develop a methodology to facilitate the process and assist in obtaining the optimal design. The purpouse of this methodology is to find the best combination of the position of the tubes in the polyethylene matrix to obtain a maximum efficiency and a flat response for a range of initial neutron energy values.

Contents

List of Figures

List of Tables

Chapter 1
Introduction

1.1 Motivation

Neutron detectors are widely used at almost every nuclear research facilities. Their range of application covers nearly all the topics in basic and applied nuclear research: in nuclear structure, for decay studies; in nuclear reactions, for the identification of the reaction channels and reconstruction of the complete kinematics; in nuclear astrophysics, for determining the neutron emission probabilities; in nuclear technology, for nuclear data measurements, new requeriment on neutron cross sectios data for the generation IV reactor concepts, and as monitors; in nuclear medicine, as radiation monitors and dosimeters and in material science, for neutron imaging techniques.

In the nuclear physics community, one topic of interest is improvement of the accuracy of β-delayed neutron emission probabilities (P_{n} values), which will help theoreticians to improve their models and, in turn, make extrapolations to more neutron-rich isotopes more reliable. New measurements in the heavier mass region A>150 are desired, and also more measurements of multiple neutron emitters will become possible in the next years. To study decay of neutron rich nuclei there are existing facilities like IGISOL/JFLTRAP[1], ALTO-Orsay[2], FRS at GSI[3], ISOLDE at CERN[4] and RIKEN[5], and in the short term perspective, as soon as the DESPEC experiment at FAIR[6] (Germany), S3 and DESIR at SPIRAL2[7] (France), SPES at LNL (Italy)[8] and FRIB at MSU[9] (USA) become available, it will be possible to produce ion beams of very neutron rich isotopic

[1]Jyväskylä Ion Guide Isotope Separator On-Line (IGISOL) facility
[2](Accélérateur Linéeaire auprès du Tandem d' Orsay
[3]FRS :FRagment Separator at GSI
[4]ISOLDE:On-Line Isotope Mass Separator
[5]RIKEN: Large research institute in Japan
[6]FAIR: Facility for Antiproton Ion Research
[7]SPIRAL2:Système de Production d'Ions Radioactifs en Ligne
[8]LNL:Labs of the Italian Institute of Nuclear Physics (INFN).
[9]Facility for Rare Isotope Beams from Michigan State University (MSU),

species with unprecedent intensities, as high as several orders of magnitude larger than is possible nowadays.

The HISPEC/DESPEC experiments are intended to address questions in nuclear structure, reactions and nuclear astrophysics by means of high-resolution gamma-ray spectroscopy based on cutting edge germanium detector technology. The 4π germanium detector arrays are complemented by a suite of ancillary detector systems for charged particles and neutrons as well as devices dedicated to specific types of nuclear structure observables such as decay or single-particle strengths or electromagnetic moments, to name but a few.

In the DESPEC (DEcay SPECtroscopy) experiment, the radioactive ions are slowed down and come to rest in a stack of a highly segmented silicon-based, implantation and decay detector system (AIDA[10]). This system will be surrounded by a compact high resolution Ge array, neutron detectors, fast BaF_2 detectors and/or a total absorption gamma ray spectrometer. A magnet for isomeric moments measurements is an additional option. Here, decay studies of dripline nuclei will be the core interest, in particular towards the neutron-rich r-process lines. It will also be possible to combine HISPEC and DESPEC for recoil decay studies, with the DESPEC detectors being placed at the end of the magnetic spectrometer.

The device described in this thesis is the BEta-deLayEd Neutron detector (BELEN) that is being developed for experiments at the future FAIR facility [30] within the DESPEC (DEcay SPECtroscopy) collaboration [11]. Meanwhile different prototypes of the detector have been employed at several installations for the study of β-delayed neutron emitters and in particular the determination of the neutron emission probability P_{n}.

1.2 Overview of BELEN

The DESPEC experiment at FAIR will perform high resolution and high efficiency spectroscopy with radioactive ion beams. The focus of the experiment will be to address key questions in nuclear structure and astrophysics for nuclei very far from the valley of stability. The radioactive beams will be delivered by the energy buncher of the Low Energy Branch

[10] AIDA:Advanced Implantation Detector Array
[11] HISPEC/DESPEC technical design report

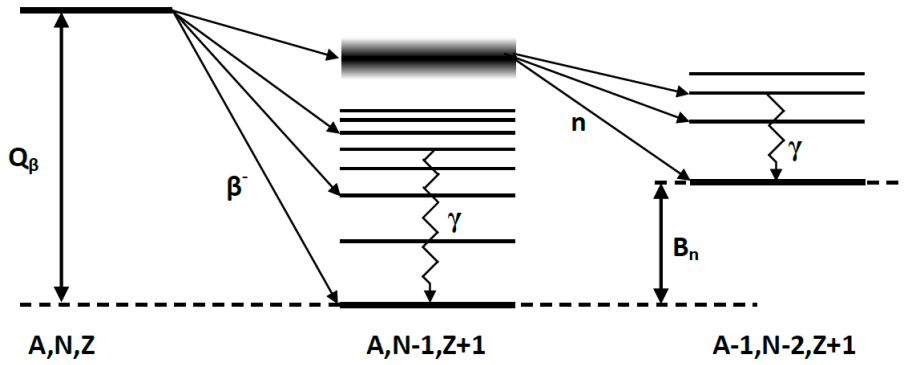

Figure 1.1: *Decay scheme of a β-delayed neutron emission.*

(LEB)[12] of the Super-FRS[13] (Fragment Separator). These radioactive beams will be formed of secondary reaction products following Coulomb excitation, direct reactions, fragmentation or fission reactions of relativistic radioactive ion beams.

DESPEC is conceived as a modular experiment where different setups can be coupled together in order to study different aspects of decay spectroscopy. The ions of interest will be implanted on an array of a Double Sided Silicon Strip Detector (DSSSD) called AIDA where their β-decay will be measured. A variety of other detectors will be placed around this DSSSD array according to the experimental needs, such as a compact Ge array, neutron detectors, fast timing BaF_2 detectors, a total absorption spectrometer and equipment for g-factor measurements.

The detector BELEN has been designed to measure the probability of neutron emission after β-decay (P_n), and of very neutron-rich nuclei. The detector uses ^{3}He proportional counters embedded in a polyethylene neutron moderator matrix to detect neutrons. The detector concept is a modular one, which allows an easy adaptation to different experimental environments and the optimization of the detector efficiency by changing the number of counters and their positions in polyethylene matrix.

The β-delayed neutron emission takes place when a precursor nucleus beta-decays and the resulting daughter nucleus emits a neutron, see figure 1.1. This neutron emission is energetically allowed if the excitation energy of the state populated in the beta-decay, Q_β, is larger than the neutron separation energy of the daughter-nucleus, B_n.

[12]LEB technical design report
[13]SuperFRS technical design report

The study of β-delayed neutron emission probabilities, P_n, is of interest for different fields, such as nuclear structure, nuclear astrophysics and nuclear technology applications. In the astrophysical r-process, the delayed neutron emission influences the r-process progenitor abundances along the decay of neutron-rich nuclei back to stability during stellar nucleosynthesis and constitutes a source of late neutrons during freeze-out [7, 12, 35]. Improved experimental data from delayed neutron emission represents an important input for theoretical calculations since properties of nuclei on the expected r-process path can only be predicted by extrapolation on the basis of systematics of experimental $T_{1/2}$ and P_n values.

Furthermore, in nuclear structure, β-delayed neutron emission constitutes an important probe for the structure of neutron-rich nuclei far away from the valley of stability where other measurements are not yet possible [15, 40, 44]. The probability of neutron emission after β-decay, P_n, carries information on the β-strength above the neutron separation energy, B_n. The technological interest of this type of study is related to nuclear power generation. Research of such nuclei is, therefore, fundamental for the design of safer and more efficient nuclear reactors. In this sense in year 2011, the IAEA (International Atomic Energy Agency) boosted the creation of a Coordinated Research Project (CRP) on β-delayed neutron emission evaluation [4] to study the need for Compilation and Evaluation of β-delayed Neutron Probabilities, define β-delayed neutron precursors as "standards" for the purpose of data evaluation and measurements, and elaborate a list of priorities for evaluation and new experiments for reactor physics and nuclear structure/astrophysics.

Despite the high interest in accurate P_n data and the amount of experimental data available nowadays, its quality is not sufficient for the various scientific and technical applications and it is necessary to perform new high precision measurements. The new FAIR facility will contribute to this quest for accurate data by granting access to very exotic nuclei that could not be explored in the past.

1.3 Monte Carlo Simulation

Monte Carlo techniques provide essential assistance in design work by closely modeling the actual geometry of a problem and by having imaginary neutrons that simulate the motions and interactions of real ones. The probability of a neutron interaction occurring is an important feature in the description of neutrons traveling through matter. Calculational tech-

niques that predict neutron events, with generation of random numbers in a computer, are called Monte Carlo methods.The response of a detector can be calculated from the transport of many individual neutrons, despite the inclusion of a few improbable neutron histories that deviate drastically the average behavior. The Monte Carlo method can allow a detailed geometrical model to be constructed mathematically to simulate a physical situation. The modeling of BELEN detector have been performed with two different Monte-Carlo codes, GEANT4, and MCNPX 2.5.0.

GEANT4 is a toolkit for simulating the passage of particles through matter. It includes a complete range of functionality including tracking, geometry, physics models and hits. It has been created exploiting software engineering and object-oriented technology and implemented in the C++ programming language [5].

MCNPX is a general-purpose Monte Carlo radiation transport code for modeling the interaction of radiation with everything. MCNPX stands for Monte Carlo N-Particle eXtended. MCNPX is written in Fortran 90, runs on PC Windows, Linux, and unix platforms, and is fully parallel (PVM and MPI). During the time we've done the work explained in this thesis, have been used several versions of Geant4 from 9.2 to 10.1, in early versions clear discrepancies between Geant4 and experimental results found so the detectors design was based on simulations MCNPX.

1.4 Detector calibration

Calibration tests of BELEN detector, have to be done for each experimental campaign to assure the correct operation of the detector before starting the measurements. Calibration can be performed with isotropic neutron sources such as ^{252}Cf, Am-Be, etc., which produce neutrons in a continuous spectrum and from specific reactions for neutron productions with narrower energy spread such as those that can be obtained at PTB [27].

1.5 Objectives of the thesis

The BEta-deLayEd Neutron (BELEN) detector has been designed for FAIR as part of the DESPEC setup. The purpose of this detector is the measurement of neutron emission probabilities after β-decay. The BELEN neutron detector will be used jointly with an implantation setup called

AIDA that will be placed inside the beam hole. The beam of ions will be implanted on the DSSSD where they will β-decay and the subsequent neutrons will be detected by BELEN.

The main objective of this thesis is to design BELEN detector for FAIR. The design of the detector has been developed using Monte Carlo simulations with MCNPX and GEANT4 codes at UPC-SEN (Universitat Politècnica de Catalunya - Secció d'Enginyeria Nuclear). The aim of the simulations was to choose a positon of tubes to achieve the maximum neutron detection efficiency while keeping a flat efficiency along the expected energy range for the neutrons. Moderation is used by BELEN detector to obtain a flat efficiency. Different aspects about the neutron moderation in the polyethylene have been studied. A large simulation process has led to the final decision on the design of the final detector.

Prior to FAIR detector design, we have developed several prototypes. These prototypes have been calibrated and used to measure different neutron emissions from various nuclei after a β-decay at JYL and GSI facilities. All this previous experience in the design of detectors, has served to develop a tool to automate parts of the process and assist in obtaining the optimal design.

1.6 Structure of the thesis

Chapter 2 describes the main elements of BELEN detector and also some neutron detectors that employ the same technique to measure neutrons. Chapter 3 describes the methodology to find the optimal configuration and details about the configuration of the detector BELEN and the design and construction of different prototypes of the neutron detector. Chapter 4 covers the development of an application to facilitate finding the best configuration of tubes and some approximations to reduce the number of required simulations to find that configuration. Chapter 5 describes the calibration with a ^{252}Cf source of BELEN-30 and BELEN-48 detector, and another calibration for BELEN-48 detector done with some neutron production reactions (^{51}V(p,n)^{51}Cr, ^{13}C(p,n)^{13}N and ^{13}C(α,n)^{16}O) at PTB.

Chapter 2
State of the art

2.1 Introduction

The neutrons are not directly detectable by most detectors, can be detected through the interaction with an intermediate material. Such material has to have a high cross section for the interaction of neutrons which leads to the creation of a detectable secondary particle with an energy of reaction (Q) high enough to allow a simple pulse height discrimination of gamma rays which are usually present in neutron fields.

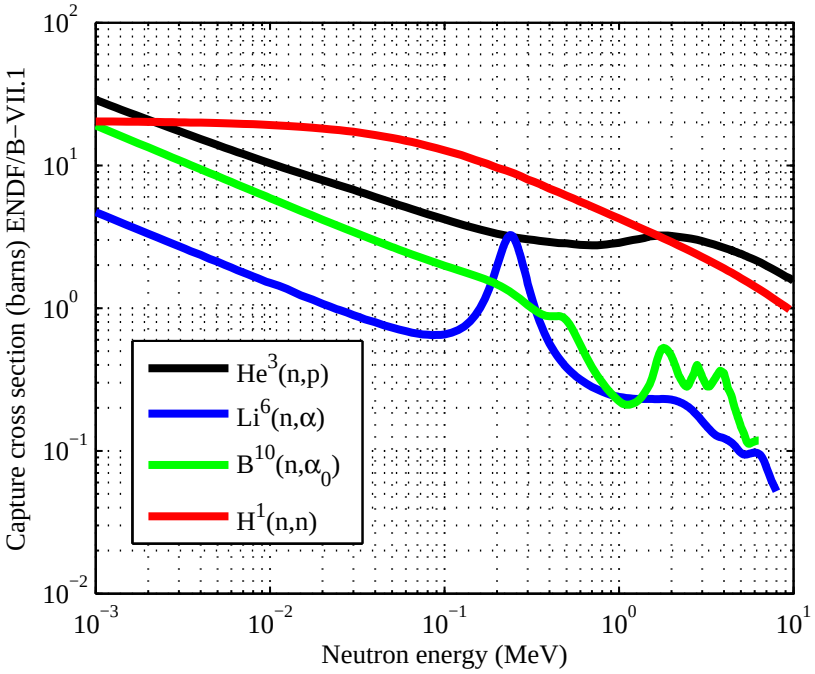

Figure 2.1: *Some cross sections of most common materials used in neutron detection*

Some of the main technical factors that have to be considered when designing a neutron detector are the neutron energy range and the efficiency

for each energy. The energy range is limited by the detector geometry and materials, because the neutron can interact anywhere within the detector volume, good detection efficiency requires covering a large solid angle with bigger detectors to increase the neutron's probability of interaction. There are trade-offs between these factors, and designing the detector for more than one experiment requires some of these factors to have a higher priority than others.

The neutron energies can be roughly divided into two groups, slow neutrons which have energy below so called cadmium cut off (0.5 eV) and fast neutrons with energy above this level [34]. The cross section for neutron interactions in most materials strongly depends on neutron energy, as shows figure 2.1., and thus rather different techniques have been developed for neutron detection in different energy regions. A detector whose counting efficiency does not depend on the neutron energy (flat response) is an useful device in many areas of neutron physics. The low detection efficiency for fast neutrons of any slow neutron detector can be somewhat improved, as in BELEN detector, by surrounding the counters with few centimeters of hydrogen-containing moderating material. The following sections describe this moderator technique, and some other features of the BELEN neutron detector.

2.2 Moderated neutron detectors with flat response

The combination of a BF_3 tube and cylindrical moderator was first suggested as a flat response neutron detector by Hanson and McKibben [20]. A later design by McTaggart is shown in figure 2.2 and has achieved farily widespread acceptance as the standard long counter [34]. A number of instruments have been developed using this technique and we describe briefly some of them in the next sections.

MAINZ LONG-COUNTER

Constructed by the group of K.-L. Kratz at Mainz (Germany) and used in the European laboratories, including CERN-ISOLDE 5 (Switzerland), GANIL (France) and GSI (Germany). It has High Density Polyethylene (HDPE) housing, with a 100 mm diameter central hole, and a side hole for insertion of a germanium counter perpendicular to the beam axis. The latter opening reduces the number of usable ^{3}He tubes to about 50.

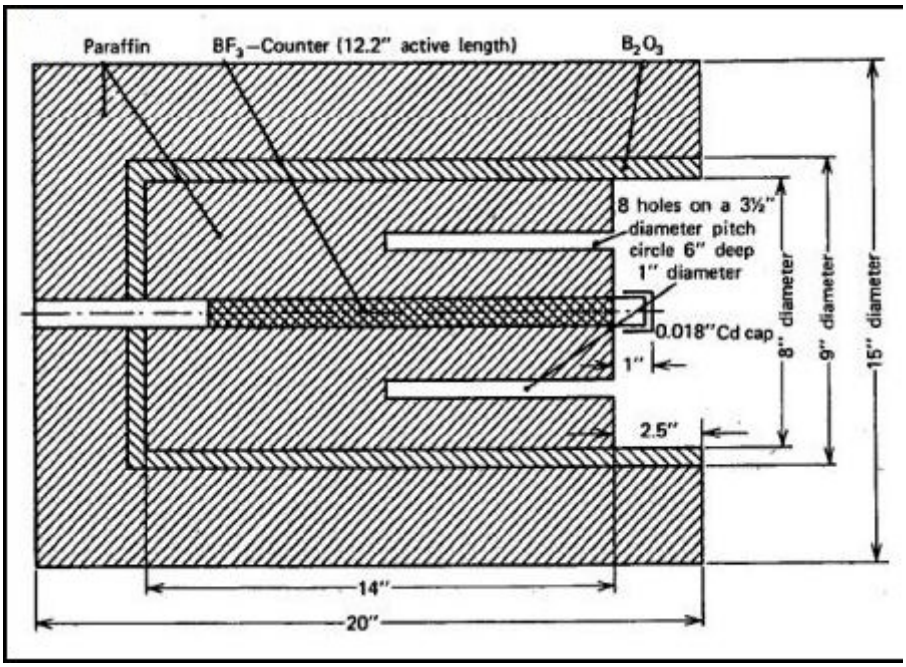

Figure 2.2: *Cross secion of the McTaggart long counter (from Knoll 4 edition [34] [20])*

These tubes, 3 feet long and 1" diameter, also operate at 10 atm gas pressure [38].

LONIE

The new LOng-counter with ENergy Independant Efficiency (LOENIE) [37] is an octagon (diameter of 42 cm face-to-face) with an axial hole. Eighteen proportional counters filled with ^{3}He at 10 atm pressure embedded in a polyethylene matrix in two concentric rings. The inner ring at 8 cm contains three ^{3}He tubes whereas the outer one at 17cm contains the fifteen remaining tubes. The detector efficiency can be seen in figure 2.4 The central hole is rectangular-shaped and wide enough (8.5 cm × 11 cm) to contain a vacuum chamber. A lateral hole was dug to house the tape moving system in order to remove the long-lived activity far from the detectors and to prevent them from increasing the beta and gamma ray background. Around the detector, two layers of neutron shielding are placed: a 5 mm-thick B4C layer surrounded by a 2.5 cm-thick borated polyethylene layer.

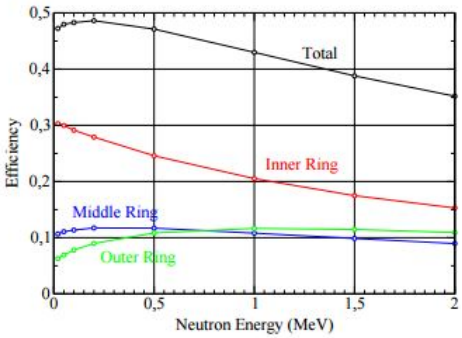

Figure 2.3: *Efficiency for neutron detection as a function of energy from MAINZ Long-counter detector [38]*

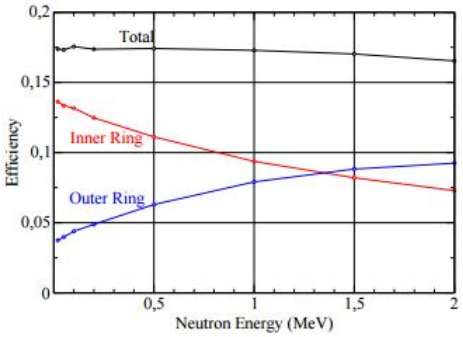

Figure 2.4: *Efficiency for neutron detection as a function of energy from LONIE detector [37]*

NERO

The Neutron Emission Ratio Observer (NERO) [13, 25] operated at the National Superconducting Cyclotron Laboratory (NSCL) located at Michigan State University, has an even larger central opening (22.4 cm diameter) to accommodate the NSCL beta telescope. NERO consists of three concentric rings of proportional counters (one inner ^{3}He and two external BF_3 gas tubes rings) embedded in a 60 x 60 x 80 cm3 polyethylene matrix, with a 22.4 cm diameter central cylindrical hole to hold the Beta Counting System (BCS) inside [1]. In the final setup, layers of boron carbide and water can be placed around the detector to minimize neutron background mainly beam-induced and from cosmic rays. The sum of efficiencies of all three rings is the total efficiency of the detector. It is constant at a value of approx. 45% for 1keV up to 300 keV and decreases to 42% at 1 MeV and to 26% at 5 MeV [14, 22, 24] as can be seen in figure

2.5. The NERO detector, together with the Beta Counting System, has been employed in numerous r-process motivated experiments performed at NSCL.

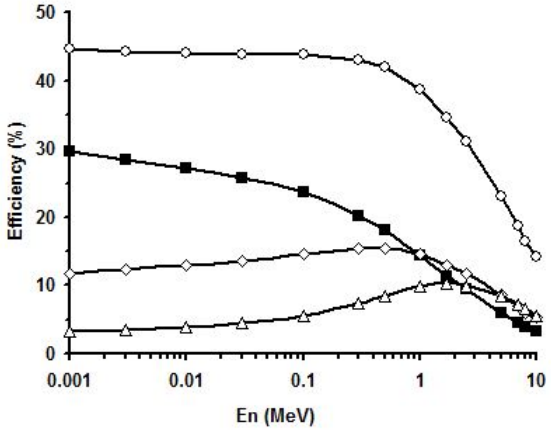

Figure 2.5: *Efficiency for neutron detection as a function of energy from NERO detector [1]*

3HEN

3HEN is based on commercially available, 1" and 2" diameter tubes filled with ^{3}He at 10 atm pressure. The ^{3}He tubes will be embedded in an axially symmetric 2-foot long cylinder, made out of a High Density Polyethylene (HDPE) moderator. By Monte-Carlo simulations was obtained a nearly constant neutron detection efficiency, around 75%, for low energy neutrons (<2 MeV). The proposed counter is also very efficient for counting higher energy neutrons, with efficiency above 50% at 5 MeV.

Beta detectors and X-ray or clover γ-counters will be placed in an adjustable opening along the detector axis. Such flexibility allow to optimize the low-energy vs high-energy gamma counting without compromising the detection efficiency for emitted neutrons. Neutron transitions to excited states will be identified via neutron-γ correlations obtained with the X-ray or γ-ray detector. To reduce background neutrons present at the accelerator facilities, additional shielding plates of 1 mm cadmium surrounded by the HDPE and paraffin bricks are placed around the neutron counter [19, 45].

The design criteria of the neutron detector included a high neutron detection efficiency with a flat response to low-energy neutrons, a small

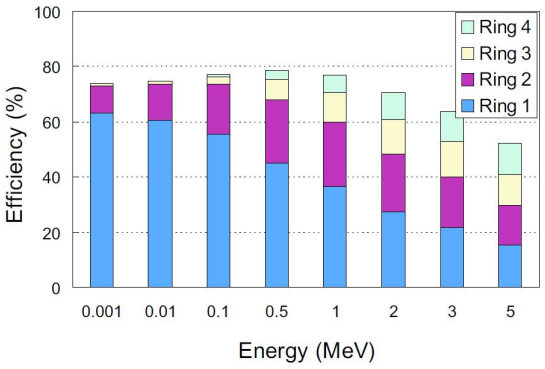

Figure 2.6: *The efficiency-per-ring for neutron detection as a function of energy from proposal 3HEN [45]*

outer diameter enabling it to easily fit inside existing support structures, system portability and a flexible construction that would allow for the use of auxiliary beta and gamma detectors.

2.3 BELEN detector

BELEN detector it is based on the moderator technique described before. The detector combine an array of ^{3}He proportional tubes with a neutron energy moderator matrix made from polyethylene as can be seen in figure 2.7. ^{3}He tubes are embedded in a moderator matrix made of high density polyethylene. The polyethylene block dimensions vary according to the arrangement of the neutron source and the position of the other detectors related to the experiment.

The detector BELEN has been designed to measure the probability of neutron emission after β decay (P_n), and half-lives of very neutron-rich nuclei. β-delayed neutron emissor precursors are implanted on a tape placed in the center hole of the BELEN detector and β detector is placed next to the implantation point in the tape in order to detect the β decay and be able to correlate this signal with the neutron detection from the BELEN. The main difficulty to detect the correlation, is the long moderation time of the neutron in the polyethylene (around 200 μs) as can be seen in figure 2.9, which in a conventionally triggered system will require opening a long time window for the correlation. Such a long correlation window would cause a large dead time in the system. Therefore the BELEN detector works with a purpose-built triggerless DACQ [32], developed at Insti-

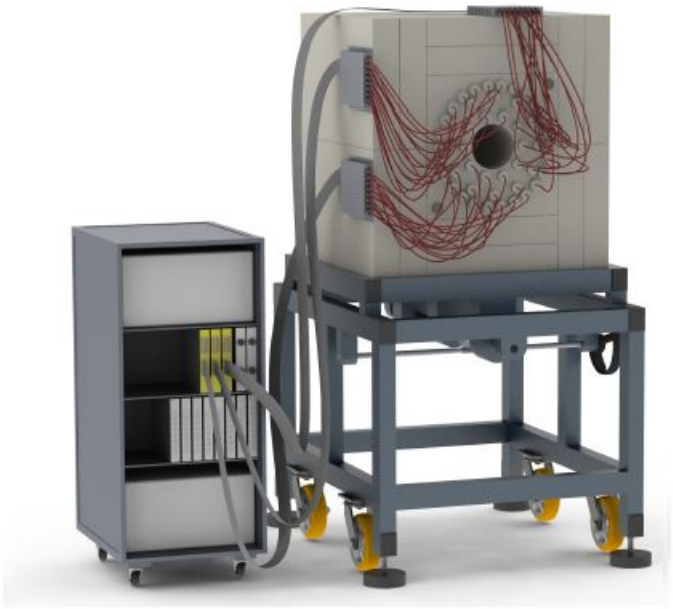

Figure 2.7: *3D view of the BELEN-48 prototype. It can be seen the tops of the ^{3}He tubes embedded in the polyethylene matrix and its connection by wiring with the electronic module on its rigth.*

tuto de Física Corpuscular (IFIC), Valencia (Spain), where for energy signals above a certain threshold, time and energy pairs are registered independently for every channel. The GasificTL DACQ software builds the β-neutron coincidence with the desired correlation time.
The following sections describe other BELEN neutron detector main elements and some details of the BELEN-20A the first prototype developed.

2.3.1 ^{3}He tubes

A typical tube detector consist of a gas-filled tube with a high voltage applied across the anode and cathode. A neutron passing through the tube could interact with a ^{3}He nuclei to produce tritium and a proton see equation 2.1:

$$^3He + n \rightarrow ^1H + ^3H + 765\ keV \tag{2.1}$$

The proton ionizes the surrounding gas atoms to create charges, which in turn ionize other gas atoms in an avalanche-like multiplication process. The resulting charges are collected as measureable electrical pulses. A

very important feature of the ^{3}He gas is the fact that it has no lower detection threshold for the neutron energy. Furthermore it has almost negligible sensitivity to gamma-rays, which takes away the concern about neutron-gamma discrimination. The energy released in the reaction will be deposited in the gas and collected by the electronic chain. In the cases that the reaction takes place close to the walls of the detector, one of the particles could deposit part or all its energy in the wall and therefore the collected energy will be reduced. This depends of course on the products range which depends on the characteristics of the detector as its pressure and density. If the range is comparable with the detector dimensions they have higher probability to escape from the detector leaving only part of its energy. This wall effect spreads the expected energy of the neutron detection reaction from 191 keV to 765 keV, as it can be seen in figure 2.8The cross section for the reaction decreases with increasing neutron energy, being more than 150 times smaller at 1 keV than at thermal energies (0.025 eV). At higher neutron energies there are elastic scattering of the neutrons from the helium nuclei; the resulting ionizing nuclei may have sufficient kinetic energy to produce a recordable event in the gas, the contributions of these events may be negligible, but in code simulations can be accounted considering ionization energy deposited by event in detection medium rather than only capture reactions. It must be noted gamma rays also can produce secondary electrons within the walls of the detector. However, the electrons have very long range within gas. Thus, they only deposit a fraction of their energy within the proportional gas. These parasitic pulses are therefore very small when compared to the pulses due to the ionization caused by the reaction products.

2.3.2 Polyethylene matrix

The first step of the simulations of BELEN was to evaluate the neutron moderation effect in a polyethylene matrix in order to determine where ^{3}He tubes should be placed. When neutrons interact with nuclei by elastic or inelastic scattering their energy is degraded. The number of interactions to produce this degradation depends upon several factors including the initial energy of the neutrons and the type of scattering (elastic or inelastic). Inelastic scattering generally requires that the incoming (captured) neutron have sufficient energy to excite the nucleus to a level that will result in the ejection of a neutron. Hence inelastic scattering occurs only at high neutron energies and the resulting neutrons will have very much lower energies. Elastic scattering, on the other hand, occurs at

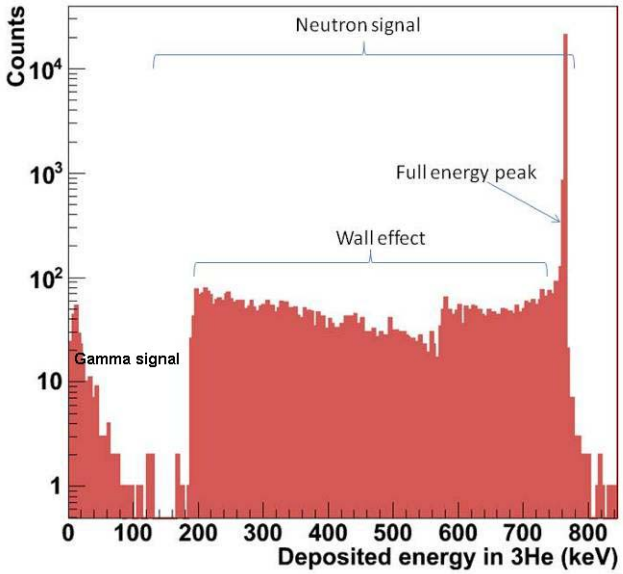

Figure 2.8: *Simulation of a deposited energy in ^{3}He tube (keV).*

all neutron energies and may not necessarily degrade the neutron energy very much. Hence most collisions are elastic.

The interaction length is depending on the energy of the neutrons arriving to the shielding. For each neutron energy the interaction length has been calculated using the relationship between the interaction length and the inelastic cross section. Different simulations were performed considering a polyethylene block of dimensions 4 x 4 x 4 m^3 with an 8 cm radius beam hole, and assuming monoenergetic neutrons emitted isotropically from the center of the beam hole. The results can be seen in figure 2.9, where each figure show the projection of the spread of the neutrons through the polyethylene block. The rows shows different initial neutron energies and the columns shows the time elapsed from the moment of the neutron emission. The colour shades indicate the density of neutrons with an energy below 10^{-7} MeV, red showing the highest density (>200 neutrons/cm^2) and light blue the lowest (<20 neutrons/cm^2). As can be seen in the figures, the higher the initial energy of the neutron, the longer time the neutron requires to be moderated inside the polyethylene matrix and the further it scatters away from the center of the detector. From this figure it was concluded that the maximum spread away from the origin of a 10 MeV neutron in the polyethylene block was around 30 cm whereas a 1 eV-neutron could only spread about 15 cm. This confirms

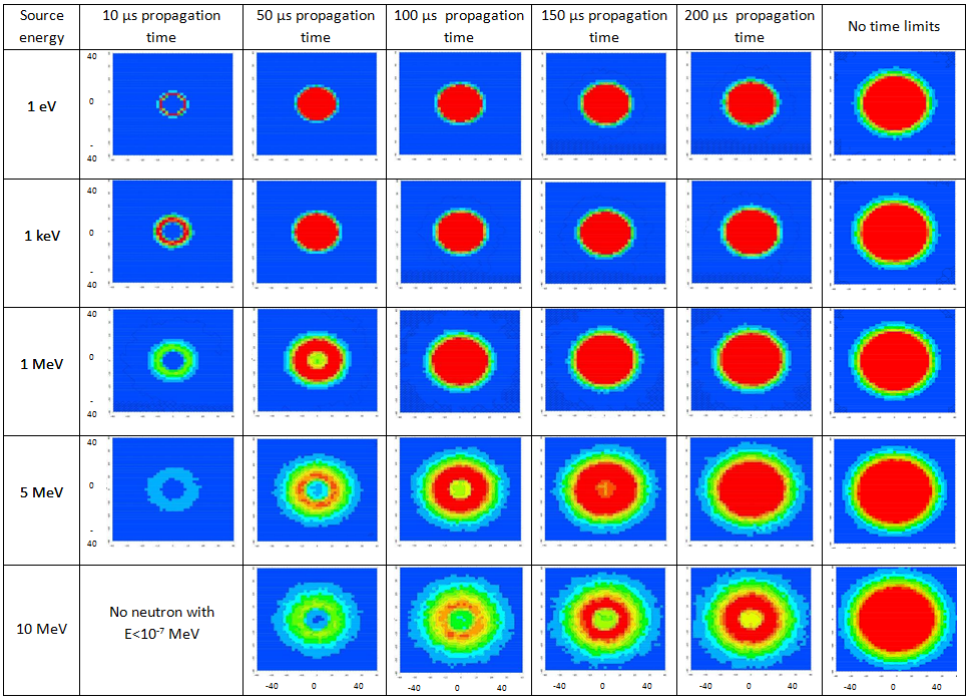

Figure 2.9: *Summary table of neutron flux in the polyethylene block for different source energies and neutron propagation times. The neutron source is located at the center of the polyethilene block and the emission is isotropically. The flux showed is the projection of the spread of the neutrons through the polyethylene block. Dimensions of x and y-scale are in cm. The colour shades indicate the density of neutrons with an energy below 10^{-7} MeV, red shows the highest density (>200 neutrons/cm^2) and light blue the lowest (<20 neutrons/cm^2)*

that lower energy neutrons would be mainly detected in the ring with the detectors closest to the beam hole, whereas higher energy neutrons would be detected in the rings further away.

2.3.3 Gas pressure and tube length analysis

Monte Carlo simulations have been performed using GEANT4 to determine the optimum gas pressure and tube length. The setup of these simulations is a single ^{3}He tube, embedded in a 1 x 1 x 1 m^3 polyethylene block. This block has a cylindrical hole in the center where the neutron point source is located. The dimensions of the tube are all fixed except its effective gas length. This length (represented in the figure 2.11 as L) in

conjunction with the moderation distance D and the gas pressure are the key factors to find the configuration that optimizes the neutron detection. It is significantly important to estimate the optimal gas pressure in order to avoid an overrun cost, since the cost of the ^{3}He gas increases linearly with the quantity, and a higher pressure directly means a higher density. A simulation with the previous setup (figure 2.11) has been carried out changing the gas pressure from 2 atm to 20 atm for 9 different initial neutron energies (from 10^{-4} to 10 MeV). It is important to specify that the moderation length (D in the figure 2.11) is defined by the 1 MeV energy neutrons at 65 mm. At the same time, the effective length of the tube (variable L) is set at 600 mm.

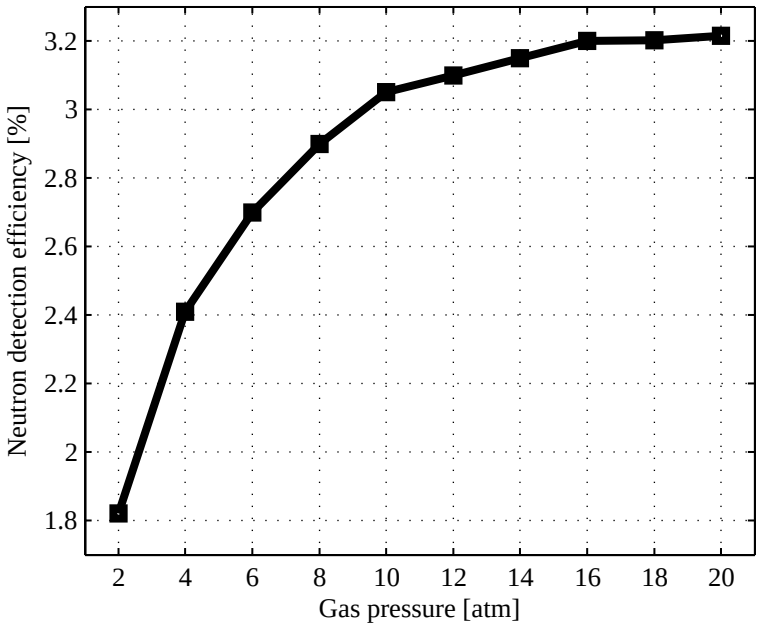

Figure 2.10: *Single detector efficiency for gas pressure at average of initial energy*

The results shows that it is possibly to assume that the efficiency has the same tendency for all initial energies. Thus, the average efficiency for energy from thermal to 5 MeV, has been calculated to find the optimal pressure. Observing figure 2.10, which represents the average efficiency for all the energy range, a pressure between 8 and 10 atm is considered as the optimal pressure for the ^{3}He gas inside the detector tubes due to the fact that above this point the increase of the detection efficiency is lower than the increase of the ^{3}He cost.

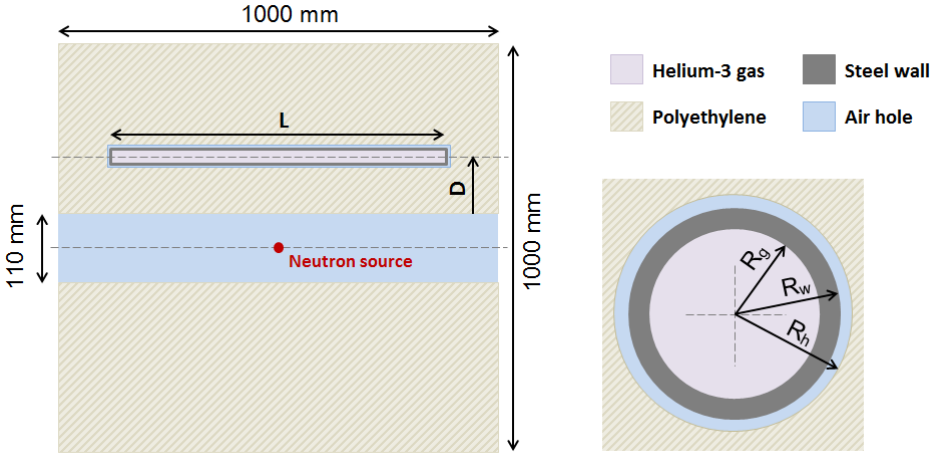

Figure 2.11: *Sketch of the simulation. The gas radius is R_g; the external tube radius is R_w; the hole radius where the tube is inserted is R_h; D is the distance from tube axis to the beam hole axis; L is the tube length. The beam hole diameter is 110 mm*

In order to determine the dependence of effective length of gas tubes with efficiency, different GEANT4 simulations have been done ranging the tube length from 300 to 900 mm and the distance from 90 to 180 mm (L and D, figure 2.11) for the whole energy spectrum. The gas pressure has been set at 8 atm. It is easy to extract from there that the closer to the center the tube is located, the higher is the efficiency. At the same time, increasing the length of the tube, the efficiency enhances too. To see the best coupling of L and D parameters is defined the *Change of efficiency*. That magnitud is calculated by dividing each value of efficiency by the efficiency of a tube with a length of 30 cm and then plotted in function of the change of this ratio with a increase of 100mm of tube lengths as can be seen in figure 2.12

The location of the tube has a great influence on the detection efficiency regardless of tube length; limiting the tube length is important as regard to the cost. Taking into account the different increments of length, an increment of length from 400 to 500 mm contributes with an efficiency gain higher than a 6%, while the next increments lead to an efficiency gain below the 3%.

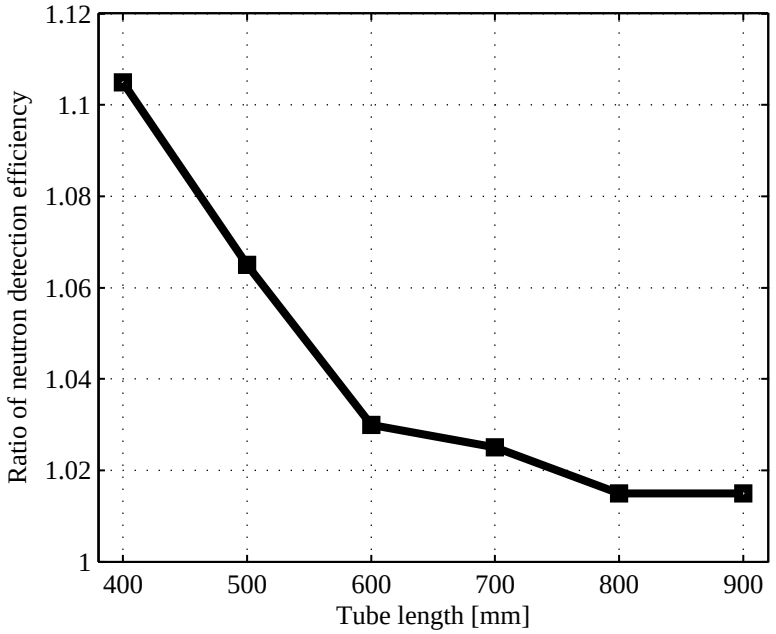

Figure 2.12: *Ratio between efficiency for a tube with an increase of 100 mm of tube lengths*

2.4 BELEN-20A

BELEN-20A was the first prototype of the neutron detector BELEN. The settings for the design of the detector BELEN-20A consisted on 20 ^{3}He proportional tubes with an effective length of 60 cm, a diameter of 2.54 cm and a gas pressure of 20 atm and a polyethylene block of dimensions $90 \times 90 \times 80$ cm^3 with 11 cm diameter central hole. The experiment for the characterization of BELEN-20 detector and its self-triggered acquisition system was performed in November 2009 at Cyclotron Laboratory of the University of Jyväskylä (JYFL), to measure the β-delayed neutron emission from the fission products ^{88}Br, ^{94}Rb,^{95}Rb and ^{138}I. Measurements were performed for neutron rich isotopes with well known neutron emission probability (P_{n}) values and with a ^{252}Cf source. These measurements were used to obtain the tube detection efficiency and verify the previous Monte Carlo simulations [18] , [17] table 2.1. Within the relatively large uncertainty of the experimental value there is a fair agreement with the simulations. The results of this experiment prove the suitability of the BELEN-20 detector and the triggerless DACQ to perform these measurements.

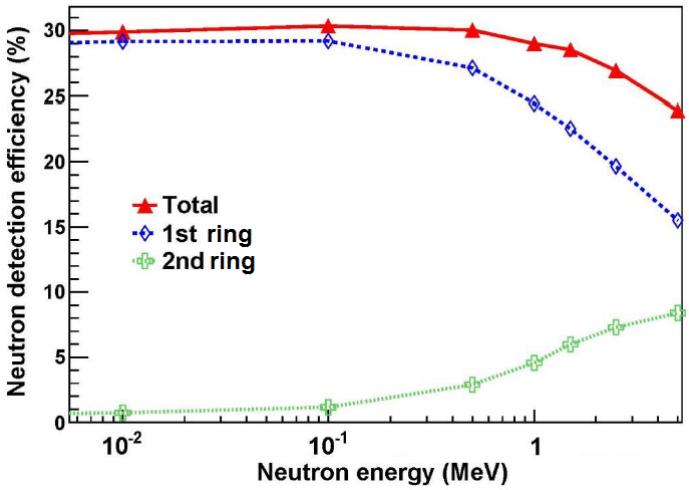

Figure 2.13: *Efficiency for BELEN-20a prototype (2009) obtained by Monte Carlo simulations with MCNPX code*

BELEN-20a		Efficiency		
Isotope	Mean Energy	Experimental	MCNPX	Geant4
^{94}Rb	437 keV	0.302(8)	0.298	0.300
^{95}Rb	525 keV	0.301(16)	0.296	0.298

Table 2.1: *Experimental and theoretical (simulated) efficiencies of BELEN-20 for two neutron energies, corresponding to neutrons from ^{94}Rb and ^{95}Rb*

Chapter 3
Design of BELEN detector for DESPEC, GSI and JYL experiments

3.1 Introduction

The BELEN neutron detector is being developed within the DESPEC (DEcay SPECtroscopy) collaboration[1] for experiments at the future FAIR facility[2]. The DESPEC experiment at FAIR will perform high resolution and high efficiency spectroscopy with radioactive ion beams. The detector BELEN has been designed to measure the probability of neutron emission after β-decay (P_n), and half-lives of very neutron-rich nuclei. Different prototypes of the detector have been developed and have been employed at several installations for the study of β-delayed neutron emitters. This prototyping model has allowed to find improvements in various aspects of development as optimal pression of tubes, electronics and design, in order to achieve a better final system developed for the DESPEC collaboration. With regard to the subject of this thesis, this model has helped to define a methodology to facilitate the design of such detectors. The purpouse of this methodology is to find the best combination of the position of the tubes in the polyethylene matrix (configuration) to obtain a maximum efficiency and a flat response for a range of initial neutron energy values. This chapter includes the details about that methodology and its application to define some BELEN detector prototypes.

3.2 BELEN configuration design

3.2.1 Definition of the problem

A *configuration* is the set of positions of each tube in the polyethylene matrix. The aim of the configuration design, is to combine different groups

[1]HISPEC/DESPEC technical design report
[2]FAIR: Facility for Antiproton Ion Research

of tubes (forming a partition of the set of available tubes) at some positions in the polyethylene matrix that gives the best compromise between high mean efficiency and flat response for the neutrons of all energy range defined for each experiment. The distribution of tubes also is made to obtain maximum symmetry to give us a better statistics when analyzing the results. One easy way to obtain that symmetry is distribute the tubes in a ring around the central axis of the polyethylene matrix. Is important to note that although the position of a tube where the efficiency is maximum for a given neutron energy can be easily determined, the interaction between different tubes complicates the way to get it.

To choose between the configurations, we define some quantitative parameters that help quantify the configurations. These parameters are defined according to the purpose of the experiment. The common feature of the main experiments involving the detector, is both the not well known energy spectrum of neutrons emitted by the source and the low intensity of the neutron emission associated with a limited time of measurement. To obtain the maximum information of the experiment, is necessary to design the detector so that combines maximum efficiency and, due to ignorance of the initial neutron spectrum, constant efficiency as constant as possible in the range of expected source neutron energies (flat factor). These two features are numerically represented by parameters: *mean efficiency* and *planarity(flat factor)*. The value of these two parameters serve to choose the best configuration of the detector.

Mean detector efficiency

The **mean detector efficiency** (η_{mean}) is defined as the value of the expression 3.1

$$\eta_{mean} = \int_{rang(E)} \eta(E)s(E)dE \tag{3.1}$$

where $\eta(E)$ is the detector efficiency at energy E and $s(E)$ is the function, normalized to 1, describing the neutron spectrum of the experiment:

$$\int_{rang(E)} s(E) = 1 \tag{3.2}$$

For Monte Carlo simulations, the efficiency calculation is performed with a numerical integration by choosing specific values for energy in order to have a good estimate on the entire range of energy. The efficiency

generally behaves as a smooth function, so that the errors obtained are small if the points selected for the calculation are distributed to the appropriate energy range. The expression for the **mean detector efficiency** is:

$$\eta_{mean} = \sum_{i \in rang(E)} \eta(E_i) s(E_i) \tag{3.3}$$

In order to get an accurate measure of the **mean efficiency** of a particular experiment would be necessary to have a priori the neutron energy spectrum, but in most of the experiments with BELEN neutron detector we don't have this information. To assign a parameter to give us information about the mean efficiency of our detector, are defined several types of characteristics spectra to have a measure of the **mean detector efficiency**. The usual way to define the efficiency of a BELEN neutron detector is with a flat spectrum, with the same value for all range of experiment expected energies.

$$s(E) = u(E) = \frac{1}{\int_{rang(E)} dE} \tag{3.4}$$

Another neutron spectra used is obtained from an experimental calibration with the source ^{252}Cf.

Flat factor

The flat factor, *f*, is the ratio between maximum efficiency and minimum value of the efficiency in a range of energy :

$$f = \frac{\eta_{max}}{\eta_{min}} \quad E \in rang(E) \tag{3.5}$$

so that the minimum ratio corresponds to the best planarity which guarantees that the **mean efficiency** calculated is a good measure for all energies in the range.

3.2.2 Methodology to find the optimal detector configuration

To choose the number and types of tubes for one group of them is necessary a previous study of the efficiency obtained for some basic configurations. As an example of this kind of study, in Figure 3.1 can be seen the value of efficiency versus energy for different groups of tubes

distributed in a ring at different radius (8 cm to 13 cm with 0.5 cm intervals) to the center of the block of polyethylene with a cylindrical central hole of 5 cm. The labels of the plot gives the values of the different parameters to evaluate the configuration: e is mean efficiency, M is maximum eficiency, m is minimum efficiency for the range of energy defined $[e : \eta_{mean},\ M : \eta_{max},\ m : \eta_{min}]$. As can be expected, the maximum detection efficiency is obtained at the lower distance to the center of the ring (8 cm with a mean efficiency of 31 %) . And the flatest one is the ring at 11.5 cm, but with a mean efficiency of only 18%.

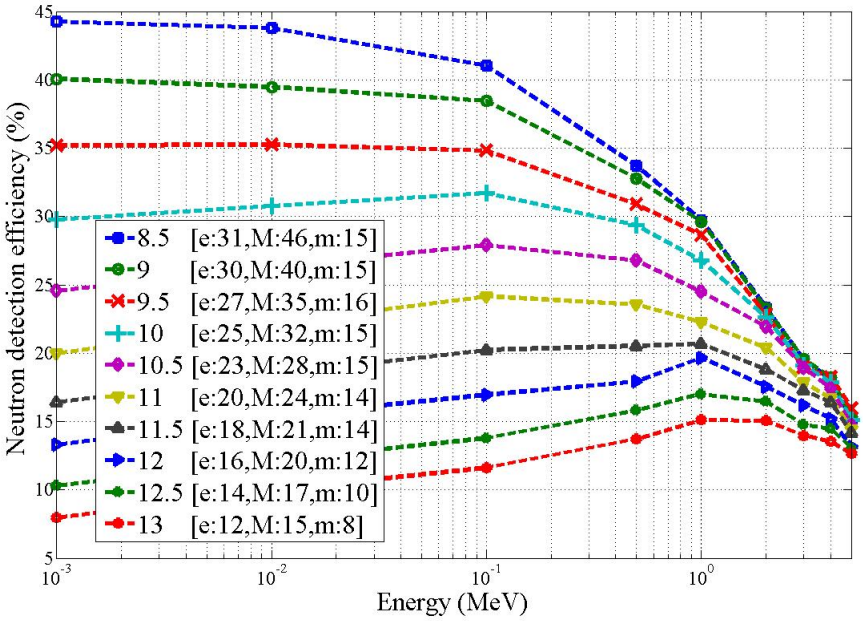

Figure 3.1: *Efficiency for the same number of tubes distributed in a ring at different radius (8 cm to 13 cm with 0.5 cm intervals) to the center of the block of polyethylene for the range of energies below 5 MeV*

The next step is to combine different groups of tubes as it can be seen in Figure 3.2 with a combination of three groups of tubes distributed in three rings (G1 inner ring, G2 middle ring and G3 outer ring). The sum of efficiencies of each group can be seen also in this figure. In the plot, the horizontal axis shows the range of the energies defined by the experiment and the vertical axis the percentatge of efficiency for each group and its sum. The total efficiency seems relatively flat but is not optimal, there are more configurations with a better combination of mean efficiency and

flat factor. Note that the efficiency of each group is calculated with the presence of the other ones and is not the same that we obtain for the group isolated in the polyethylene matrix.

As has been explained, is important to note that the influence of the presence of the other tubes complicates the way to get the total efficiency for the configuration with the tubes of all groups, and it is necessary to do a new simulation for each combination of groups. We can see this in the figure 3.3 that shows the efficiency versus energy of two tubes at different distances to the center the polyethylene matrix (8 cm and 11 cm) with a cylindrical central hole of 5 cm. In the same figure can be seen the efficiency versus energy of the configuration with the two tubes in the polyethlene matrix at the same initial polar angle (aligned), and with 15, 30 and 45 degrees polar angle between tubes. In the figure 3.4 it can be seen in percertatge the difference between this four configurations in reference with the efficiency sum of the two efficiencies of the isolated tubes. The influence of the presence of the other tubes is higher when they are aligned, more than 15% for the overall energy range. The issue of influence between the tubes efficiency is discussed in more detail in the next chapter.
Summarizing and adding some details, our basic steps of the methodology for the configuration design of BELEN neutron detector are:

1. Simulate some configurations of tubes to estimate the range of expected efficiencies. For example, one configuration with all the tubes nearest to the central hole as can be possible, to obtain a maximum efficiency for low range energies and another with a first rough estimate value of efficiency for the highest energy range.

2. A systematic study putting just one tube at different distances from the origin of neutrons to obtain an estimation of the profile of efficiencies for different energies (one time for each type of tube that we have available). This result for an isolated tube will not be the same for this tube into a configuration with more tubes, because interference between the tubes makes it change, however, it is a first reference to define combinations of rings for subsequent tests.

3. With the data obtained in the previous step, we calculed a first approach of the efficiency for the configurations distributed in two rings. This efficiency has been calculated using an approach of efficiency as a sum of individual tube efficiency (obtained in the previous step) adding a term that fixes in part the interference between tubes. This approaches will be explained in detail in the next

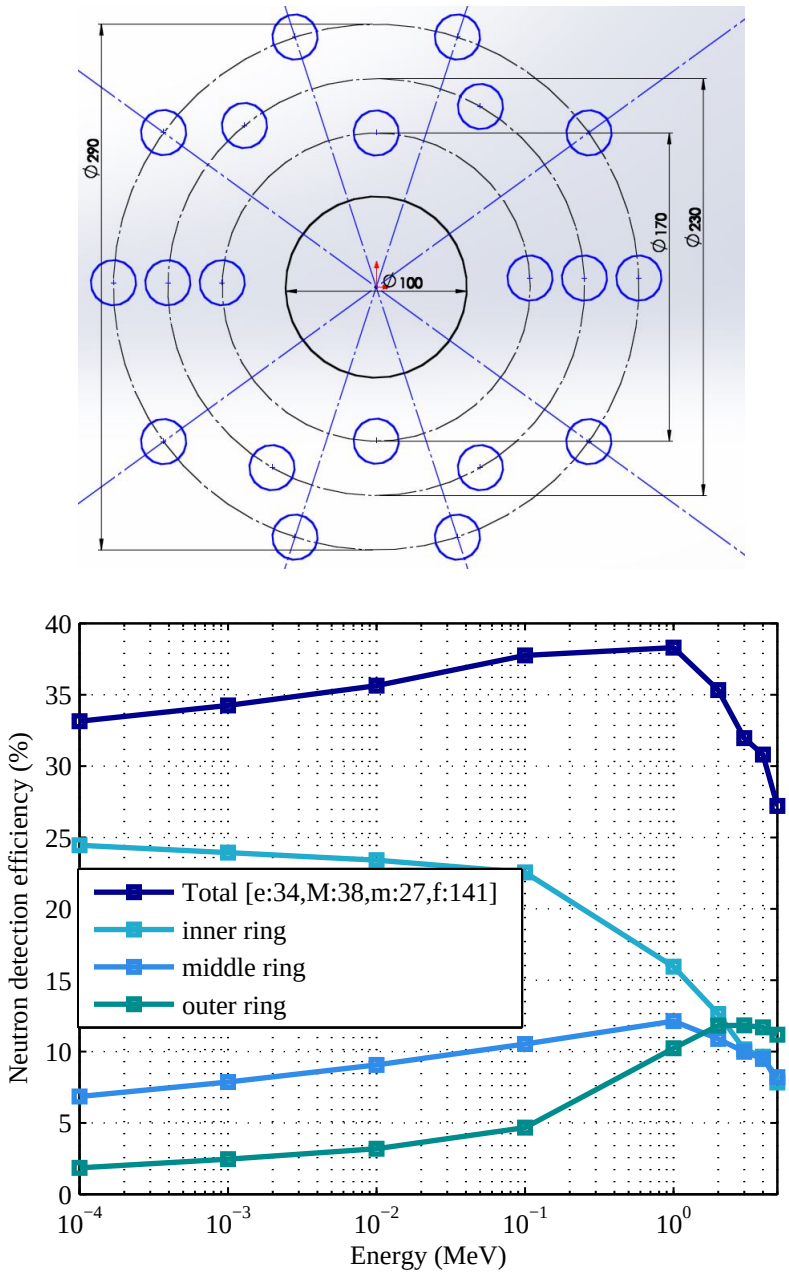

Figure 3.2: *Front view of a possible BELEN configuration with a 10 cm diameter central hole and three rings (G1 inner, G2 middle , G3 outer) with 4,6,10 tubes respectively and an efficiency plot for a range of energy from 100 eV to 5 MeVs of that configuration*

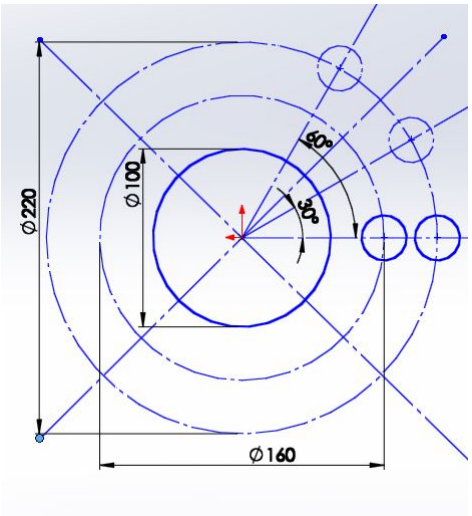

Figure 3.3: *Schema of two tubes at distances of 8 cm and 11 cm aligned, with an polar angle of 15, 30 and 45 degrees between them*

chapter. This result serves as a reference for subsequent simulations and save a great number of Monte Carlo simulations. Several areas of parameters (the parameters used are the radius of the rings, and the number and types of tubes for ring) are choosen with a good combination of mean efficiency and flat factor.

4. The efficiency of the choosen configurations of last step are calculated by Monte Carlo simulations. Then a large number of simulations are performed with minor modifications (number or type of tubes and radius of rings) of those configurations.

We repeat whole process adding more rings until it is geometrically possible or there is no improvement in the result.

For the step 3 we need to define a part of the space of parameters to do a more accurate search of the optimal configuration. In the case of a large number of tubes, as in BELEN-48 or BRIKEN, there are a lot of odds and it has been decided an alternative option, we choose a partition of the set of tubes available and dedicate each of those elements of the partition to obtain just one of the goals. The main idea is to subdivide the searching of the best configuration in a sequence of subproblems with different goals in several steps. For each step we use a number of tubes to achieve the goal (or to get as close as possible to the goal). To describe the goal, we define a figure of merit with different weights of the following list of variables:

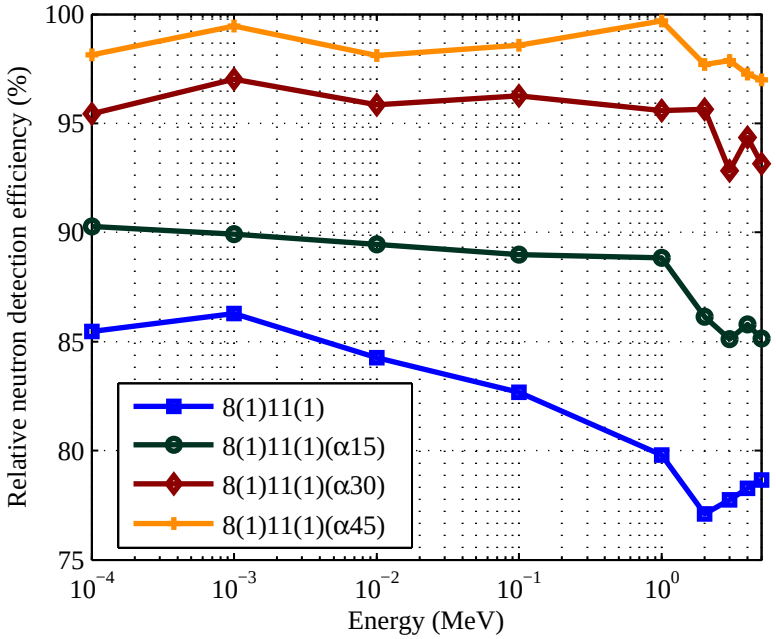

Figure 3.4: *Efficiency relative to the sum of efficiencies of two isolated tubes at distances of 8 cm and 11 cm of the four configurations of these two tubes aligned, with a polar angle of 15, 30 and 45 degrees between them.*

- Flat factor (defined in differents range of energy)
- Mean efficiency
- Symmetry of the ring tubes

The first and second parameter are the same as defined in this section. The third is defined to impose symmetry to the final configuration. The detail of the computed process to obtain the goal for each group is explained in the chapter 4.

3.2.3 Simulation details

The modeling of BELEN detector have been performed with two different Monte Carlo codes, GEANT4, and MCNPX. Such an independent cross check could reveal possible mistakes in the geometric model and physics used. Monte Carlo calculations always have some errors which arise from the nature of the calculations. These errors are, statistical uncertainty, discrepancies in material composition and geometry, errors

in nuclear data libraries and theoretical models. The statistical uncertainty decreases with increasing computation time, the estimated relative error, caused by the statistical uncertainty falls with the number of simulated particle histories, N, according to $1/\sqrt{N}$. The error arising from geometrical model was supposed to be small because geometry is not so difficult to represent. Material used in the experiment were well known and relatively simple, the final error caused by differences between the physical experiment and the simulation is expected small. We can not calculate the error caused by nuclear data libraries, because the data in the libraries often does not present its error. BELEN detector simulations to search the final prototype configuration have always been held with a number greater than 1M (million) neutrons (for each simulated energy) , only when we have wanted an approximate value of efficiency we have simulated with 0.1M neutrons.

The MCNPX code offers options based on physics packages. For neutron transport the free gas model down to 4 eV is used and for lower energies the treatment takes into account the crystalline structure of materials for thermal neutrons interactions. In this particular, we used poly.60t (hydrogen in polyethylene at 293 degrees Kelvin) from ENDF/B6.0 [2].

The Geant4 simulation toolkit supports various physics models which are assigned to a particle through processes. There are no default physics models to deal with particle transport, which means that depending on the application we can choose one physical model and also to assign cross-section data libraries [3]. The BELEN simulation code are based on GEANT4 release 9.5 but has been updated to later release and end up with the release 10.1. The list of physical processes employed in the BELEN detector simulation within GEANT4 toolkit is based on the standard models of physics lists, modified to include additional interactions of neutrons with polyethylene. Concerning the neutronc interactions, this package includes the data driven high precision neutron package (NeutronHP) to transport neutrons below 20 MeV down to thermal energies. But it is well known fact that the moderation of neutrons with kinetic energies below 4 eV in polyethylene should be considered in a special way [39]. In this low-energy region the scattering of neutrons on the hydrogen nuclei in polyethylene cannot be treated as scattering on free protons due to the possible excitation of vibrational modes in polyethylene molecules. Such collective motion of molecules significantly change the thermal neutron scattering characteristics in polyethylene, so dedicated thermal scattering dataset and model should be included for neutron energies less then 4 eV to allow the correct treatment of neutron moderation and capture

processes in the elements of BELEN. The complete list of the GEANT4 classes for neutrons is given in table 3.1. Another modification used, is the software tool for transforming any evaluated neutron cross section library (ENDF/B, JEFF, JENDL, CENDL, BROND...) in the ENDF-6 format into the G4NDL format [39]. In this way, GEANT4 have access to the complete list of standard evaluated neutron data libraries when performing Monte Carlo simulations with GEANT4 since release 9.5.

Process	Model		Cross section data
	Name	Range	
Elastic	G4NeutronHPThermalScattering	<4 eV	G4NeutronHPThermalScatteringData
	G4NeutronHPElastic	4eV-20MeV	G4NeutronHPElasticData
Inelastic	GBinaryCascade	< 30 MeV	G4NeutronHPThermalScatteringData
			G4NeutronHPInelasticData
Capture	G4NeutronHPCapture	< 20 MeV	G4NeutronHPCaptureData

Table 3.1: *Physics list used for neutron interactions with GEANT4 in this work (Fission process is in the soft but not used)*

In order to model a ^{252}Cf source, a customized Geant4 fission library developed by the Lawrence Livermore National Laboratory is used. This customized library is not only capable of simulating neutron and gamma-ray multiplicities of various spontaneous fission sources but also of neutron-induced fission sources [33].

3.2.4 Configuration design for some BELEN detector prototypes

As you can see in Figure 3.5, the first two prototypes of BELEN consisted on 20 tubes (BELEN-20) and were tested in two experiments at JYFL[3] in 2009 and 2010. The next prototype BELEN-30 was tested at GSI in 2011 and was composed by 30 tubes. The BELEN-48 has been designed for FAIR as part of the DESPEC setup. Meanwhile have been designed also two prototypes BELEN48-M1 and BELEN48-M2 that have been employed in JYFL in 2014. Previously BELEN48-M1 have been tested at PTB in 2013. The last BELEN like neutron detector designed is BRIKEN and in this work we show our proposed configuration.

[3]Cyclotron Laboratory of the University of Jyväskylä

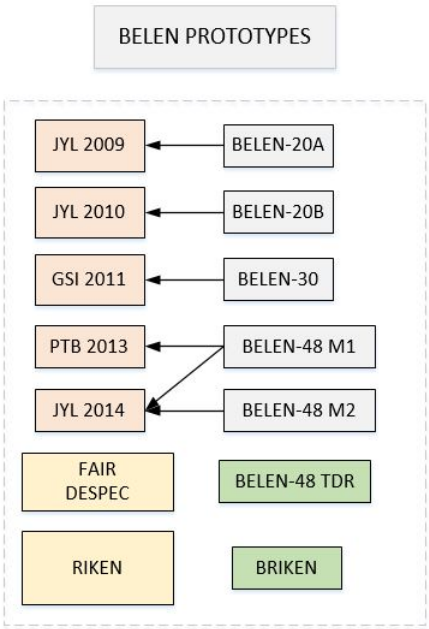

Figure 3.5: *Belen prototypes and its related experiments*

The next sections includes the details about the methodology employed and the final configuration for some prototypes of the BELEN neutron detector. The settings have been made to meet the initial specifications of each facility, the value of efficiency per energy of neutron source, and the flat response of that efficiency.

3.3 BELEN-20B

3.3.1 Experiment setup

An update of the BELEN-20A prototype was designed, built and tested in June 2010. A novelty in our setup is the introduction of a trigger-less data acquisition system. Its use allows continuous control of data quality, which leads to greater accuracy, with a minimum acquisition dead time [32]. The use of delayed-neutron precursors with different neutron emission windows allowed the study of the effect of energy dependency on neutron, and -neutron rates. The BELEN prototype was validated at JYFL using the pure beam delivered by the Penning trap where radioactive species were produced by deuteron inducing fission on an uranium target. Figure 3.6 shows the detection setup used at JYFL including a

HPGe detector that was used to detect the gamma rays in coincidence with the β-decay and the neutron emission. The isotopically pure beams were directed inside a vacuum tube inserted to the centre of the BELEN detector, where they were implanted on a movable tape. β-delayed neutron emissor precursors were implanted on a this tape and a Si detector was placed next to the implantation point in the tape in order to detect the β-decay and be able to correlate this signal with the one from the BELEN. This experiment was designed to mesure β-delayed neutron emission of fission fragment of the elements ^{95}Rb,^{88}Br,^{85}As,^{86}As,^{85}Ge,^{91}Br,^{137}I.

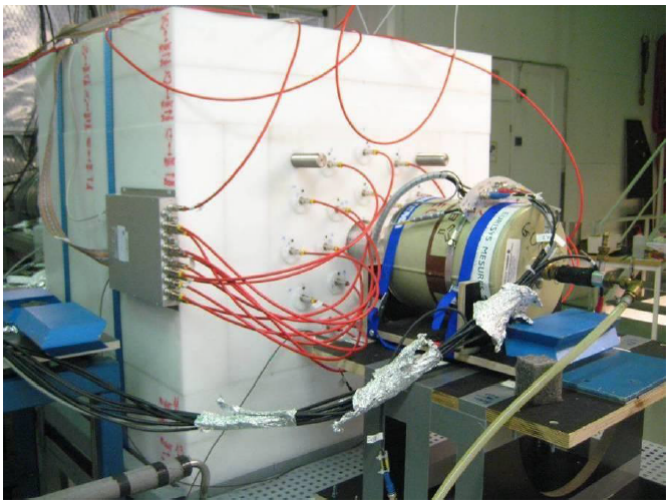

Figure 3.6: *BELEN-20 and HPGe detector in the JYFLTRAP beam line.*

3.3.2 BELEN-20B configuration design

The settings for the design of the detector BELEN-20B consisted on 20 ^{3}He proportional tubes with an effective length of 60 cm, a diameter of 2.54 cm and a gas pressure of 20 atm, and a polyethylene block of dimensions 90 × 90 × 80 cm^{3}and with 11 cm diameter central hole. The methodology to design the detector was the same as described above. Initially we did a simulation with a configuration with all available tubes nearest to the source of neutrons. This first result is far from the optimal result because it will give us a very bad value of flat factor (maximum efficiency of the order 70% for 1 keV and 42% for 1 MeV) but good for the mean efficiency (over 50%). To study the best position of the tubes, we simulated configurations with just one tube at different distances from

the origin of neutrons to obtain an estimation of the profile of efficiencies for different energies. It can be seen in figure 3.7 that 1 MeV efficiency is higher compared to the rest of energies when the tubes are located at 10.5-11 cm from the centre of the polyethylene matrix.

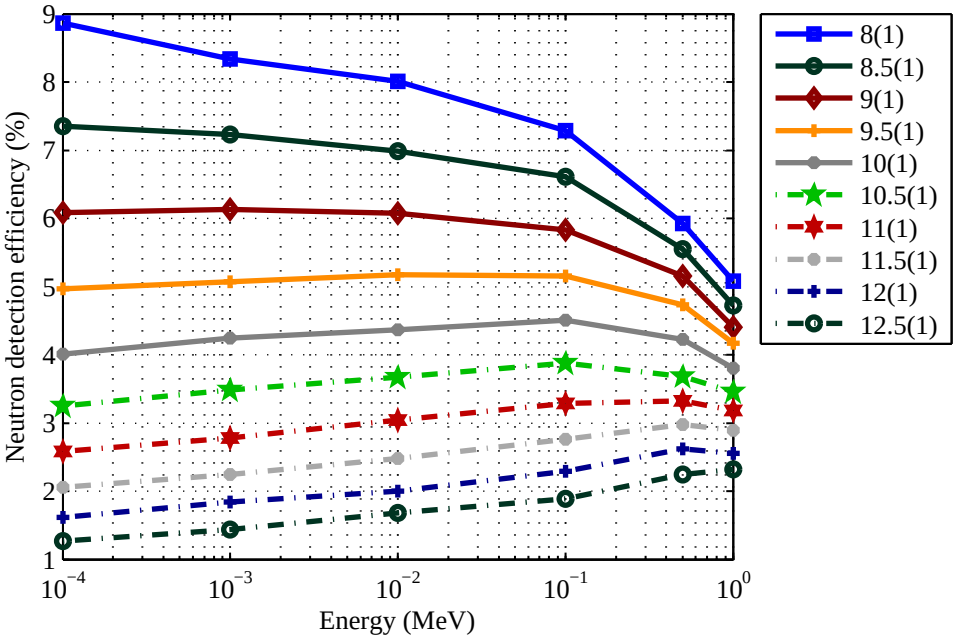

Figure 3.7: *Efficiency for one tube at distances of 8 cm to 12.5 cm*

With the data obtained for individual tubes, we calculated a first approach of the efficiency of configurations for tubes distributed in two rings. This efficiency has been calculated as the sum of the efficiency of a single tube obtained in the previous step. This result serves as a reference for subsequent simulations. Several solutions are choosen with good efficiency average and flat factor and are simulated by Monte Carlo simulations. Then, a large number of simulations are performed with minor modifications (in number or type of tubes and radius of rings) of those configurations. Afterwards it was observed that we can improve some configurations adding a small hole of 1 cm in the central block.

To ensure that the configuration with two rings is optimal we have splitted one of the ring in two rings in several ways obtaining some new configurations of three rings. By Monte Carlo simulation we can see that there is no improvement in efficiency/flat factor in those new configurations. For simplicity, in case of equality of results, we choose the solution with the lowest number of rings.

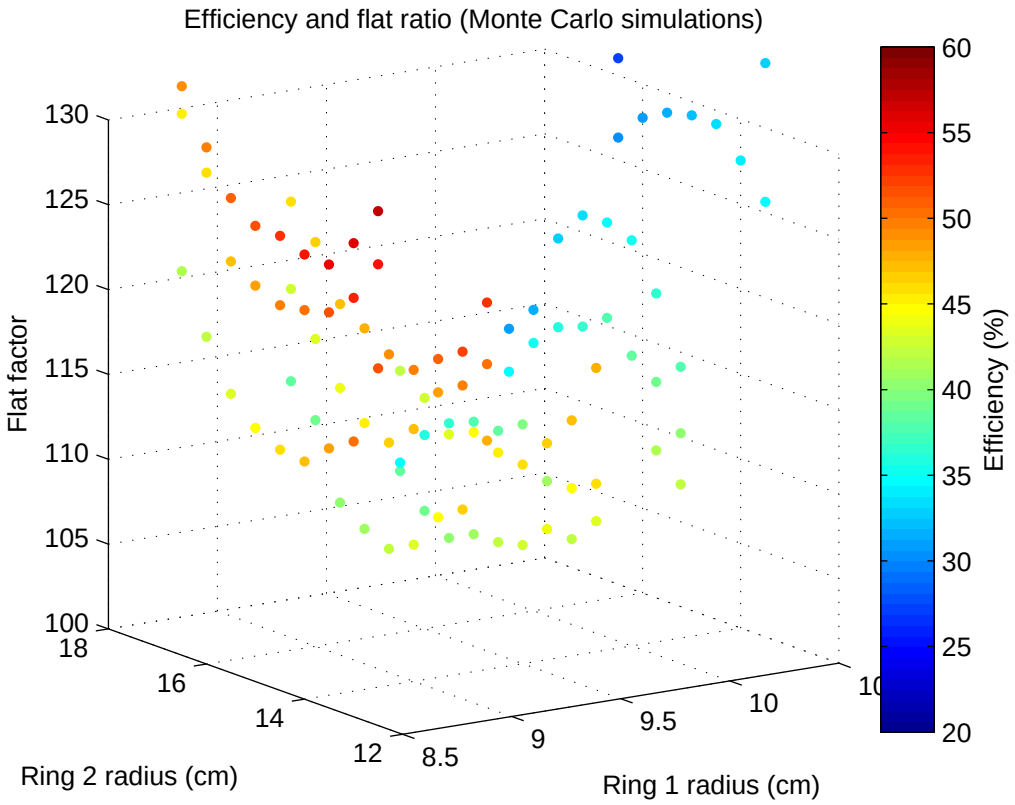

Figure 3.8: *Flat factor and efficiency for two rings from Monte Carlo simulations*

Finally the tubes are placed at a radius of 9.5 cm (8 tubes) and 14.5 cm (12 tubes) around a central longitudinal hole of 11 cm diameter with a small slit of 1 cm in the central block of 10 cm polyethylene. Figure 3.10 illustrates the detection efficiency for this prototype, nearly constant below 1 MeV reaching 46% and decreases for higher energies. The figures 3.11 shows the front view of the polyethilene matrix with the beam hole of 10 cm and the 20 tubes around in two rings.

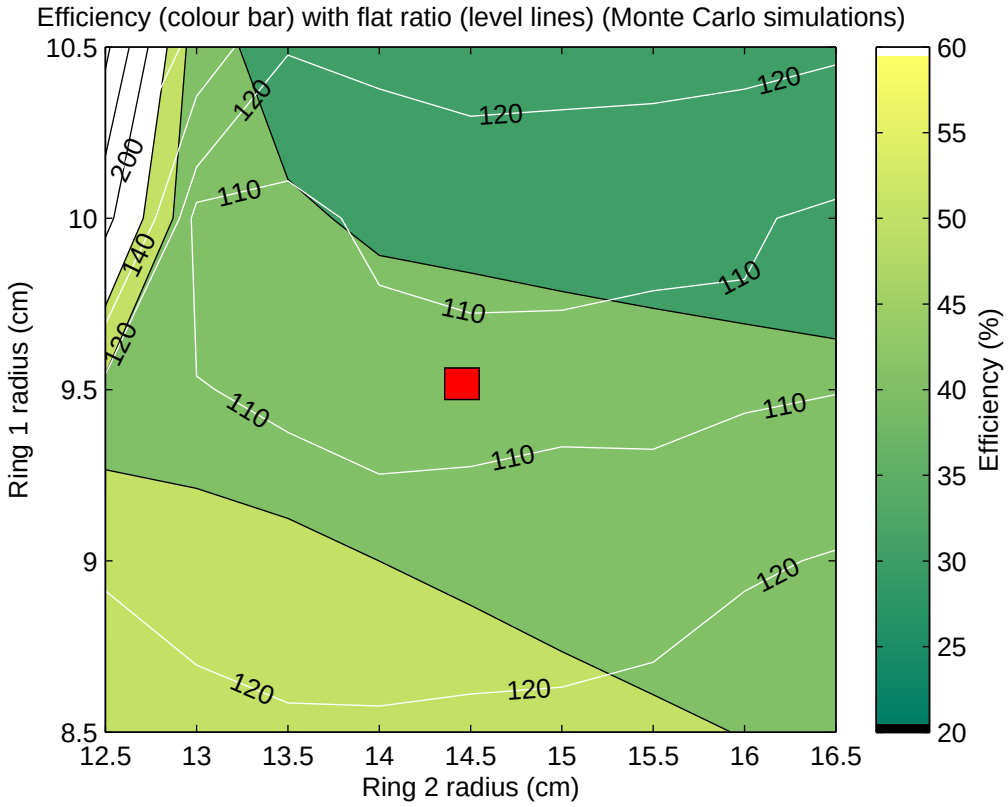

Figure 3.9: *Flat factor and efficiency for two rings for BELEN-20B from Monte Carlo simulations*

BELEN-20B/Rings	inner (G1)	outer (G2)
Radius (mm)	95	145
Number of ^{3}He tubes at 20 atm	8	12

Table 3.2: *Positions and characteristics of groups of tubes for BELEN-20b*

Table 3.3 shows efficiency and flat factor for the energy range below 1 MeV and 2 MeV obtained with MCNPX simulation codes. That results have been compared to the experimental ones using the ratio between efficiency of the inner ring and outer ring. In table 3.4 are compared the experimental values with the values obtained by Monte Carlo simulation, and we see a good agreement between these values.

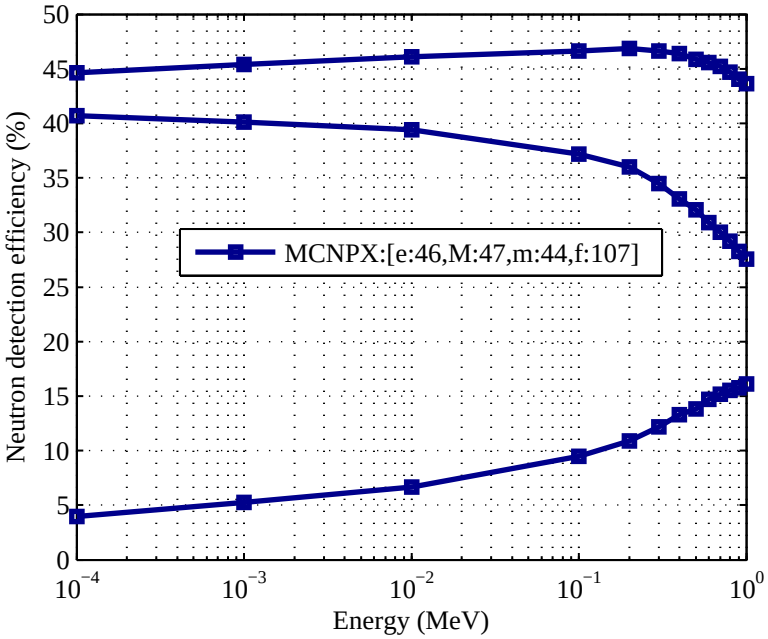

Figure 3.10: *Contribution of each ring to the neutron detection efficiency and total efficiency for the BELEN-20*

BELEN-20b	MCNPX	
	efficiency (%)	flat factor
100eV-1MeV	46	1.07
100eV-2MeV	43	1.21

Table 3.3: *Efficiency and efficiency ratio of BELEN-30 detector*

3.3.3 Experimental results and remarks

For the characterization of BELEN-20B detector setup we employed fission products which are delayed-neutron precursors with well known properties. The instrumentation includes BELEN-20B and a Si detector, a fairly common arrangement. The observed efficiency is well reproduced by Monte Carlo simulations. We used a calibrated ^{252}Cf source to measure the neutron detection efficiency and obtained a value of 40.9(8)% in very good agreement with the simulation made with MCNPX. The ratio between the counts of the inner and the outer ring of ^{3}He tubes is

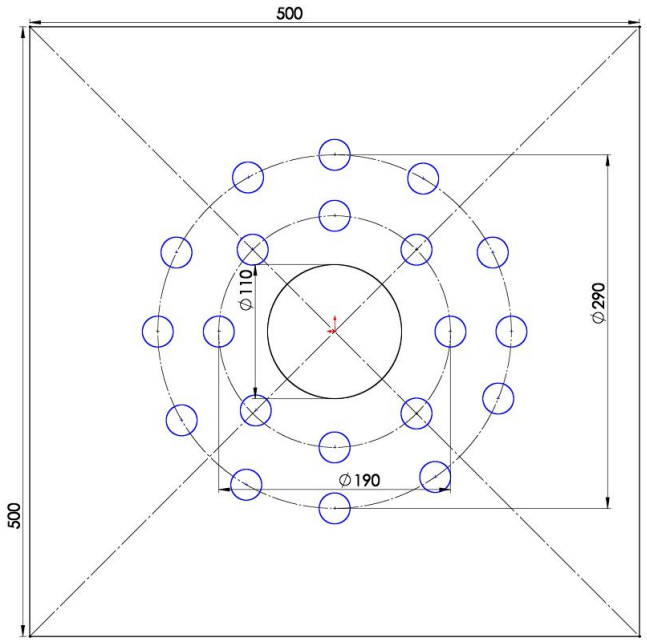

Figure 3.11: *Front view from the BELEN-20B final configuration design with 8 tubes at 9.5 cm and 12 tubes at 14.5 cm from center of polyethylene matrix*

quite sensitive to the neutron energy distribution. The measured ratio is 1.499(3) in quite good agreement with the result of the simulations.

BELEN-20B		Inn/out ratio efficiency	
Isotope	Mean Energy (keV)	Experimental	MCNPX
^{88}Br	247	3.04(2)	3.27
^{94}Rb	437	2.51(2)	2.66
^{95}Rb	525	2.52(3)	2.62
^{137}I	625	2.20(2)	2.22
^{252}Cf	2200	1.499(3)	1.56

Table 3.4: *Experimental and simulation ratio between outer ring and inside ring efficiency obtained for calibration sources with BELEN-20B*

Nuclei	Implanted ions	$T_{1/2}$(s)	P_{n}(%)
^{213}Tl	1015	23.8±4.4	7.6±3.4
^{214}Tl	598	11.1±2.5	27.4±10.9

Table 3.5: *Summary of some results obtained for the measured thallium isotopes with SIMBA and BELEN-30*

3.4 BELEN-30

3.4.1 Experiment

In August 2011 a new BELEN prototype was used at GSI laboratory in an experiment using the FRS (Fragment Separator) facility [26]. The aim of the experiment was to determine for very exotic neutron-rich nuclei in the region around N=126, half lifes ($T_{1/2}$) and β-delayed neutron emission probability (P_{n}) , such data can be compared with some theoretical models that have been developed on the basis of experimental data of nuclei. [8, 9, 43]. An initial calibration measurements was performed with ^{252}Cf source, as it can be in the table **??** the results are good enougth. In order to determine the P_{n} value, all implant β-particles events in the SIMBA silicon detectors have been analyzed by opening a window of 400 μs forward and backward (considered as background) in time to detect correlation neutron events. This time window is determined according to the expected neutron moderation time in polyehylene, to maximize the neutron detection efficiency.

$$P_n(\%) = \frac{100}{\eta_n}\frac{N^{fwd} - N^{bwd}}{N} \tag{3.6}$$

where η_n is the BELEN neutron efficiency, N^{fwd}, N^{bkd} are the number of forward and backward correlated neutrons envents and $N_\beta$the number of parent β-decays.
The analysis of data confirms the ^{213}Tl as a neutron emiter and ^{214}Tl gives the largest value of P_{n} mesured of this experiment (Table 3.5).

The experiment was based on the fragmentation of a ^{238}U beam accelerated up to 1 GeV/u with the linear accelerator UNILAC coupled to the SIS-18 synchroton. Ions were tracked and identified with tracking detectors, such as plastic scintillators, MUlti Sampling Ionization Chambers (MUSIC) and Time Projection Chambers (TPCs). They allow to obtain the atomic number (Z), the mass-to-charge (A/Q) ratio and the position

of ions along the FRS. Finally, at the final focal plane, a passive degrader was located in order to adjust the energy of the ions of interest to implant them in the central layers of an implantation detector. At the end of the beamline the detection system comprised the Silicon IMplantation Beta Absorber (SIMBA) [23, 47] detector, which is made with a stack of silicon layers consisting of three highly segmented double-sided silicon strip (DSSD) and 4 single-sided silicon strip (SSSD) detectors for measucrown ion-implants and β-decays [43]. The kinetic energy deposited in the BELEN detector is collected and processed with a new Digital Data Acquisition System (DDAS), developed at Instituto de Física Corpuscular (IFIC), Valencia (Spain).

It was performed a measure with a calibration neutron source ^{252}Cf verifying the efficiency results obtained in the Monte Carlo simulations coincided, within a margin of error, with the experimental. The details of this calibration are explained in Chapter 5.

3.4.2 BELEN-30 configuration design

The BELEN-30 detector was used to measure the delayed neutrons produced after β-decays of very neutron-rich nuclei implanted in SIMBA. The search of the optimal configuration has been done by means of systematic Monte Carlo (MC) simulations. There are 30 ^{3}He tubes available from GSI and UPC, 10 tubes at a pressure of 10 atm (from GSI) and 20 tubes at 20 atm (from UPC). The tubes were embedded in a polyethylene block of dimensions 90 × 90 × 60 cm^3 with additional 20 cm shielding against room background and thus a total weight of 600 kg and with 23 cm diameter central hole. An additional polyethylene wall with another 30 cm shielding was installed before the setup in order to reduce the in-beam neutrons produced by the S4-degrader. The steps performed to find the best configuration are similar to those of BELEN-20B but for this prototype we have two types of tubes and maximum neutron energy expected range up to 2 MeV. We did a first simulation with a configuration using all availables tubes nearest to the source of neutrons. The maximum efficiency is of the order of 60% for an initial energy of neutrons of 1 keV and 20% for 2MeV.

To study the best location of the tubes, we simulated configurations with just one tube at different distances to the origin of neutrons. We obtained an estimation of the profile of efficiencies for different neutron energies, and for the two types of tubes. This result for an isolated tube will not be the same for this tube into a configuration with more tubes

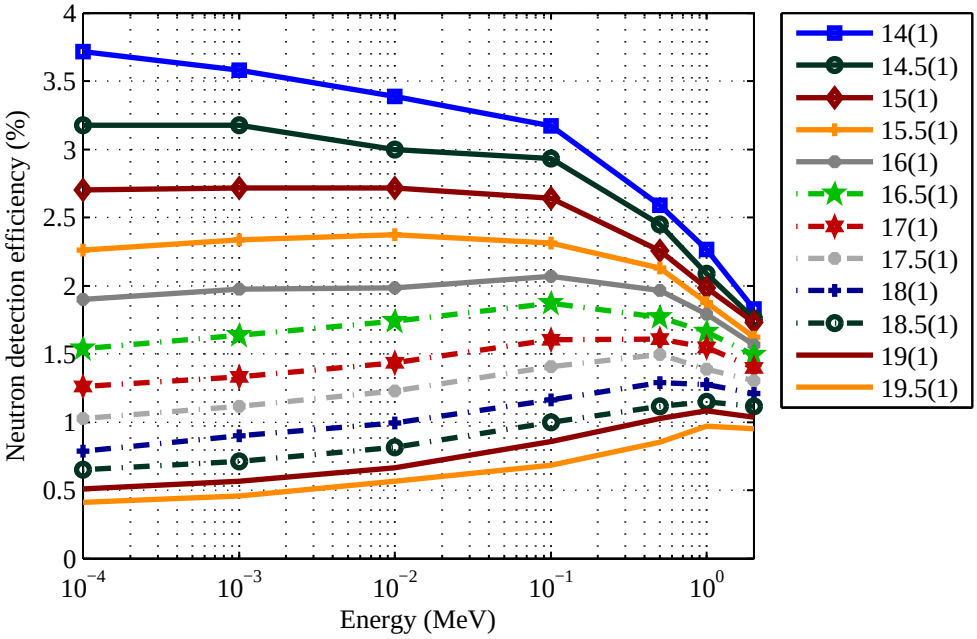

Figure 3.12: *Efficiency for one tube at 10 atm at distances to the matrix center from 13.5 cm to 18.5 cm.*

because interference between the tubes of the different rings makes it change, however, if it is a first reference to create combinations of rings for the subsequent tests. In case of BELEN-30 it can be seen in figures 3.12 the approximate distance of the maximum efficiency for the energy of 2 MeV appears at 17 cm from origin of neutrons. As seen in the figures refered before, the efficiency obtained for tube at 20 atm is only slightly higher than for the tube at 10 atm. This behavior of efficiency, discussed in chapter 2, is because of that we have to distribute the helium gas in tubes with lower pressure.

As in the case of BELEN-20B, with the data obtained in the previous step, we calculated a first approach of the efficiency of configurations with combinations of the the two types of tubes distributed in two rings. This efficiency has been calculated as the sum of the efficiency of a single tube obtained in the previous step. This analysis serves to detect in the parameter space (radius of the rings, number of tubes per ring, ring type) areas where we can find the best combinations of flat factor and mean efficiency saving us a large number of Monte Carlo simulations. When analyzing those configurations, for simplicity we have chosen some in which higher symmetries appear, for instance, tubes of the same type (at

the same pressure) are grouped together in one ring. The first ring have only tubes at less pressure. This was decided to compensate the higher efficiencies obtained at lower energies in the inner rings is better to put in it less tubes (and at less pressure) than in the outer rings.

The efficiency of the choosen configurations of last step are calculated by Monte Carlo simulations. Then a large number of simulations are performed with minor modifications (number or type of tubes and radius of rings) of those configurations. In some configurations, we observe that we can improve the result by rotating an initial angle the external ring respect its axis and we decide to analize the results of simulations adding this new parameter. We added a third ring and we did not significantly

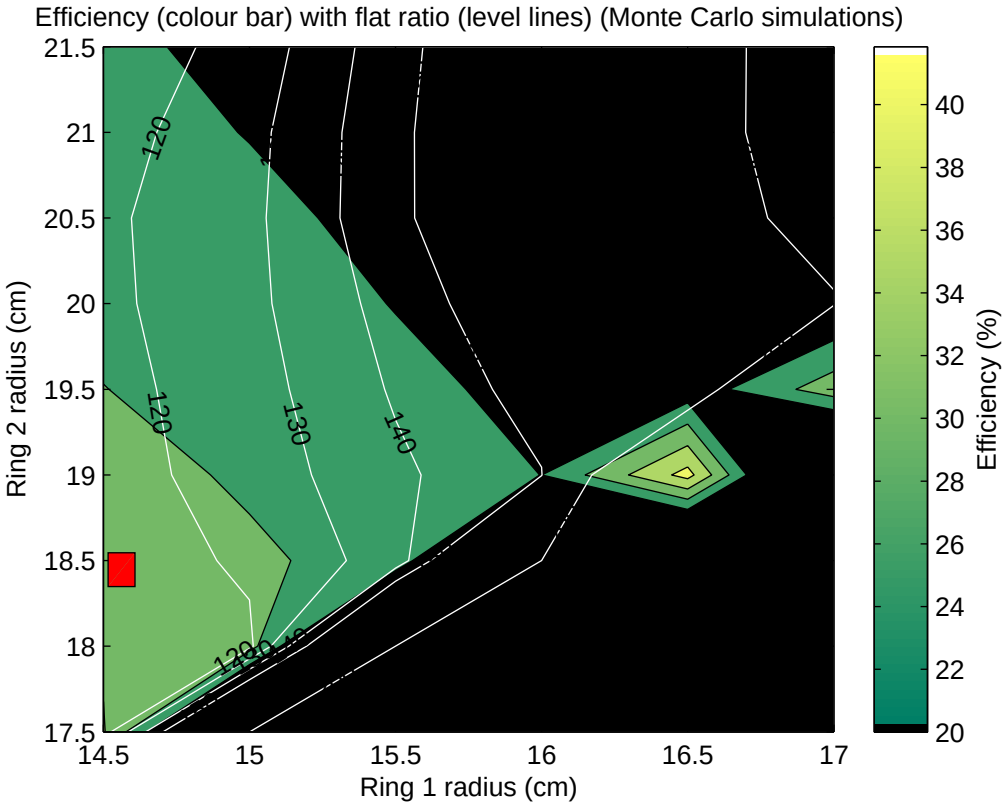

Figure 3.13: *Result of Monte Carlo efficiency and flat factor simulations for BELEN-30 with the better configuration along inner and outer radious since 2 MeV.*

improve the results in efficiency/flat factor. Finally we did a final selection of the best combination of flat and efficiency ratio and the simulations

are performed with a large number of neutrons so that the end result is confirmed with high accuracy as possible to choose the final configuration.

	inner ring (G1)	outer ring (G2)
Radius (mm)	145	185
Number of tubes^{3}He at 10 atm	10	0
Number of tubes ^{3}He at 20 atm	0	20

Table 3.6: *Positions and characteristics of groups of tubes for BELEN-30.*

BELEN-30	MCNPX		GEANT4	
	efficiency (%)	ratio	efficiency (%)	ratio
100eV-1MeV	40	1.10	41	1.10
100eV-2MeV	38	1.21	40	1.26

Table 3.7: *Efficiency and flat factor of BELEN-30 detector.*

The configuration choosen for BELEN detector consisted of 30 ^{3}He tubes distributed in two rings around the 23 cm diameter central hole. The best configuration found with those tubes available for maximum efficiency and up to 2 MeV flat factor was with an inner ring, with a radius of 14.5 cm with 10 tubes at a pressure of 10 atm and with an outer ring, with a radius of 18.5 cm formed by 20 tubes at 20 atm. Figure 3.15 shows the front view of the polyethylene matrix. Figure 3.14 illustrate the detection efficiency for this prototype, nearly constant below 2 MeV reaching 40%. In table 3.7 can be seen the results of mean efficiency and flat factor for different energy ranges obtained by MCNPX and GEANT4. Also, the experimental results for a ^{252}Cf calibration source, have been

BELEN-30	Efficiency			Inn/out ratio efficiency		
Isotope	Exp.	MCNPX	Geant4	Exp.	MCNPX	Geant4
^{252}Cf	0.351(8)	0.348	0.350	0.726	0.758	0.764

Table 3.8: *Experimental and simulation results for BELEN-30 with ^{252}Cf calibration source*

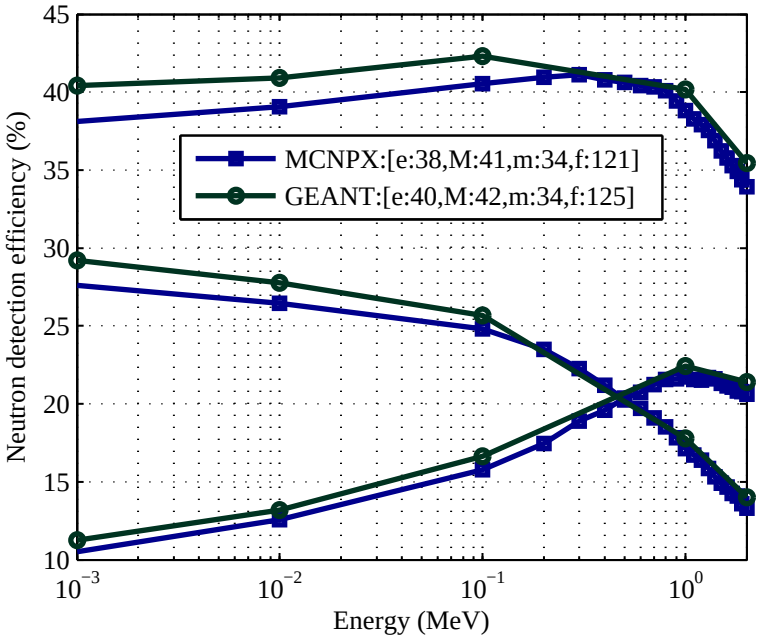

Figure 3.14: *Contribution of each ring to the neutron detection efficiency and total efficiency for the BELEN-30*

compared to the results obtained with MCNPX and Geant4 simulations (table 3.8) and are in fair agreement with the simulations.

3.5 BELEN-48

The BELEN-48 detector is the final prototype of BELEN detector included in TDR [16] documentation designed for FAIR as part of the DESPEC setup. The purpose of this detector is the measurement of neutron emission probabilities after β-decay. The BELEN-48 for DESPEC will be employed jointly with an implantation setup called AIDA [29] that will be placed inside the beam hole. Meanwhile two prototypes (BELEN-48M1 and BELEN-48 M2) was designed for experiments at JYFL in 2014. BELEN-48 M1 previously was calibrated at the PTB Braunschweig at June 2013.

DESPEC is conceived as a modular experiment where different setups can be coupled together in order to study different aspects of decay spectroscopy. The ions of interest will be implanted on an array of a Double Sided Silicon Strip Detector (DSSSD) called AIDA where their β-decay will be measured. This system will be surrounded by a compact high

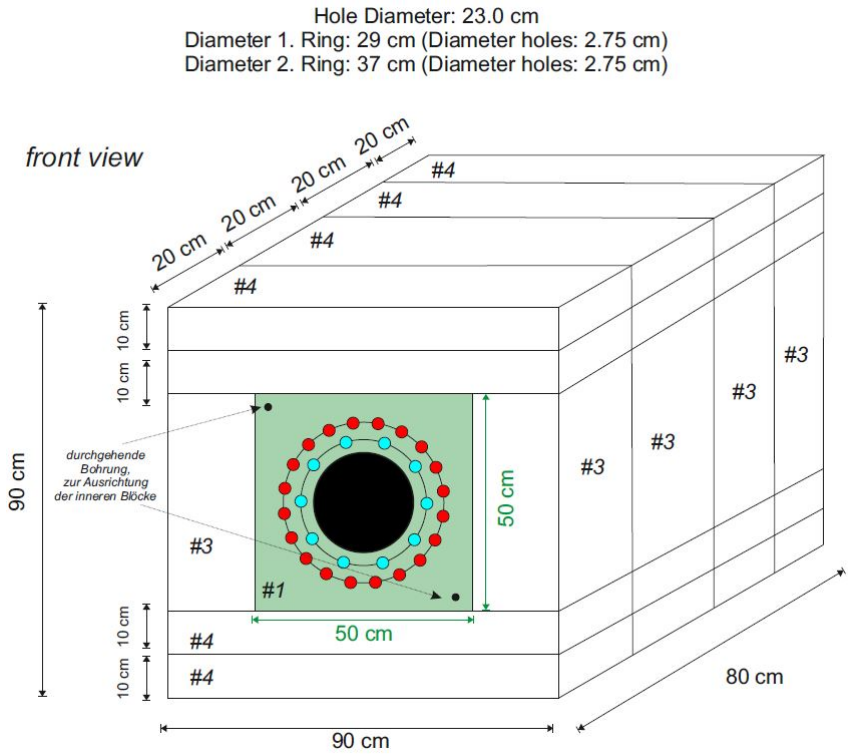

Figure 3.15: *Schematic diagram of Belen-30*

resolution HPGe array, by the neutron detectors, the fast BaF2 detectors and/or a total absorption gamma ray spectrometer. The design of the polyethylene moderator of the neutron detector matrix is adapted to this conditions with a central hole of 16 cm.

The experiment at JYL consist in the first measurement of 2-neutron β-delayed emission (β_{2n}) emitters with the BELEN detector and thus an important test for future measurements of more neutron-rich isotopes at RIKEN and FAIR. This experiment is part of a Coordinated Research Project (CRP) for a "Reference Database for Beta-Delayed Neutron Emission" from International Atomic Energy Agency (IAEA) . The aim of this project is a careful evaluation of the existing data of P_n-values and also a re-evaluation of important β-neutron emitters, half-lives, and a careful investigation of β_{1n}+β_{2n} cases. Those new measurements could be done at the new generation of radioactive-beam facilities which are able to produce neutron-rich isotopes. The beam will be implanted onto a movable tape in vacuum at the center of the detector. In this way counting losses

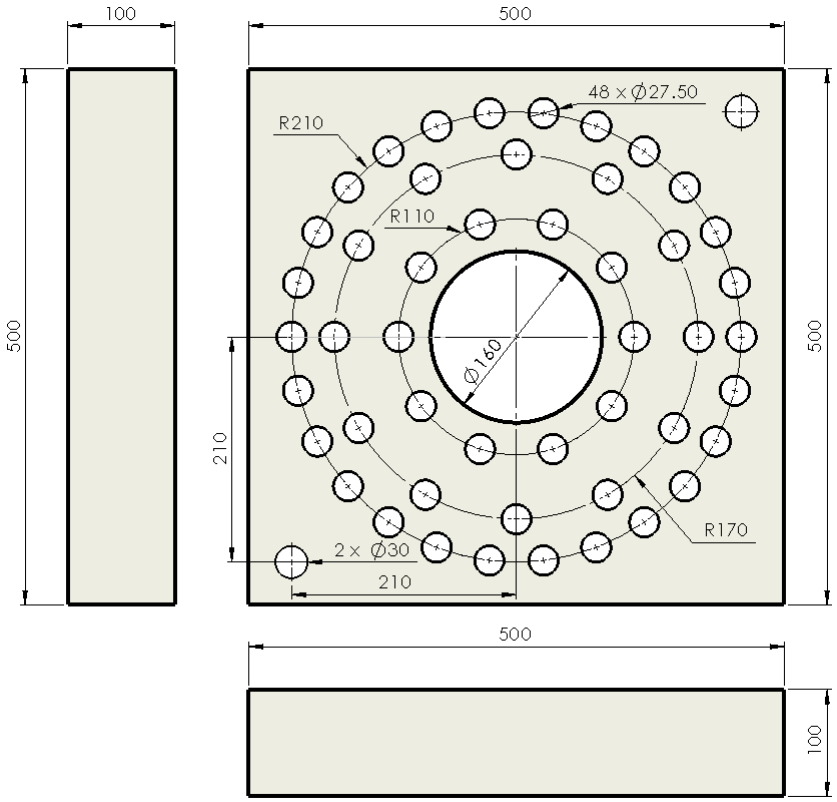

Figure 3.16: *Front view of a single block of B48-AIDA.*

due to the short half-lives are minimized. The beam tube contains a collimation system to ensure proper implantation on the tape. Closely behind the tape (also in vacuum) a Si detector (25.2 mm x 0.9 mm) acting as β-tube with an efficiency of about 25%.

3.5.1 BELEN-48 detector

The detector BELEN-48 consists on 48 high-pressure ^{3}He proportional tubes from GSI and UPC as can be seen in table 3.9 embedded in a polyethylene matrix which acts as a neutron moderator. Additional polyethylene shielding (20 cm thick) will be added on the lateral sides of the matrix in order to reduce the level of detected neutron background signals to about 1 n/s.

The polyethylene (high density 0.95 g/cm^3) matrix is composed of 8 slices or blocks of 10 cm thickness that are assembled together to conform the central block with dimensions 50 x 50 x 80 cm^3. Except the first block

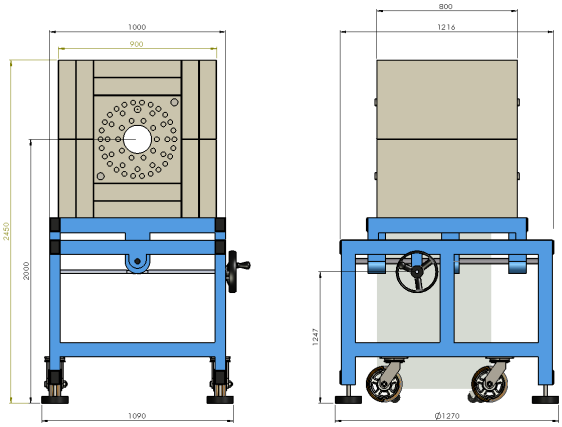

Figure 3.17: *Front and side views of the BELEN support structure.*

Owner	P (atm)	Diam.(inch/cm)	Eff Length(inch/cm)	#tubes
GSI	10	1/2.54	23.62/60	10
UPC	8	1/2.54	23.62/60	42

Table 3.9: *Tubes available for the Belen-48*

(A), that has only the beam hole, the next 6 blocks (B) are pierced also with the holes for the tubes. The rear block (block C), is pierced like a block B but the tube holes are threaded to screw caps. The caps are used to fix the tubes inside the holes. The blocks are held together by two stainless steel bars. A technical drawing of a block B of BELEN-48AIDA detector is presented in figure 3.16. The shielding consists of different polyethylene blocks adding 20 cm more of polyethylene thickness per side to the matrix. Hence, the total dimensions of the polyethylene structure are 90 x 90 x 80 cm^3.

A mechanical test has been done at the UPC workshop to find the minimum distance between the tube holes in order to prevent possible problems during the manufacturing of the polyethylene matrix. Although the drilling tool of GSI could be different to that of UPC, a minimum thickness between tubes of 3 mm has been set to avoid mechanical failures of the polyethylene matrix. This aspect is considered as a constraint to be taken into account to define the distribution of tubes in the matrix.

A supporting structure for the polyethylene block is going to be designed and constructed at the workshop of the UPC. This structure will be adapted to the final design of BELEN-48 , the facility and the implan-

tation detector. During the GSI experiment in 2011 at the FRS, such a structure was not required since the full detector setup was placed on the existing FRS rail structure and only slightly adjusted to the beamline center of 198 cm. However, a possible structure is described below. It consists of a mobile table with a sliding tray to place the detector on. This sliding tray can be moved through a stirring wheel connected to a worm gear system that allows moving the detector precisely in order to center the detector respectively to the beam implantation spot. A technical draw of the possible support structure is presented in figure 3.17 with its main dimensions.

3.5.2 BELEN-48AIDA, BELEN-48M1, BELEN48M2 configuration design

Three prototypes of BELEN-48 have been designed to obtain flat response (flat factor near 1) and good efficiency for the range of energy up to 2 MeV (but also with analysis up to 5MeV)

1. BELEN-48AIDA neutron detector will be used jointly with AIDA placed inside the beam hole radius of 8 cm
2. BELEN-48M1: Matrix 1 (M1) with a beam hole of radius 5.5 cm
3. BELEN48M2: Matrix 2 (M2) with a beam hole of radius 3 cm

To design the three prototypes of BELEN-48 we followed a similar methodology that used in BELEN-20B and BELEN-30 but in this case due to the large number of tubes it was necessary to fix some conditions to facilitate searching of best configuration. First is calculated a estimation of the efficiency expected for the three cases and then we do a lot simulations with the three central hole of 16/22/6 cm with a single tube of the two types at different distances from the origin of neutrons to find the shape of efficiency along the range of energy up to 5 MeV.

As an exemple, it can be seen in Figure 3.18 for the energy of 5 MeV the distance of the tube from the origin of neutrons where we obtained the maximum relative efficiency for this energy is 21 cm for BELEN-48AIDA, the situation is similar for the other two prototypes. In a first approach, to obtain a good flat factor we have to put a ring of tubes at a distance of 21 cm and another at 12-13 cm in order to compensate efficiency at different energies of the range. In the next step we defined some configurations with two rings and find an area of solutions with better combination of

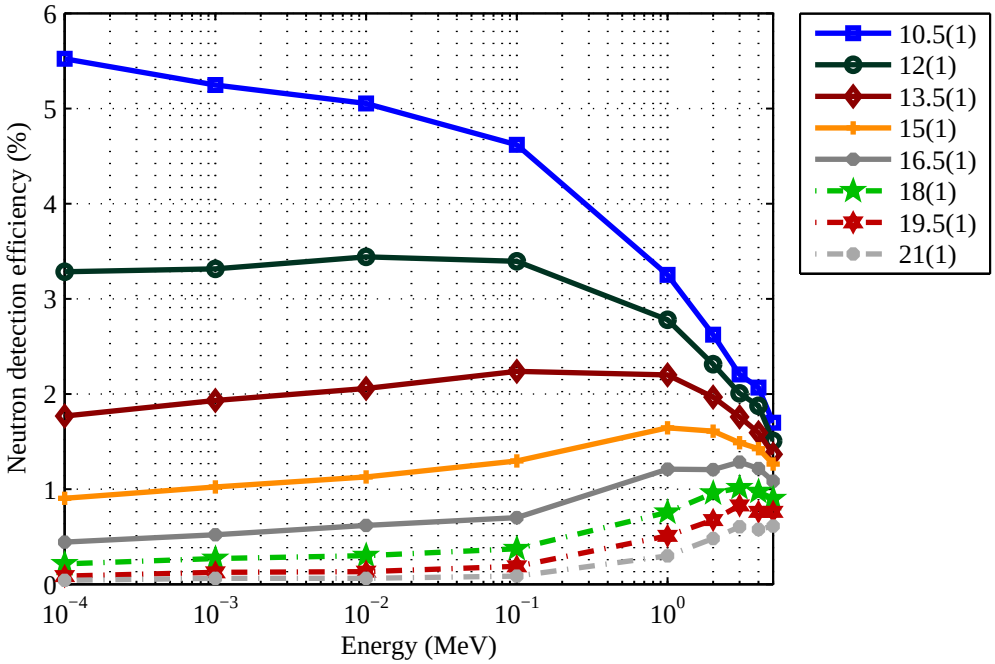

Figure 3.18: *Efficiency for a tube at 10 atm at distances of 10.5 cm to 21 cm in BELEN-48AIDA.*

flat factor and mean efficiency using an approach of efficiency as a sum of individual tube efficiency adding a term that fixes in part the interference between tubes. This approaches are explained in detail in the next chapter and it makes more important in this case than in the design of previous prototypes because the great number of tubes of each configuration. The parameters used were the two radiuos of the rings (2) and the number of tubes per ring (1). The type of the tubes is not considered in this first approach. We analyzed the results for two rings as in the previous prototypes, but we saw, due to the need to maintain planarity up to 2 MeV, that is necessary to use a third ring to obtain optimum results. We repeated whole process for three rings. As an example, in figure 3.19 it can be seen one area of parameters with a good combination of efficiency and flat ratio obtained fom an approach for BELEN48-AIDA. Finally we simulated all the areas of good parameters calculated in the previous step with Monte Carlo and obtained the configurations choosen for the three prototypes.

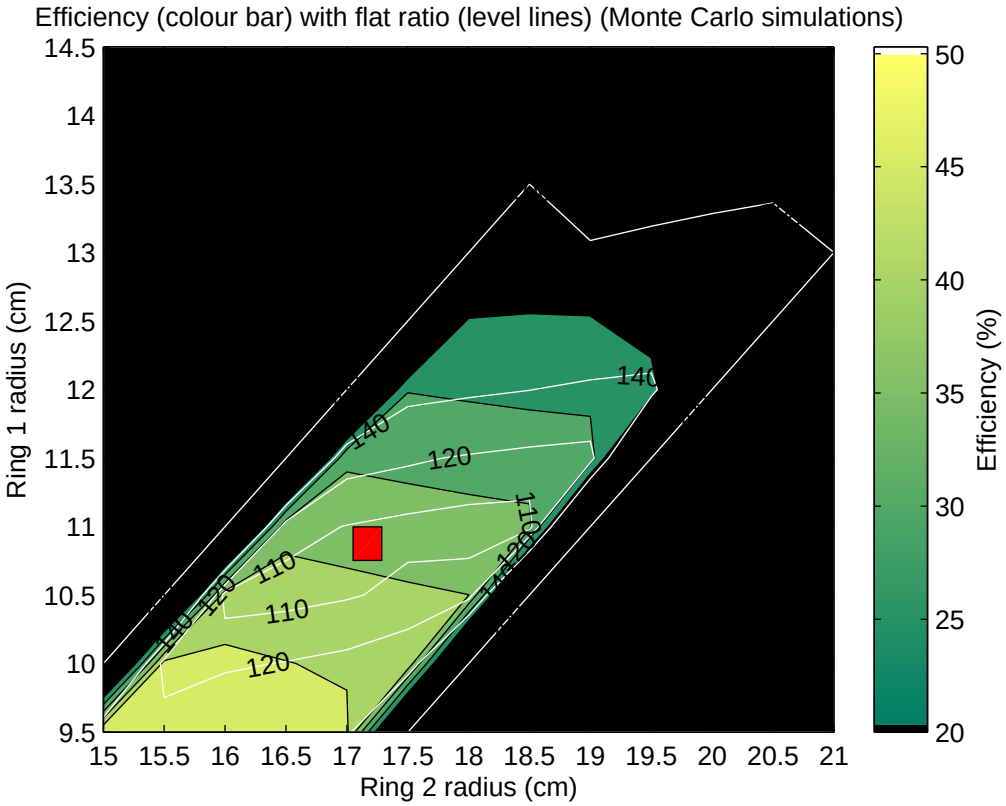

Figure 3.19: *Result of flat factor and efficiency of best configuration found along ring 1,ring 2 radius for BELEN-48AIDA.*

Configuration BELEN-48AIDA with a 16 cm diameter central hole

The final configuration found for the BELEN-48AIDA detector for this experiment can be seen in the table 3.10. A mean neutron detection efficiency of about 41% is obtained as can be seen in the efficiency figure 3.21. Also table 3.11 shows the results of mean efficiency and flat factor for different energy ranges, obtained with Monte Carlo simulation codes MCNPX and GEANT4.

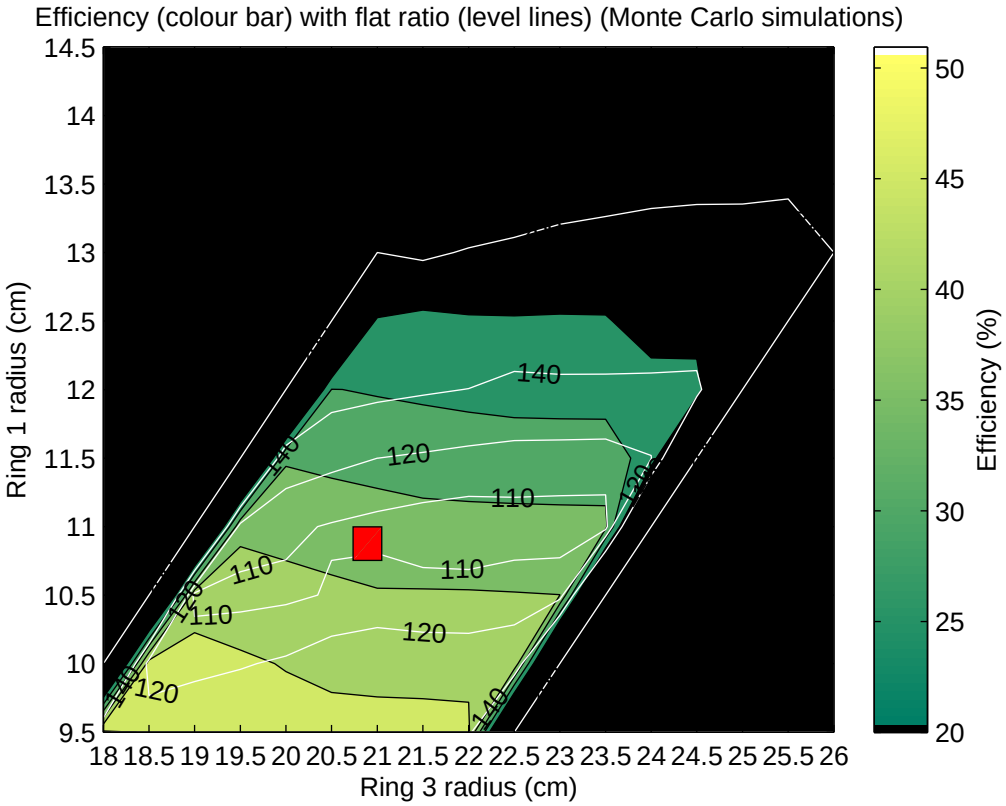

Figure 3.20: *Result of flat factor and efficiency of best configuration found along ring 1,ring 3 radious for BELEN-48AIDA.*

BELEN-48 AIDA/Rings	inner (G1)	central (G2)	outer (G3)
Radius (mm)	110	170	210
Number of ^{3}He tubes at 10 atm	0	8	0
Number of ^{3}He tubes at 8 atm	10	4	26

Table 3.10: *Positions and characteristics of groups of tubes for Belen-48 (FAIR)*

BELEN-48 AIDA	MCNPX		GEANT4	
	efficiency	flat factor	efficiency	flat factor
100 eV-1 MeV	44	1.02	47	1.07
100 eV-2 MeV	44	1.07	46	1.12
100 eV-5 MeV	41	1.30	44	1.37

Table 3.11: *Efficiency and flat factor of BELEN-48 detector*

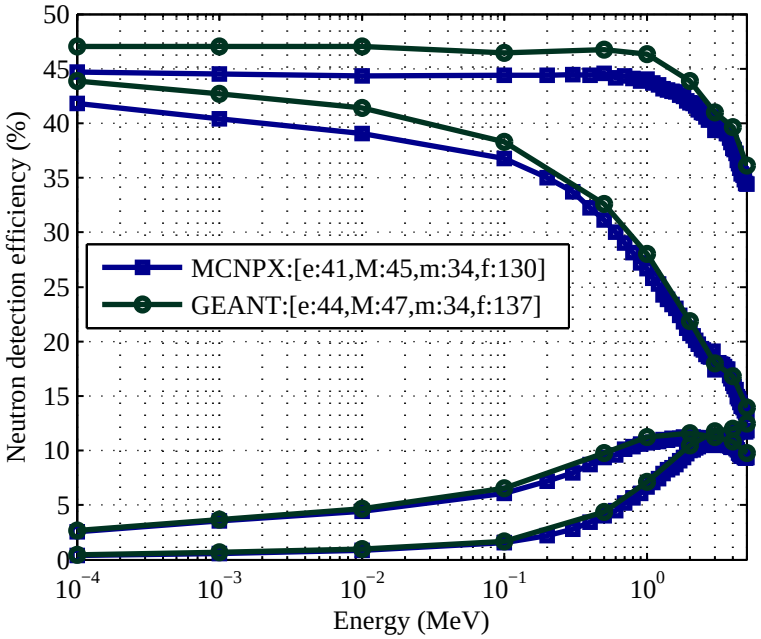

Figure 3.21: *Contribution of each ring to the neutron detection efficiency and total efficiency for the B-48AIDA detector*

Configuration M1 with a 22 cm diameter central hole

The design of the polyethylene matrix of the neutron detector to moderate the neutrons will be adapted to the conditions at the IGISOL facility with the HPGe gamma detector located at the center of BELEN-48 detector. The better configuration was obtained with the distribution of the tubes in three rings around the central hole. The average neutron detection efficiency is about 40% with small energy dependence that can be seen in the table 3.22 and figure 3.22.

BELEN-48 M1/ Rings	inner	centra	outer
Radius (mm)	85	155	195
Number of 3He at 10 atm	0	8	0
Number of 3He at 8 atm	6	4	30

Table 3.12: *Positions and characteristics of groups of tubes for Belen-48 (Matrix 1)*

BELEN48-M1	MCNPX		GEANT4	
	efficiency (%)	flat factor	efficiency (%)	flat factor
100eV-1MeV	38	1.05	40	1.07
100eV-2MeV	39	1.05	41	1.07
100eV-5MeV	38	1.15	39	1.19

Table 3.13: *Efficiency and flat factor of BELEN-48 Matrix 1 detector*

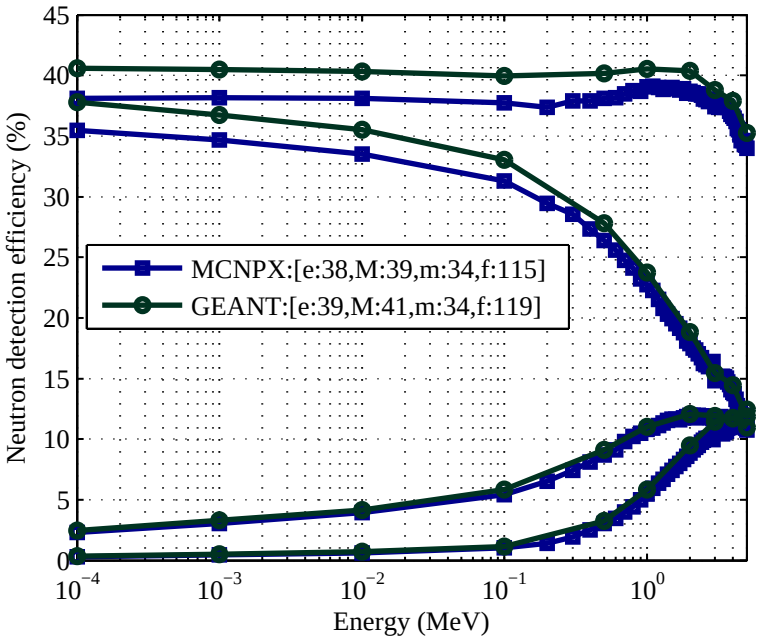

Figure 3.22: *Contribution of each ring to the neutron detection efficiency and total efficiency for the B-48M1 detector*

Configuration M2 with a 6cm diameter central hole

The configuration was obtained with the tubes distributed in three rings around the central hole as it can be seen in the table 3.14, maximizing the efficiency and optimizing flat factor for energy range from 100 eV to 2 MeV. The average neutron detection efficiency is about 60% with small energy dependence for this range, as can be seen in table 3.15 and figure 3.15 .

BELEN-48 M2/Rings	inner	central	outer
Radius (mm)	60	115	170
Number of ^{3}He tubes at 10 atm	0	8	0
Number of ^{3}He tubes at 8 atm	6	10	24

Table 3.14: *Positions and characteristics of groups of tubes for Belen-48 (Matrix 2)*

BELEN48-M2	MCNPX		GEANT4	
	efficiency (%)	flat factor	efficiency (%)	flat factor
100 eV-1 MeV	59	1.04	61	1.05
100 eV-2 MeV	59	1.06	61	1.10
100 eV-5 MeV	55	1.31	58	1.36

Table 3.15: *Efficiency and flat factor of BELEN-48 Matrix 2 detector*

3.6 BRIKEN

BRIKEN stands for β-delayed neutron emission measurements at RIKEN [31]. This detector called BRIKEN (Beta-delayed neutron measurements at RIKEN) [28] will consist of 174 ^{3}He tubes (from UPC+GSI+ORNL+RIKEN) embedded in a large, high-density, polyethylene matrix. This new experimental set-up aims for experimental campaigns to measure β-delayed multiple neutron emission properties of a large amount of very neutron-rich nuclei at the RIKEN Nishina Center. Such wealth of new information

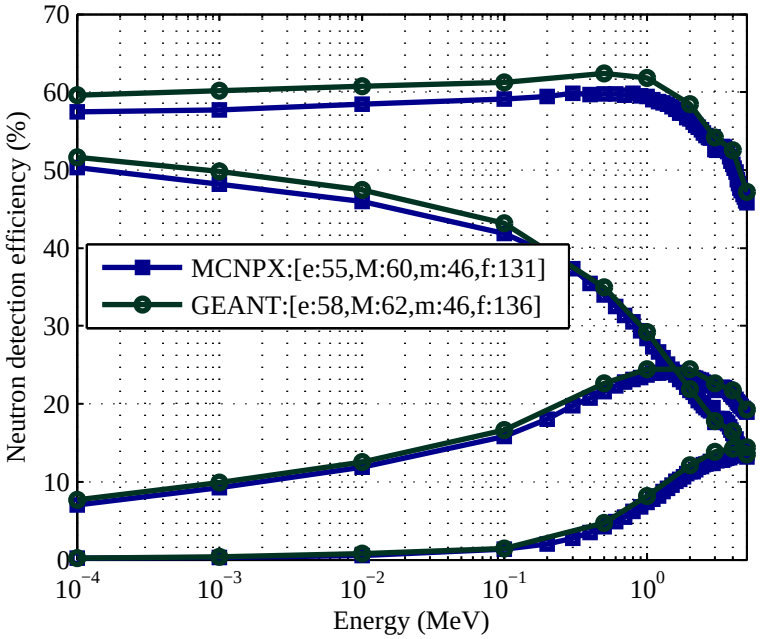

Figure 3.23: *Contribution of each ring to the neutron detection efficiency and total efficiency for the B-48M2 detector*

is expected to enhance greatly the understanding of β-strength distribution for neutron-rich nuclei, and provide an essential piece of information for r-process model calculations.

Owner	P(atm)	Diam(inch/cm)	Eff Length(inch/mm)	#tubes
GSI	10	1/2.54	23.62/600	10
JINR	4	1.18/3.0	19.69/500	20
ORNL	10	2/5.08	24/609.6	67
ORNL	10	1/2.54	24/609.6	17
RIKEN	5.13	1/2.54	118.1/300	26
UPC	8	1/2.54	23.62/600	42

Table 3.16: *Tubes available within the BRIKEN collaboration*

3.6.1 BRIKEN detector

The detector is composed of an array of cylindrical proportional tubes filled with ^{3}He gas, embedded in a high-density polyethylene matrix to moderate the neutron energies. A total 174 ^{3}He tubes of six different types are available for the BRIKEN neutron detector. They are listed in Table 3.16. Owing to the very large number of ^{3}He tubes available, it becomes possible to achieve a flat detection efficiency over a broad initial neutron energy range. The HDPE-moderator matrix has a square hole of 11 $\times$11 cm^2 size and an external size of 110$\times$110$\times$90 cm^3. Mechanically, the most challenging aspect concerns the drilling of holes, which in some cases are as close as at 5 mm distance, between them. In order to achieve a configuration which is mechanically stable, a design based on 100 mm thick polyethylene plates has been made.

The optimization of a system which combines such large number and types of tubes represents a rather complex task, it has been done by means of systematic Monte Carlo (MC) simulations.

3.6.2 BRIKEN configuration design

The high number of counters (174) and the different types of these counters (6) did us to use a different strategy for detector design than in the other prototypes. Initially, we simulated configurations with only one tube of all diferent types at some distances from the source of neutrons. With these simulations, we obtained the distances in which the relative efficiency (with respect to the other initial energies of neutrons) for different energies is maximized. Later, we simulated some configurations defined to obtain an estimation of the maximum efficiency at different energies regardless of the flat factor.

Then we focused to get a configuration with the maximum relative efficiency for maximum energy spectrum (5 MeV). To do this, we try to put the maximum possible space ocuped by detector material, choosing the ORNL tubes because they have 2 inches diameter and there are many of them, on the distance at which the efficiency at 5 MeV, over 17 cm as it can seen in figure 3.24 is maximized respect the other energies. Due to the large number of tubes, to get even better relative efficiency we decided to do some simulations to define a configuration that distribute these tubes in two rings around these optimal distance.

Once optimized this result, we focus on adding tubes in inner rings to adjust flat factor. In all the rings we try to keep some symmetry in the configuration putting tubes of the same type in the rings or at least

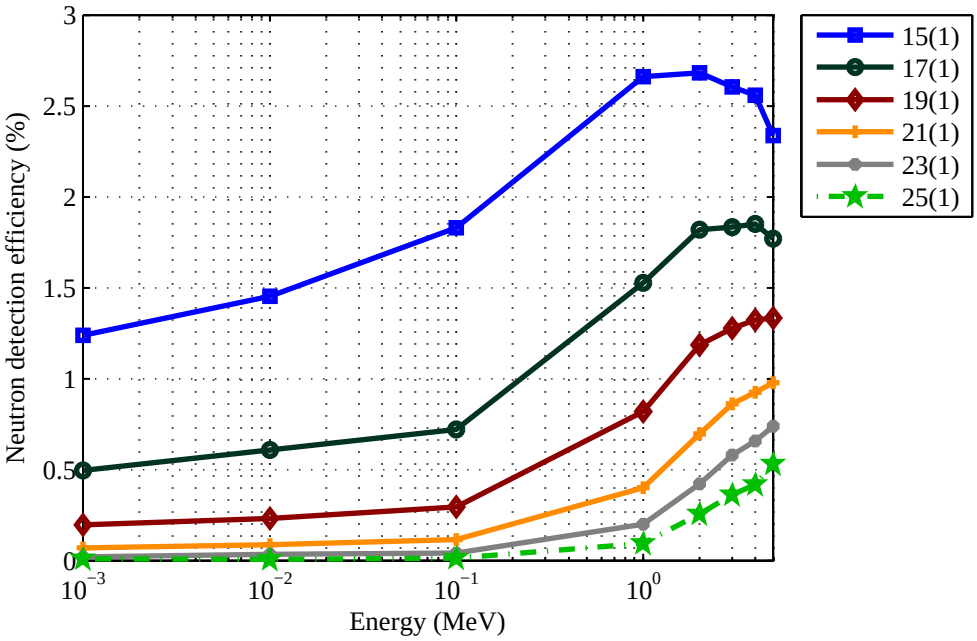

Figure 3.24: *Efficiency for one ORNL 2" tube distributed at different radius (15 cm to 25 cm with 2.0 cm intervals) to the center of the block of polyethylene for the range of energies below 5 MeV*

with a geometrical distribution as regularly as possible. This decision is arbitrary but simplifies the treatment of the problem and final solution can overcome this choice if there is some near configuration that optimize the result.

After the outer tubes distributed, we proceed to distribute the more inner tubes. Initially we placed those with less efficiency (JINR with 5 atm) in a first inner ring taking advantage of the square hole and a second ring as near as possible of hole with the ORNL tubes at 4 atm. We choose the tubes with small efficiency because one tube at a small distance of the origin of neutron, add high relative efficiency at low energies and this is difficult to compensate with the remaining tubes. From here another intermediate ring with UPC tubes are defined, we choose this type of tube because its efficiency is not very different from ORNL and GSI tubes. As it can be see in figure 3.25 the process to add a new ring implies a new optimization of the parameters of the other rings. These parameters, indicated in the axis x in the figure, correspond to the radius of the rings and the number of tubes per ring. These kind of figures serve to identify where are the best combinations of parameters and the expected range of

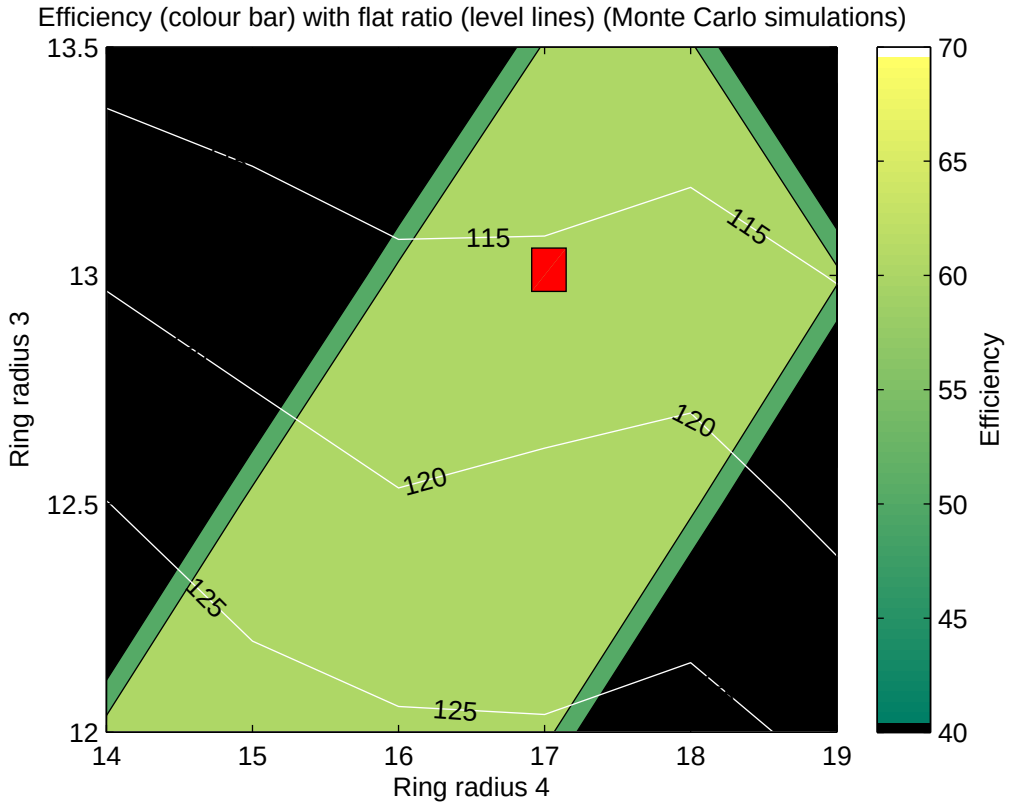

Figure 3.25: *Plot analysis of the result of simulations with radius of the ring 3 versus 4 with all the other parameters implicit. The red rectangle is located in the area of the proposed configuration*

the best result. We search an intermediate distance of the ring to the flat factor for energies of the middle of the range. As in the previous step, due to the large number of tubes we split into two intermediate rings that were complemented by ORNL and GSI tubes. This same procedure was again performed to add the JINR tubes and the RIKEN tubes.

The whole process needs to test again the radius of all the rings to ensure that the efficiency results remains the most optimal. For example, in the case of external rings, an initial distance obtained in the first optimization of the two rings at 17 cm and 22.5 cm, was changed to a final distance of 27 and 35 cm for the proposed configuration with seven rings because the effective distance traveled by the average neutrons in polyethylene is clearly less than the radius obtained without inner rings. In table 3.18 it can be seen the results of mean efficiency and flat fac-

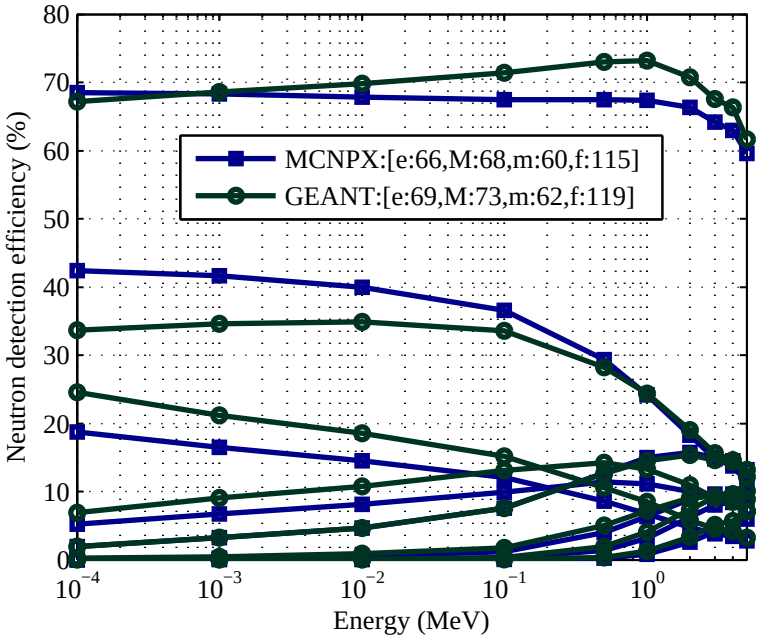

Figure 3.26: *Contribution of each ring to the neutron detection efficiency and total efficiency for the BRIKEN detector*

tor of the final proposed configuration for different energy ranges. The number of tubes, the number and radius of rings, the type of tubes in each ring, and the spacing between tubes and rings has been designed to achieve the best compromise between high and flat efficiency, while keeping a relatively large efficiency for high neutron-energies of 5 MeV. This configuration shows a good efficiency ratio of 1.15 for the range of neutron energies from 100 eV to 5 MeV, and an average neutron detection efficiency of 66%. These configuration comprises a total of 174 ^{3}He tubes arranged in six rings. Its key parameters are reported in Table 3.17 and a plot with the total efficiency for all range of neutron energies and for each ring can be seen in figure 3.26. As discussed before, multiple neutron emission represents one of the main scientific topics within the BRIKEN project. In this way, and owing to the very large detection efficiency and segmentation of the BRIKEN setup, the probability for two-neutron detection becomes also quite large, over 40%. This is shown in 3.28 where the two and three neutron detection efficiency is shown as a function of three neutron energy. In this case, as the available decay energy is shared between two neutrons, one can have confidence that those energies will be relatively small, thus being the low energy part of the

Ring	Radius(cm)	#Tubes	Pressure(atm)	Institute
1	7.8	4	5	JINR
2	9.8	16	4	ORNL
3	13	24+2+2	5.13/10/8	RIKEN/GSI/UPC
4	17	8+16	10/8	GSI/UPC
5	21.5	12+24	8/4	UPC/JINR
6	27	26	10	ORNL
7	35	38	10	ORNL

Table 3.17: *Configuration of the BRIKEN neutron detector*

efficiency curve more relevant. Based on measurements performed at the F11 area of RIBF, the neutron background is not expected to cause problems for counting ion and beta correlated neutron events. However, there are several neutron shielding elements available. There are also several plates made out of 1 inch thick HDPE and 1 mm Cd layer from ORNL and two sheets 2×1 m of borated rubber (41% boron) from GSI. They will serve as an efficient passive shielding of BRIKEN.

energy range	1n				2n			
	MCNPX		GEANT4		MCNPX		GEANT4	
	eff (%)	flat	eff (%)	flat	eff (%)	flat	eff (%)	flat
100 eV-1 MeV	68	1.02	71	1.09	46	1.03	50	1.19
100 eV-2 MeV	68	1.03	71	1.09	46	1.06	50	1.19
100 eV-5 MeV	66	1.15	69	1.19	44	1.32	48	1.41

Table 3.18: *Efficiency (eff) and flat factor of BRIKEN detector*

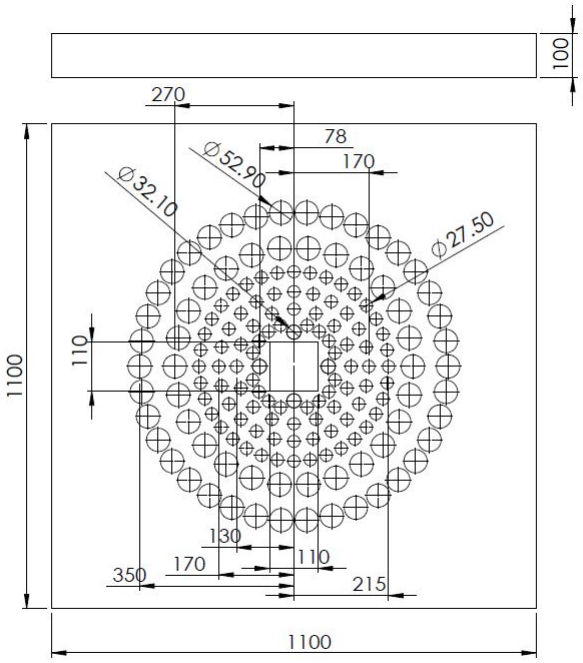

Figure 3.27: *BRIKEN frontal view (units mm)*

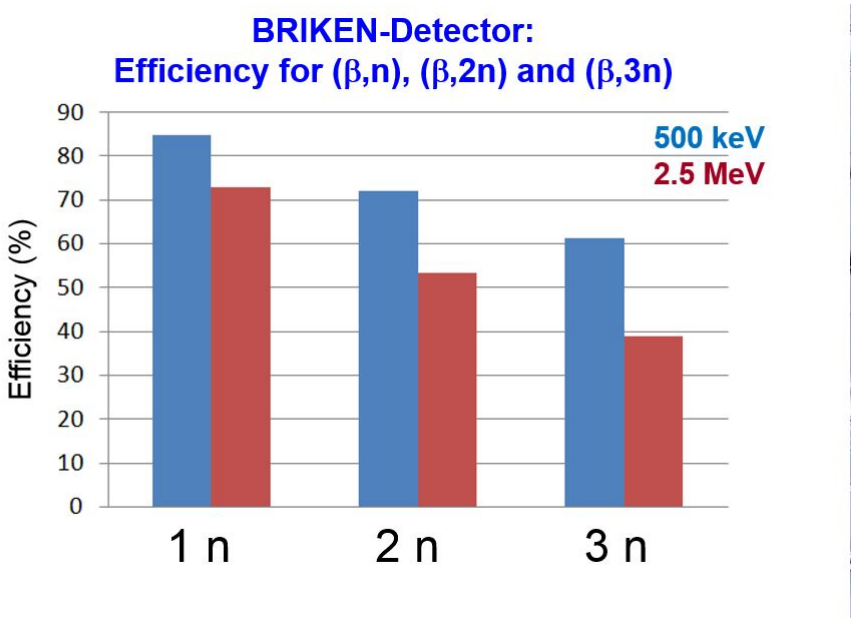

Figure 3.28: *BRIKEN detector mean efficiency for 1 neutron, 2 neutron and 3 neutron*

Chapter 4
Systematization algorithm for BELEN detector configuration design

4.1 Introduction

As seen in the previous chapter, a large simulation process has led to the final decision on the choose of the final configuration. The aim of these Monte Carlo simulations is to achieve the maximum neutron detection efficiency for BELEN detector keeping a flat response efficiency along the neutron energy range. In order to decrease the number of required simulations, has been studied some strategies to find the optimal solution. These strategies, different for each design, have been implemented in a computer code that helps in the search for the optimal configuration. To improve the time response of this code, we have also studied some alternatives to extrapolate efficiency of some complex configurations through the efficiency obtained in more basic configurations.

4.2 Systematization algorithm

The main objective is to minimize the number of Monte Carlo simulations needed to extrapolate the better configuration, but if is possible, we also try to establish a methodology to ensure that the results are close to optimal. To do this, we divide the problem of finding the best configuration in a sequence of subproblems to solve partial objectives. We define this partial objectives through a merit figure and some bonds. The bonds can fix a number maximum of rings, a maxim number of tubes per ring and an even number of tubes per ring. The merit figure have defined weigths for the following parameters:

- Flat factor close to 1.
- Increase mean efficiency
- Increase a ratio of efficiency between a defined energy and mean efficiency.

So the strategy is to define a sequence of subproblems by a figure of merit with an assigned group of tubes. For instance, with the BELEN-20 prototype we can define an easy strategy on two subproblems. The first one assign 10 tubes to improve the mean efficiency and the other 10 tubes in a second subproblem to get a flat factor close to 1. The strategy obviously is finally to use all available tubes. The order in which these subproblems are solved is very important, is not the same to improve the mean efficiency and later the flat factor than the other way around. It is also important to define which are the tubes that we designate to solve each of these subproblems. Following previous studies can be interesting to assign the tubes with less or more efficiency to get some of the objectives. It is also possible to define a fixed initial configuration and then add the rest of the tubes to the final configuration with some strategy.

To solve the subproblems, we have implemented a computer code module named OPT (Optimization module). OPT is a part of an analysis engine that is a set of modules that serves to run Monte Carlo simulation script, plot the efficiency results and do some other analysis. OPT performs the task of searching the best configuration based on the parameters passed to it , as shown in Figure 4.1. The parameters of the OPT module are:

- Initial configuration.
- The approach used to calculate the *efficiency*
- Figure of merit

The module OPT finds, from a given initial configuration and adding a number of tubes passed as a parameter, the best configuration based on a figure of merit. Initially is defined a set of positions available for the tubes in the polyethylene matrix. Given a configuration, OPT adds at each step a tube to this configuration at the position where is obtained the best value of the figure of merit. OPT does not develop a technique in the global solution space, since it is not based on a configuration that progresses according to an evolution of all possible configurations. Instead, it is a method based on local search path, since each iteration maintain one candidate solution to the problem (analogous to the state of a physical system). The method has a merit associated function (similar to an energy function of the system) for which it is intended to find the local minimum (analogous to the more stable state of the system). The search space is scanned by a transition operator (*efficiency* of the new configuration), which is incorporated in the objective function of the problem.

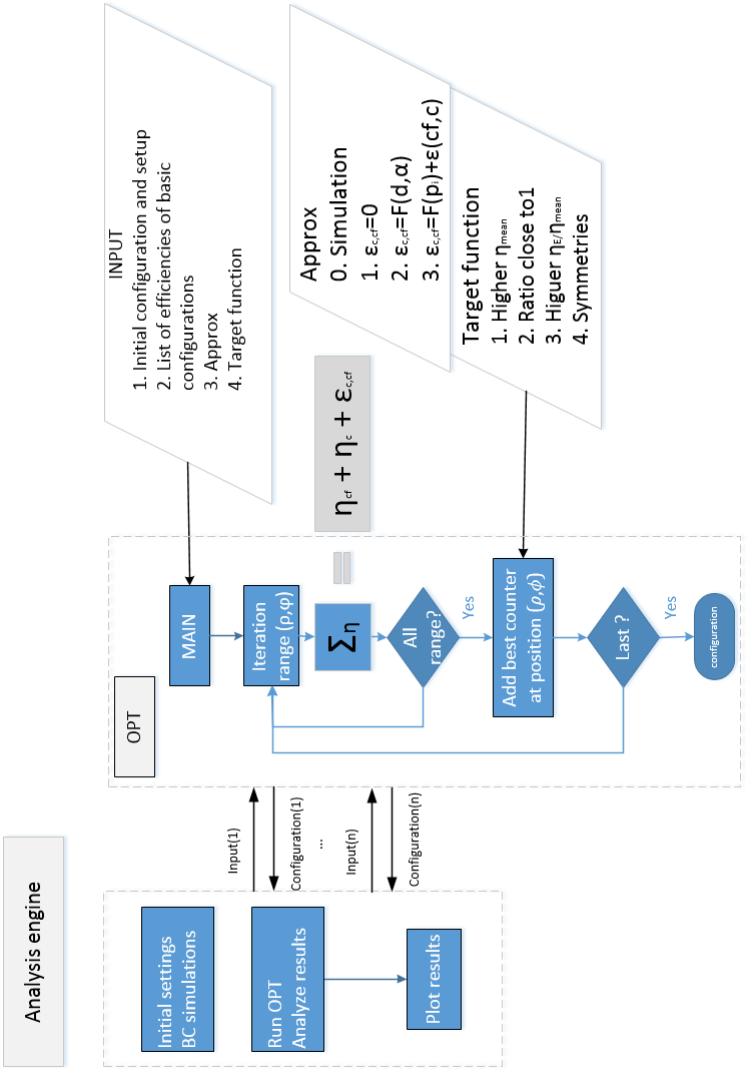

Figure 4.1: *Operating diagram of the application of analysis*

Note that the method developed could obtain a better combination of parameters for a configuration that doesn't employ all available tubes. Therefore, the method is based on a significant part in the goodness of the choice of the initial configuration and parameters that define the figure of merit. The efficiency for each new configuration defined can be calculated directly with Monte Carlo simulation or by an approach.

The algorithm makes calls with different parameters to the module OPT for each design. In section 4.4 we show some results of its use to find the optimal configuration of some of the BELEN prototypes. The module OPT used in that section calculates the efficiencies of the new configurations making use of some approaches described in the following section.

4.3 Approach of configuration efficiency

The main point is find a relation based on some geometrical parameters that gives the efficiency of a configuration as a function of the efficiency of the isolated tubes that form part of that configuration. In general, we can define that from two configurations, α and β with neutron detector efficiencies η_α and η_β respectively, the *efficiency sum* of those configurations $\eta_{\alpha+\beta}$ as the efficiency obtained in a configuration that contains all tubes of each of the configurations. We can write the equation for efficiency sum as:

$$\eta_{\alpha+\beta} = \eta_\alpha + \eta_{\beta'} + \epsilon_{\alpha\beta} \tag{4.1}$$

where $\epsilon_{\alpha,\beta}$ is a measure of the "interference" that occurs due to the presence of the tubes both with configurations together. For the OPT case, the configuration β always contain only one tube.

In the following sections we study the way to find some patterns that help us to define these generic variables and associated functions. In order to estimate the interference value, it has been used some initial simulation parameters. The calculation of the interference between tubes depend on two main factors :

- **Reduction of the number of moderated neutrons**: The presence of tubes reduces the amount of polyethylene and therefore reduces the capacity of the matrix to moderate neutrons.
- **Intersection captures**: Neutrons captured by a tube can not be

captured by another tube, therefore there is an efficiency loss due to the presence of the other tubes.

Based on these two concepts, the main idea is to obtain a model of the efficiency interference to approximate the efficiency of the new configuration. The goal is to estimate the *interference efficiency* as a function of some natural variables (distance, angles, ..) and find parameterized functions that model the behavior of the efficiency with respect to these variables. The geometrical variables involved are defined as the cilindrical coordinates with origin of the axis at the center of polyethylene matrix, with the axial coordinate z parallel to the axis of the tubes and whereρ is the distance from any point to the origin and φ is the angle to the x coordinate. To reference the positions of varios tubes, we define the variables, ρ_{ij} and φ_{ij} as the distance and angle between i and j tubes respectively as can be seen in the figure 4.2

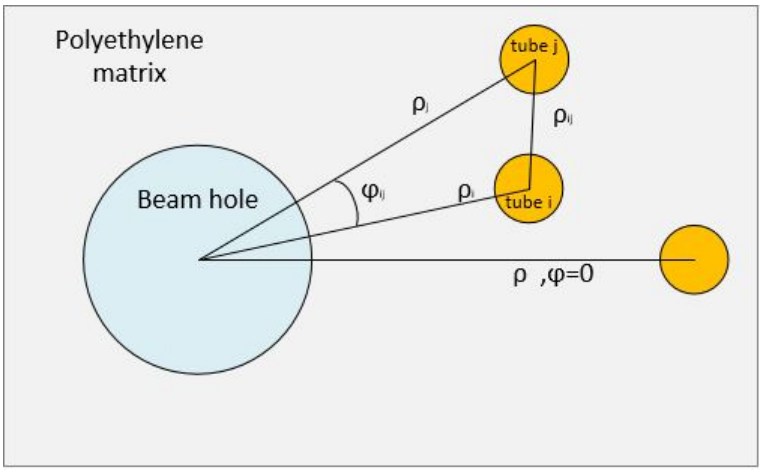

Figure 4.2: *Geometric parameters to characterizate the position of tubes in the polyethylene matrix*

To characterize the *interference efficiency*, two variables are used, the *thermal flux ratio* to get a qualitative idea of thermal neutrons distribution in the polyethylene matrix and *efficiency ratio* which gives a value of the ratio between a tube efficiency when is part of a configuration with more tubes in polyethylene matrix, respect to the efficiency of that same tube at the same location but without any other tube in the matrix.

Efficiency ratio of tubes

We need to define a variable that shows the change of efficiency between a tube as a part of a configuration with more tubes in the polyethylene matrix respect to the isolated tube in the same position of the matrix. Therefore the efficiency ratio for neutron initial energy E , k_E is defined as:

$$k_E = \frac{\eta^E}{\eta_0^E} \tag{4.2}$$

where η^E is the tube efficiency in the configuration and η_0^E is the tube efficiency in the same position without any other tube in the polyethylene matrix. This ratio will serve to assess the interference that occurs in relation to the other tubes of the configuration studied.
The reduction of efficiency for a tube in a configuration a with n tubes, is given as an approximation by the equation:

$$k_E^j = \prod_{i \neq j \, \epsilon \, \alpha}^{n} k_E^i \tag{4.3}$$

where k_E^{ti} is the efficiency ratio for neutron initial energy E for the tube t by the presence of the tube i.

Thermal neutron flux ratio

The distribution of thermal neutron flux in the detector depends strongly on the initial energy of the neutrons as can be seen in figure 4.3. The plot shows the distribution of thermal neutrons in the polyethylene according to the distance to the central axis of the detector for three different initial neutron energies. To calculate the thermal neutron fluence respect to the variable ρ we sum all the contributions of the z coordinate and angle φ. It can be seen that, in all three cases, is similar to a plot of a diffusion process, in which the diffusion coefficient, as can be expected, is greater at higher energies.

In order to observe the difference between the thermal neutron flux in the presence of tubes, is defined the thermal neutron flux ratio, u^E, dividing the flux in the polyethylene matrix with the presence of tubes over the neutron flux withouth tubes.

$$u^E = \frac{\phi^E}{\phi_0^E} \tag{4.4}$$

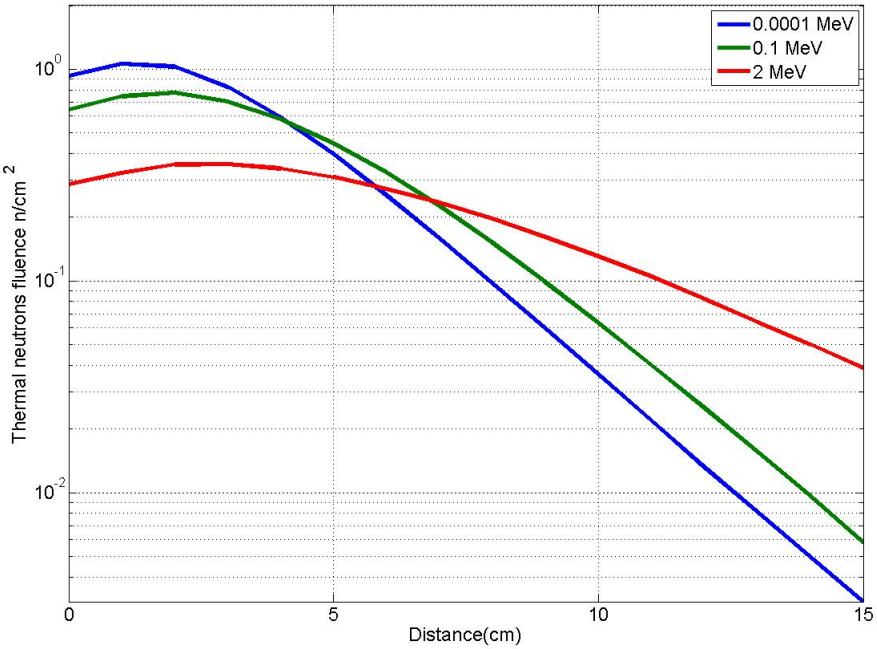

Figure 4.3: *Distribution of thermal neutron flux inside of a polyethylene matrix for three neutron energies as a function of distance from the origin of neutrons.*

where ϕ^E is the flux for neutron energy E for the configuration and ϕ_0^E the thermal neutron flux in the polyethylene matrix without any other tube in the polyethylene matrix.This ratio is used to measure the change of flux in the presence of tubes respect to the original flux and only have a qualitative use in this work to visualize the distribution of neutrons in the polyethylene.

Interference in efficiency between the same ring tubes

In order to develop a model of interference efficiency between tubes[1] , we start analyzing the simplest case for only two tubes. According to the hypotheses raised above, we study the case of intersection captures. To do this, we put the tubes at the same distance ($\rho = \rho_r$) from the origin of the neutrons forming a ring. Then, varying the angle between them

[1]Tubes used in all studies are He^3 at 20 atm with 60 cm length and diameter of 1 inch

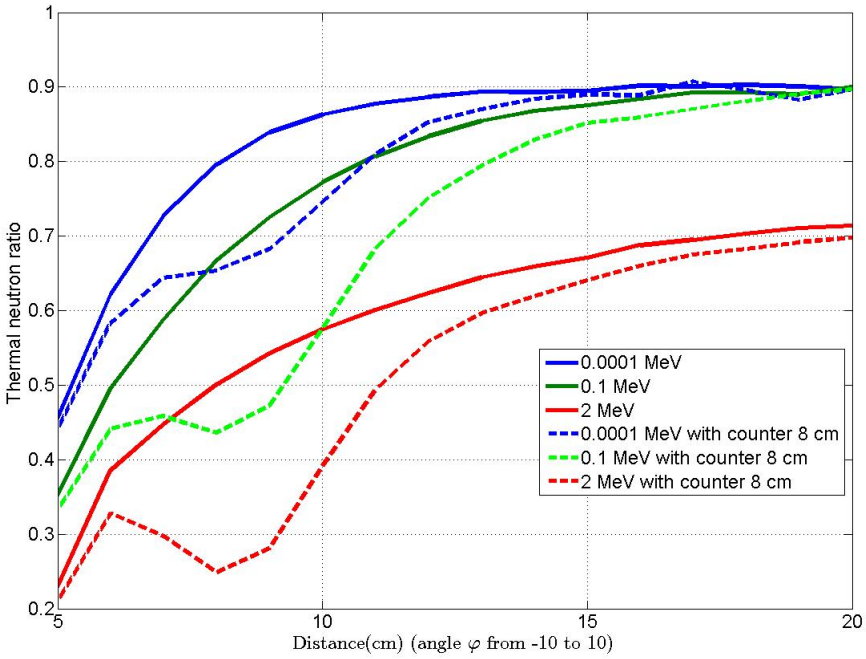

Figure 4.4: *Ratio between thermal neutron and all neutron flux with and without a tube at 8 cm from origin of neutrons flux for three differnt energies (0.0001 MeV, 0.1 MeV, 2 MeV)*

$\varphi_{12} = \varphi_1 - \varphi_2$ (distance between them is $\rho_{12} = \rho_r\sqrt{2(1 - cos(\varphi_{12}))}$), we mesure the efficiency ratio. As the tubes are at the same distance from the neutron origin, the efficiency when they are isolated is the same for each tube, and changes in efficiency ratio equally affects both tubes.

For the second case, we study the case where the tubes are located on the same path of neutrons coming from the source at different distances from the origin of neutrons. In this case, the efficiency ratio will be different for each tube and we establish some approximations in order to have a reasonable estimation of the interference. In all studies the tubes are embeded inside a polyethylene matrix, with a centered hole of 5 cm radius and conserving the symmetry with respect to the z coordinate of the distribution of neutrons.

In figure 4.5 it can be seen the efficiency ratio as a function of distance between two tubes (ρ_{12}) located at different distance from origin (ρ_r). Although there is a small dependence on radii of ring, from a certain angle between tubes, the ratio is almost 1 as could be expected (no

interference), but still having slight variations in part due to the neutrons passing through the hole in the center of the matrix of polyethylene[2]. On the behavior of ratio we can assume, with no big mistake, that the ratio tends to 1 at large distances and calculate the fit to a function of type:

$$r_\eta = a(1 - e^{-b\rho_{12}}) \tag{4.5}$$

that allows to find a and b as parameters to approximate the dependence of the sum of efficiency according to the radius of the ring and the distance between the ring tubes. We decided to keep the formula as a function of the distance between the tubes and not the angular distance in order to allow a more general formula not only applicable to the rings, the dependence is practically the same for the two variables, and although it loses sense for rings with small radius, the formula works well enough.

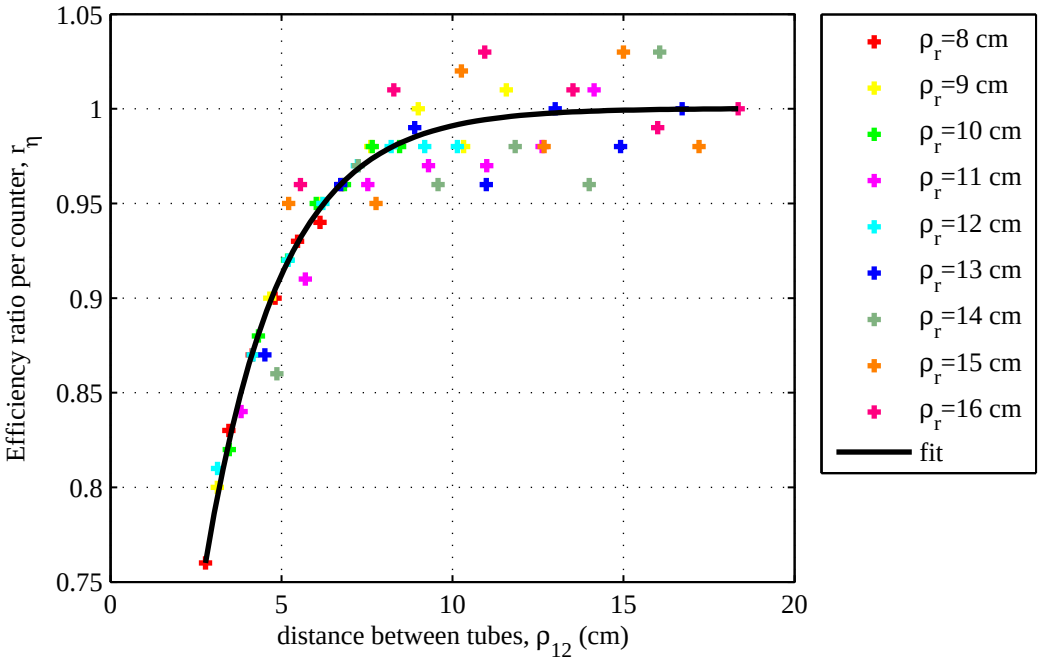

Figure 4.5: *CANVI Efficiency ratio at different rings ($\rho = 8..16$) between two tubes at different distance ρ_{12}*

In order to generalize the calculation with more tubes, we establish a way of adding new tubes to a ring, suposing that all tubes are distributed at the same angular distance (isotropically distributed in a ring). If there

[2]Polyethylene used in all studies are HDPE with density 0.93 g/cm^3

are two tubes, the angular separation between them will be 180 degrees, if there are 3 of them, angular separation will be 120 degrees and so on. To obtain the ratio efficiency of one tube, we have to apply the equation 4.5 for each pair of tubes at one ring and multiply among them.

Following this distribution of tubes in the ring, considering equation 4.3, it's easy to get a general equation that gives the efficiency of all ring for an energy E as 4.6:

$$\eta^n = \frac{n\, k^2_{\alpha\ldots} k^{2^s}_{m\alpha}}{k_0^{n-1}} \quad with\ n > 2 \tag{4.6}$$

where n is the number of tubes in the ring, $k_\alpha$is the efficiency ratio for one tube in presence of another tube at an angular distance of $\alpha = \frac{360}{n}$ (angular distance between tubes) and m corresponds to the module of the division $m = N\, mod\, 2$ and s the remainder.

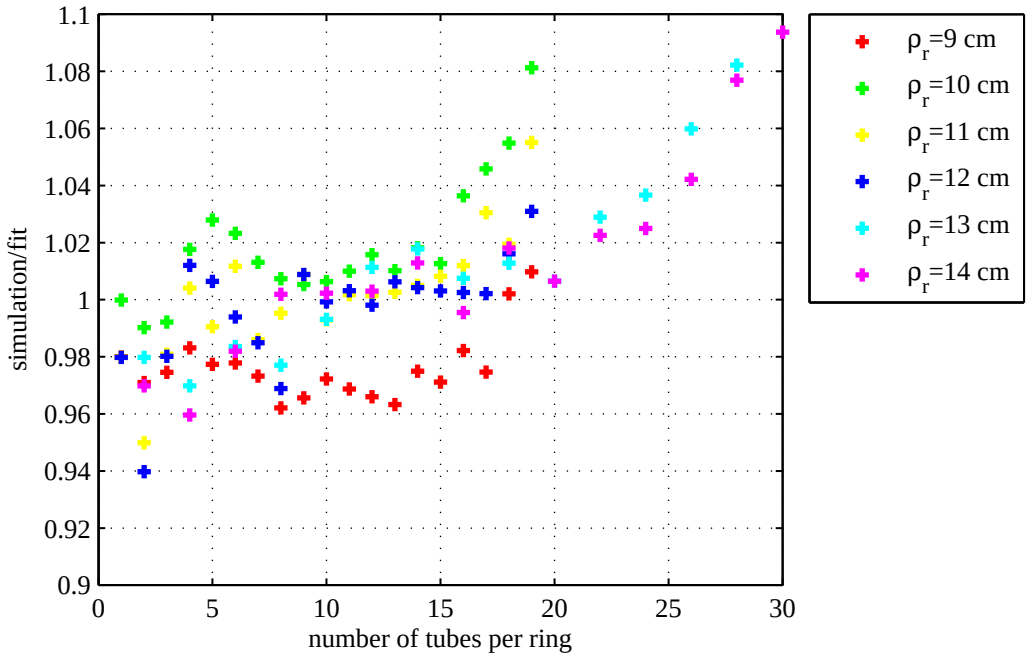

Figure 4.6: *CANVI Ratio between Monte Carlo and fit for a configuration with different number of tubes*

In the figure 4.6 is seen the result of applying the above setting to calculate the efficiency of a ring with a certain number of tubes placed at different distances from the source. The plot shows the ratio between the

result of the efficiency for Monte Carlo simulation, divided by the result of the previous function applied to all tubes of each ring. The approach fits relatively well although from a high number of rings, seems to always give a lower estimate. One reason for this difference may be the effect on the efficiency of the neutrons passing through the central hole. In any case, taking into account the purpose of the application, the adjustment is good enough.

Interference efficiency of tubes in different rings.

We proceed to study the variation in the efficiency ratio for two tubes at different distances from the source, oriented in the same direction with respect the origin of neutrons. The analysis consider the variation of the ratios as a function of neutron source energy, distance from origin of the tubes ρ, and distance between tubes ρ_{12}. In figures 4.7 and 4.8 can be seen the efficiency ratio of the inner and outer tube for different neutron source energies. The interference in ratio efficiency among tubes has a clear dependence on this energy and on the distance from the origin and between tubes. It can give some conclusions from previous studies:

1. Interference for an inner tube is only significant for lower energies and small distances between tubes.

2. For the outer tube, efficiency ratio increases with increasing neutron energy

3. Increasing distance from neutron origin reduces interference between tubes.

Two main causes can explain these effects

- Interference with the capture among tubes: neutrons captured on a tube can not be captured in the other. The consequence is a reduction in the efficiency ratio of the two tubes.

- The neutron path in polyethylene is reduced when pass through a tube. The thermal neutron flux for all source neutron energies changes in the region behind the tube (relative to the origin of the neutrons). Depending on the neutron energy the effect may be different and may therefore increase or reduce efficiency. This effect on the ratio of the neutron thermal flux can be seen in figure 4.12 where we put an empty tube to avoid the neutron absortion, it can be seen the increase of the ratio that occurs for all energies.

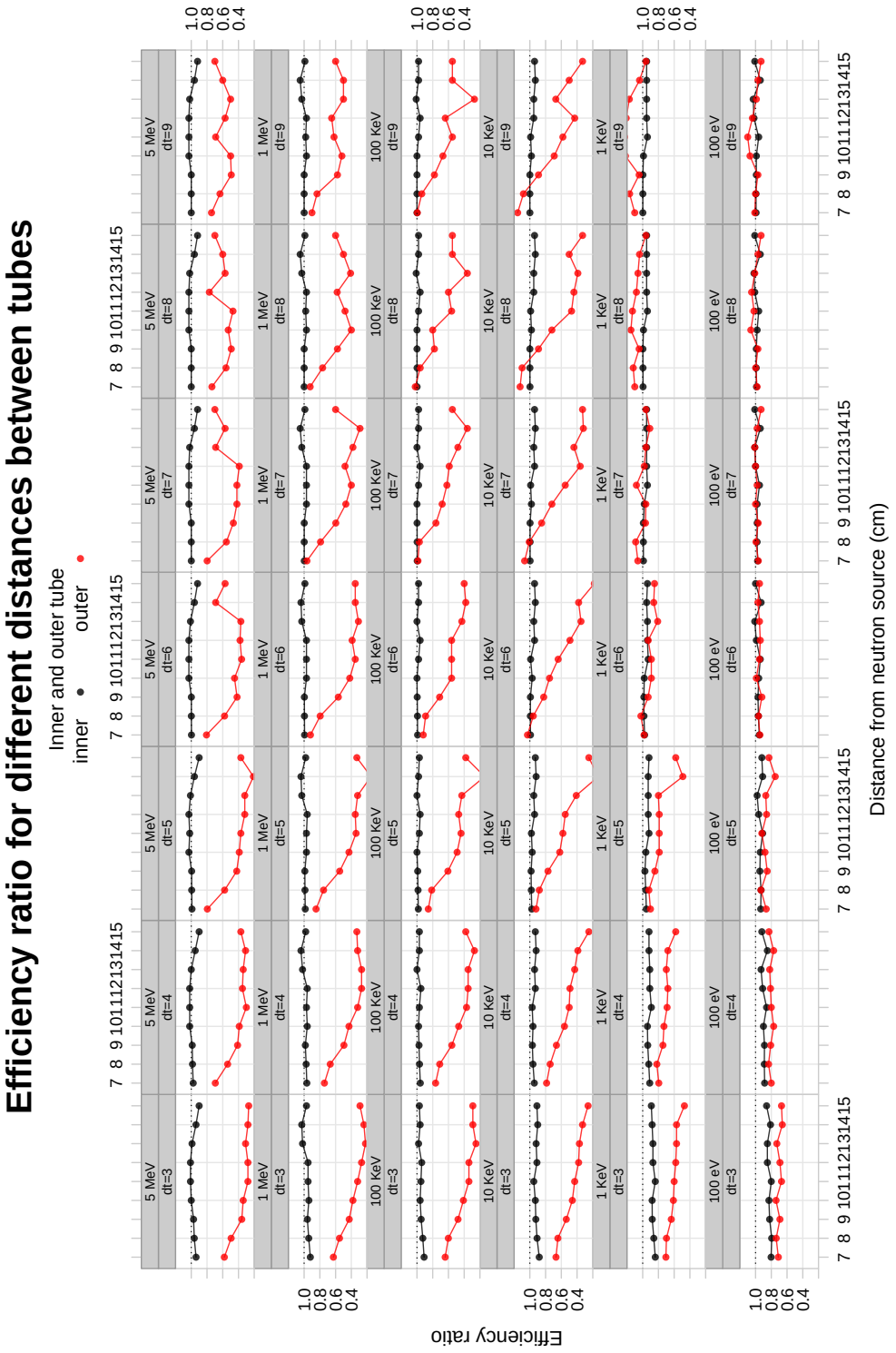

Figure 4.7: *Inner and outer tube efficiency ratio at ρ_r=7-15 cm with outer tube at ρ_{12}= 3-9 cm*

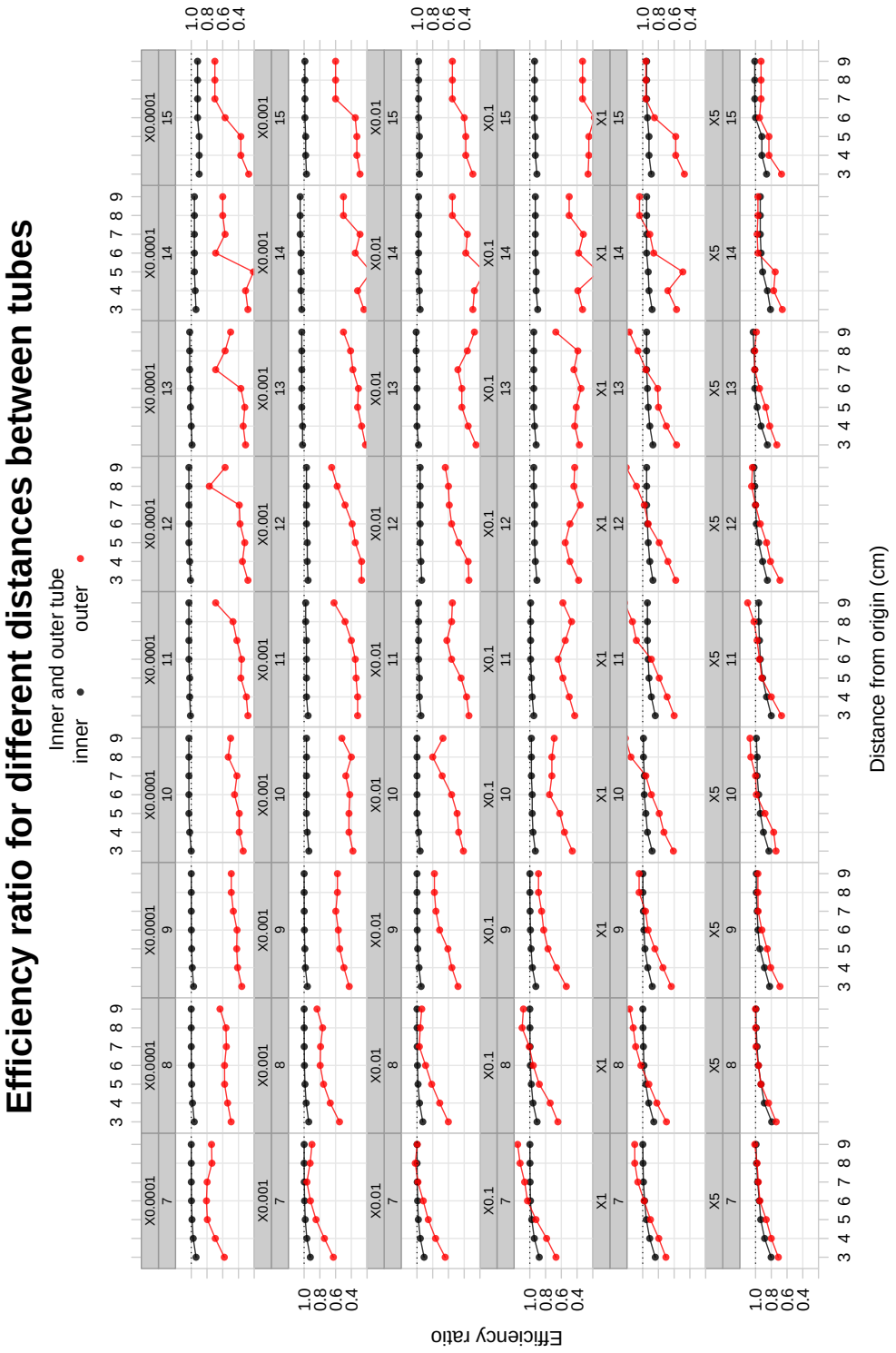

Figure 4.8: *Inner and outer tube efficiency ratio at ρ_{12}= 3-9 cm with inner tube at ρ_r=7-15 cm*

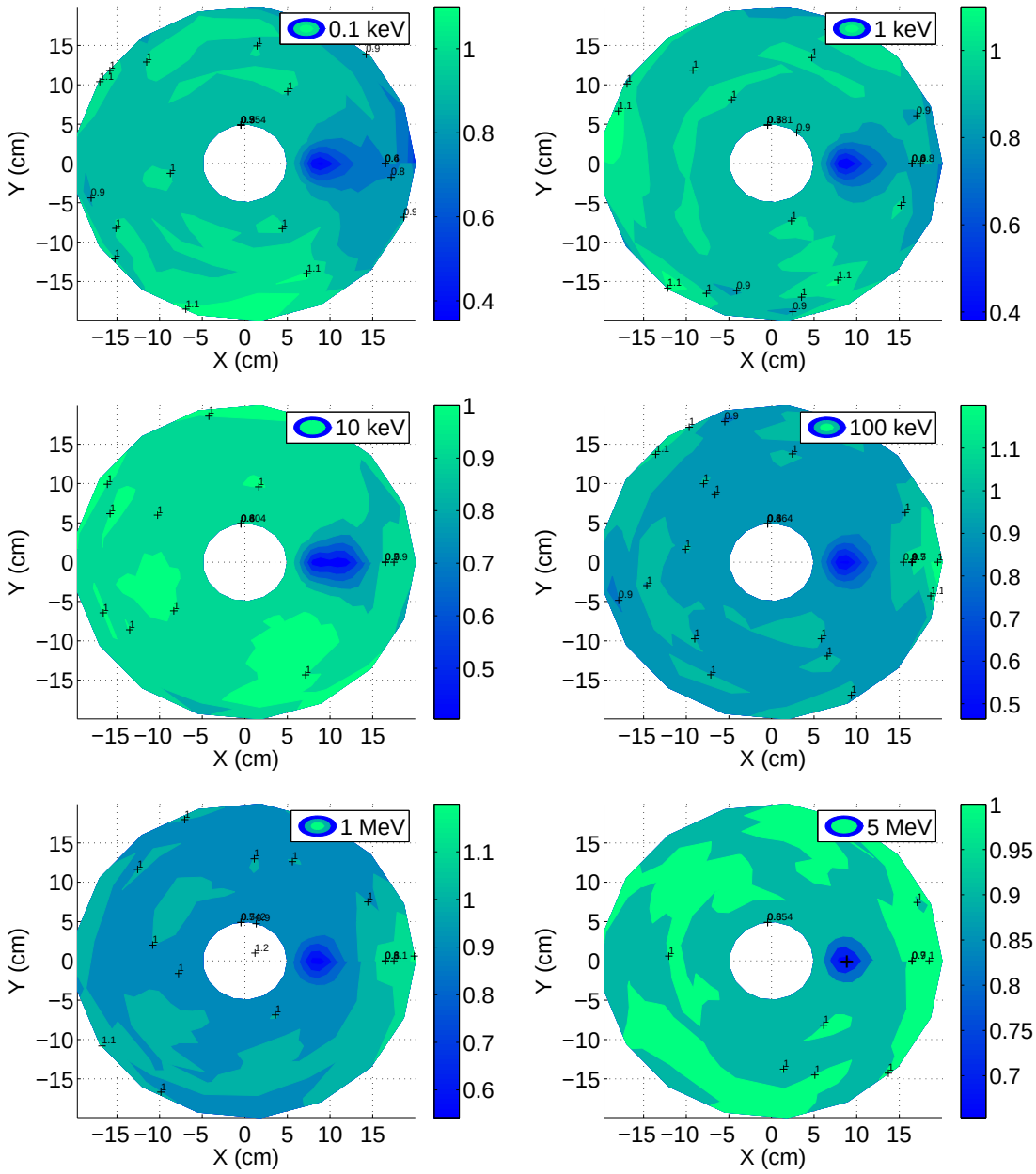

Figure 4.9: *Thermal ratio flux with one tube at r=8 cm for energies of 0.1 keV, 1 keV, 10 keV, 100 keV, 1 MeV and 5 MeV*

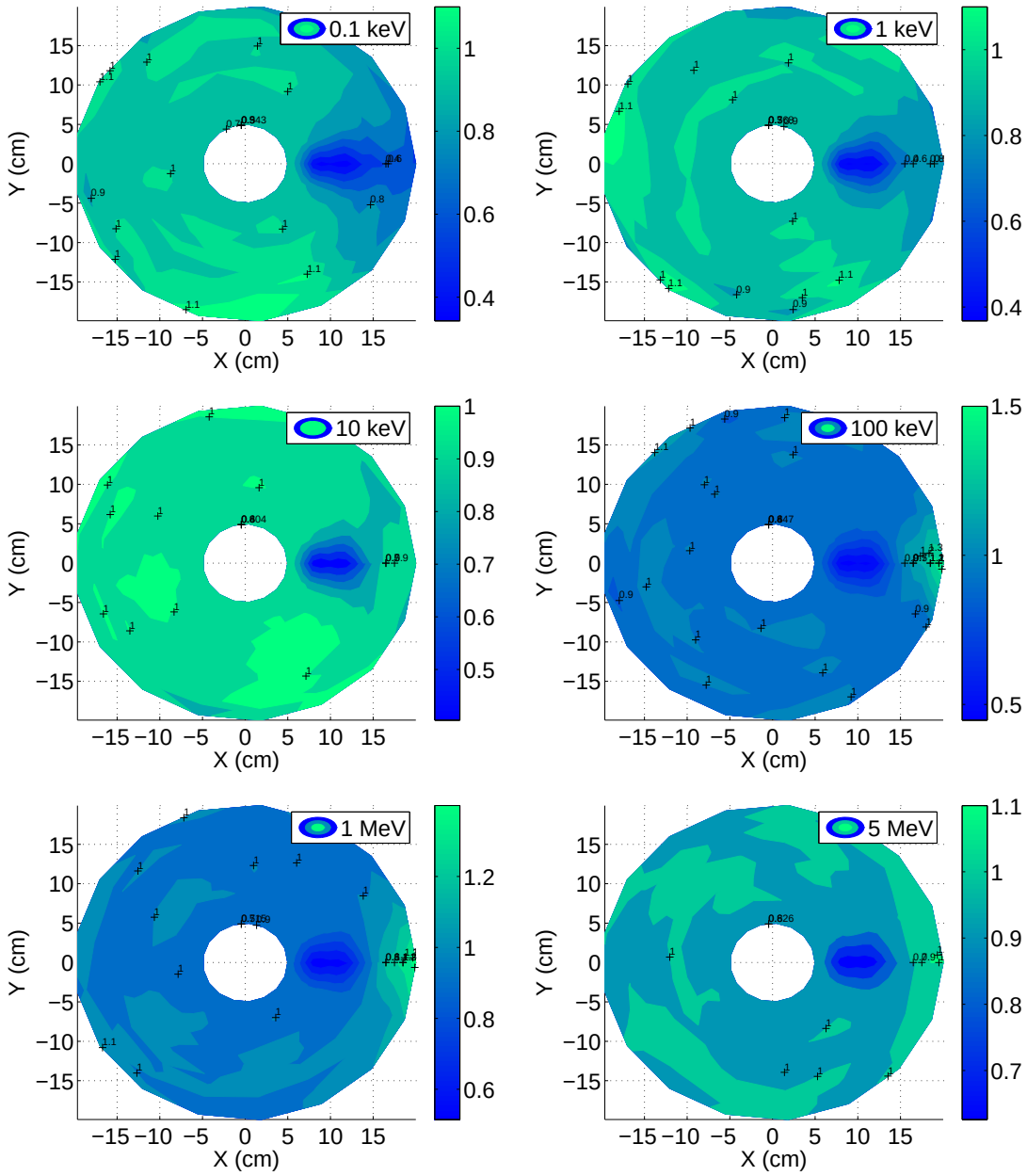

Figure 4.10: *Thermal x ratio with two tubes one at r=8 cm and other at 11 cm for energies of 0.1 keV, 1 keV, 10 keV, 100 keV, 1 MeV and 5 MeV*

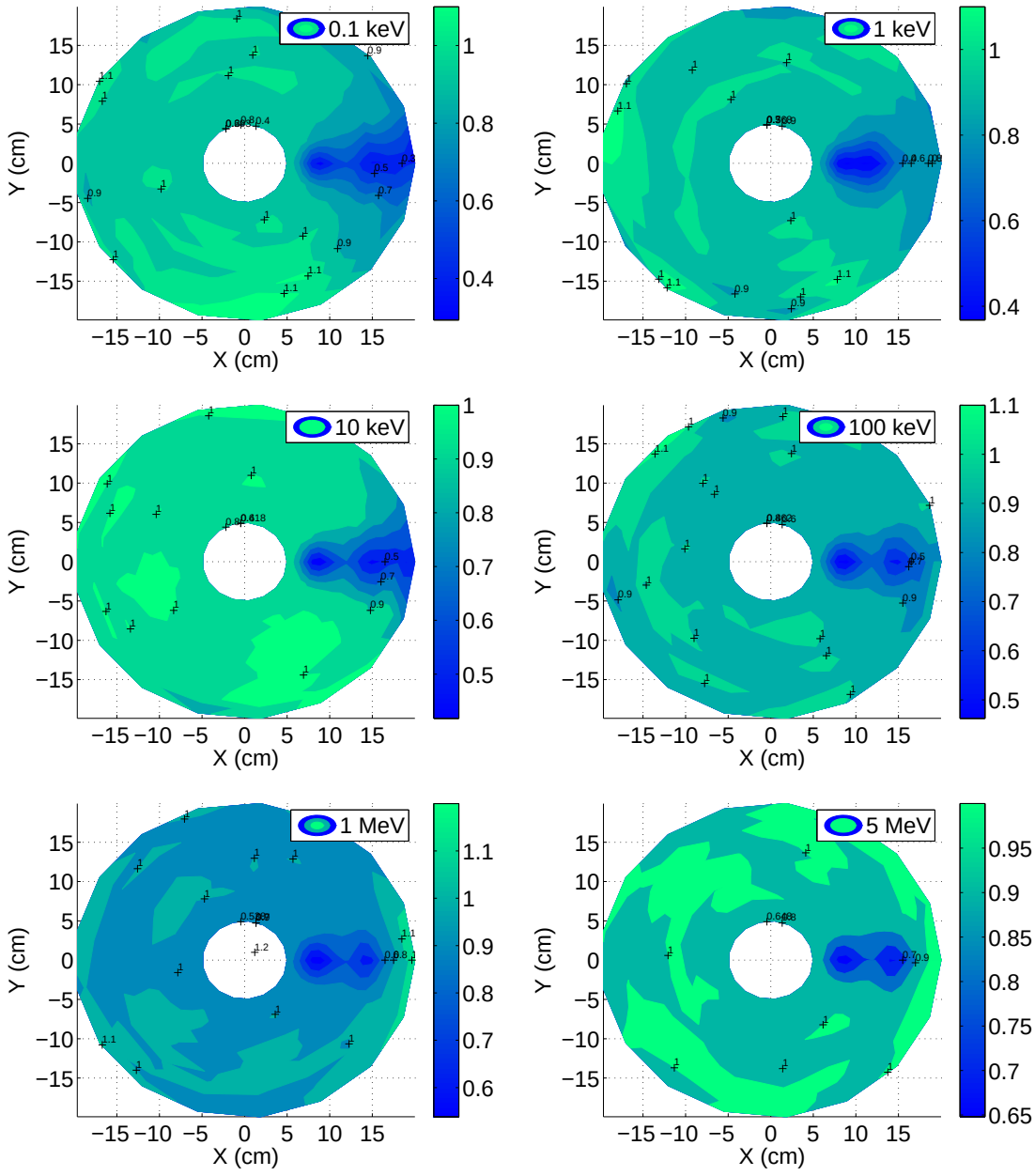

Figure 4.11: *Thermal flux ratio with two tubes one at r=8 cm and other at 14 cm for energies of 0.1 keV, 1 keV, 10 keV, 100 keV, 1 MeV and 5 MeV*

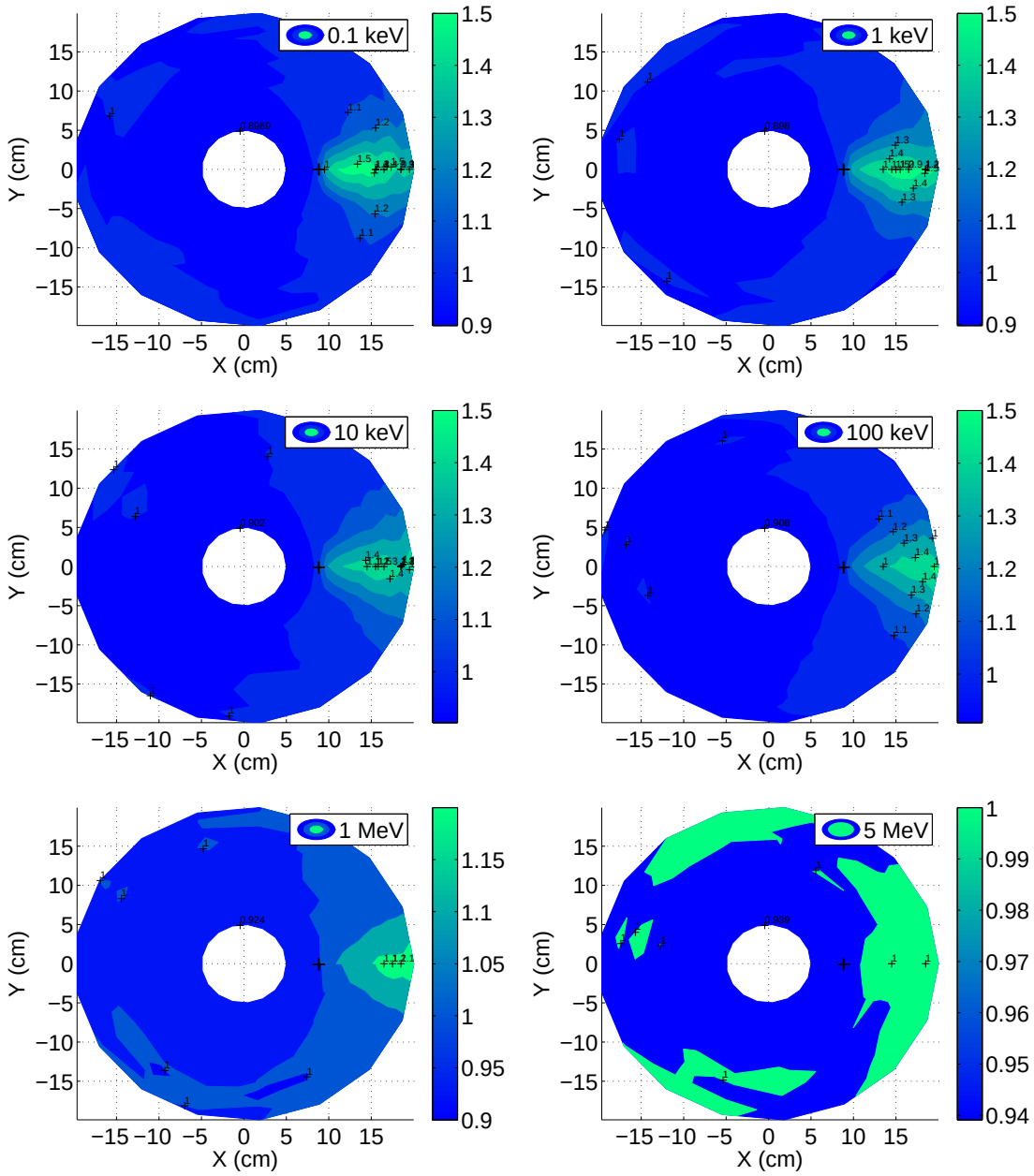

Figure 4.12: *Thermal flux ratio with one tube at r=8 cm with aire for energies of 0.1 keV, 1 keV, 10 keV, 100 keV, 1 MeV and 5 MeV*

Both effects depends on the distance between tubes and their position regarding the origin of the neutrons. Although there is always some small effect in the flux throughout the matrix of polyethylene, in general, it can be estimated that the higher effect for the efficiency of the tubes is local and decreases as a function of distance. There are notable exceptions, such as when we put a tube at a distance from source of neutrons where there is a clear reduction in the thermal neutron fluence for this energy, affects higher distances (tube at 7 cm with energy of 0.1 keV). Something similar happens with energy of 0.1 MeV and the tube at 10 cm or longer distances in the case of 2 MeV.

Given the difficulty to find an easy function that can reflect through the main variables the results obtained in this study, we decided to adopt a different approach to this case. The aim of this analysis is to find a set of values (simulations basis) in the space of parameters that characterizate the behavior of ratio efficiency. We make an statistical analysis of the data shown in figure 4.7 , where each column of a matrix represents a simulation in which a row contains efficiency ratio obtained by simulation, and the other rows contain the parameters we have been used in the simulation:

- Distance from the neutron source
- Distance between tubes
- Initial energy of neutrons

Each parameter are treated as if was an isolated variable. The aim is to study the relationship between different variables (values in the range of parameters) to quantify the relationship between them. If there is a very high correlation between variables, we expect that are dependent and therefore we can define an only one representant for all that range of variables with the same behaviour. We will do this process with the three parameters and through the study of relations between their values, we will define some ranges in which the efficiency ratio will be characterized by only one value of the range.

In a first analysis, to find a range of energies with the same behavior, we define each energy value as a parameter (for example, value 0.1 keV define the parameter "X0.1keV"). Then, we analyze the results of the efficiency ratio as a function of this variables to find a possible correlation between them. In figure 4.13 it can be seen the covariance matrix between the energy parameters for the outer and inner tube. Below the diagonal of the table it can be seen the value of correlation between the

different values of energy parameters and on top, a colored representation (color legend) of this value, in which a darker blue represents higher correlation. We want to obtain a certain structure inside the covariance matrix between the variables of energy. These structures may allow us to define relationships between variables that reduce the number of simulations required to explain the behavior of efficiency ratio. The idea is to choose different ranges of parameters with only one representant that characterize ratio efficiency in that range. In figure 4.14 it can be seen again the correlation between variables represented by the same color as the previous figure and also added the results of a significance test of this relationship. The variables are grouped according to these correlations. The confidence interval is defined by the thickness of the bar inside the cell, a greater thickness means less significance and a if is marked with a cross means no significance. The groups are displayed through a blue box which includes all values in the range. As it can be seen in the case of the outer tube, there is a strong correlation between the results obtained for energies greater than 1 MeV. Another group could be formed by the energies from 1 keV to 100 keV. While 0.1 keV needs individual treatment.

In a second analysis, we do the same for the parameters that represents the distance from the origin and distance between tubes. As can be seen in the figure 4.15 it can be made groups based on the values of correlation between the values of the parameters. In case of distance with the origin, there is a group with values between 10-15 cm, another with 8 and 9 cm and 7 cm need individual group. In the case of distance between tubes, there is a group with value 3 to 5 cm, another with 6, 7 cm and one with 8 and 9 cm.

Angular depence for the interference of the tubes.

As seen before, the main effect of interference efficiency between the tubes occurs in the direction of emission of the neutrons. We note that for distances at 3 cm (high interference) and at 6 cm, as can be seen in figure 4.16, the change in the ratio for the second tube is important from 40 degrees in case of 3 cm and about 30 degrees for the case of 6 cm. For the first tube the influence is smaller and only below 30 degrees variation exceeds 5%. The effect can be fitted on the tubes that are not in the same direction using an exponential function that depends on the difference between polar angle between tubes (φ_{cc}) (equation 4.7).

$$r_\eta(\varphi_{cc}) = 1 - [1 - r_\eta(\varphi_0)]ae^{-b\varphi_{cc}} \tag{4.7}$$

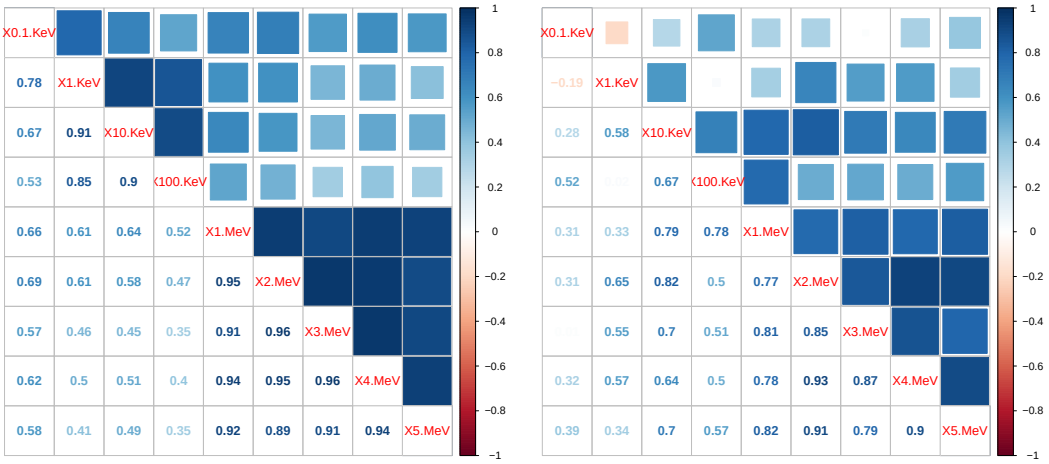

Figure 4.13: *Energy variable correlation with the outer (left) and inner (rigth) tubes*

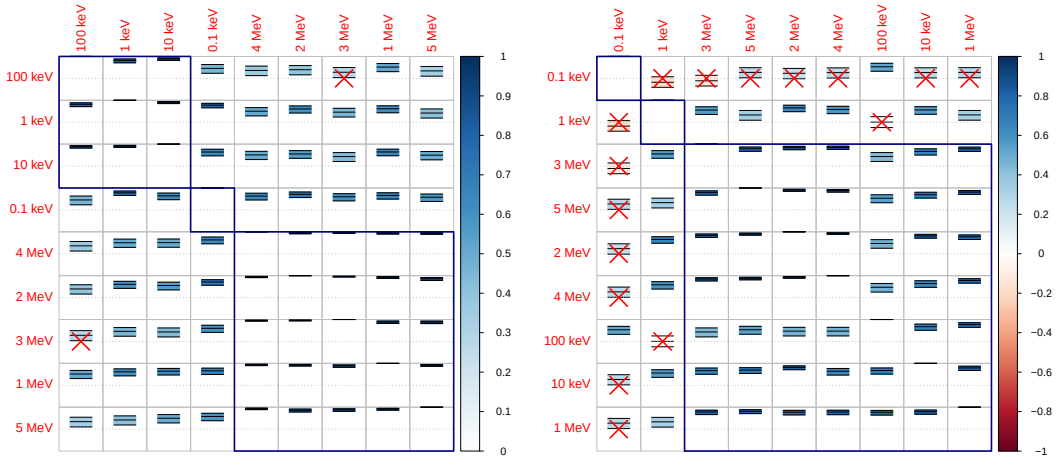

Figure 4.14: *Energy variable correlation and significant level for outer (left) and inner (rigth) tubes*

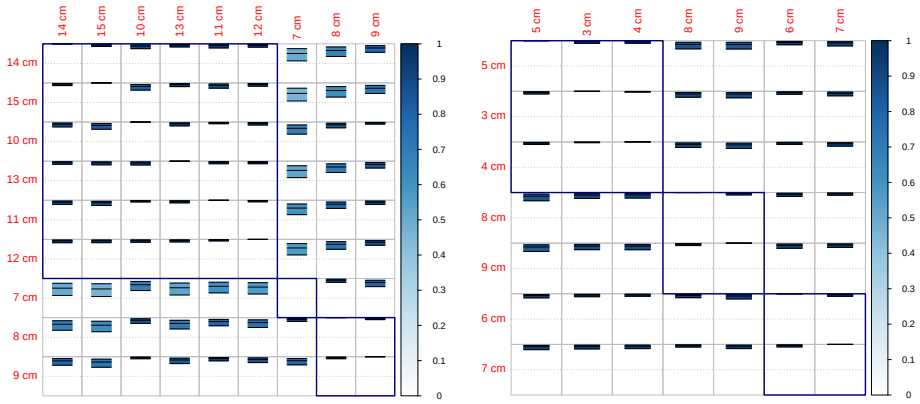

Figure 4.15: *Correlation (colour) and significant level range (upper and lower bound) for distance from source of neutrons (left) and distance between tubes correlation (rigth)*

We fit the initial approach for all initial neutron energies considering that the variation is not too large. The function is fitted according to the angle between tubes with an exponential relationship between the efficiency ratio for the case where the tubes are aligned $\varphi = 0$, with respect to the ratio we get for any single angle φ_{cc}.

4.4 Applications of the algorithm for the design of the BELEN prototypes

As explained above, the efficiency of the new configuration is calculated through the approximate formulas for tubes on the same ring and by interpolation by adding the angular effect, for tubes in different rings. In this process we are assuming that the effect in the efficiency ratio is associative. Interpolation is performed with the result obtained in the basic simulations for parameters that characterize the ranges obtained previously in the statistical analysis. The result of the application, as we have said before, give a first approach that helps us to find the optimum configuration, reducing the number of simulations required and defines a strategy for organizing the search. The prototype detectors listed below were designed as has been explained in chapter 3. The results of the algorithm seeks similar objectives to compare the resulting configurations but is not the more optimal configuration although can give a set of good

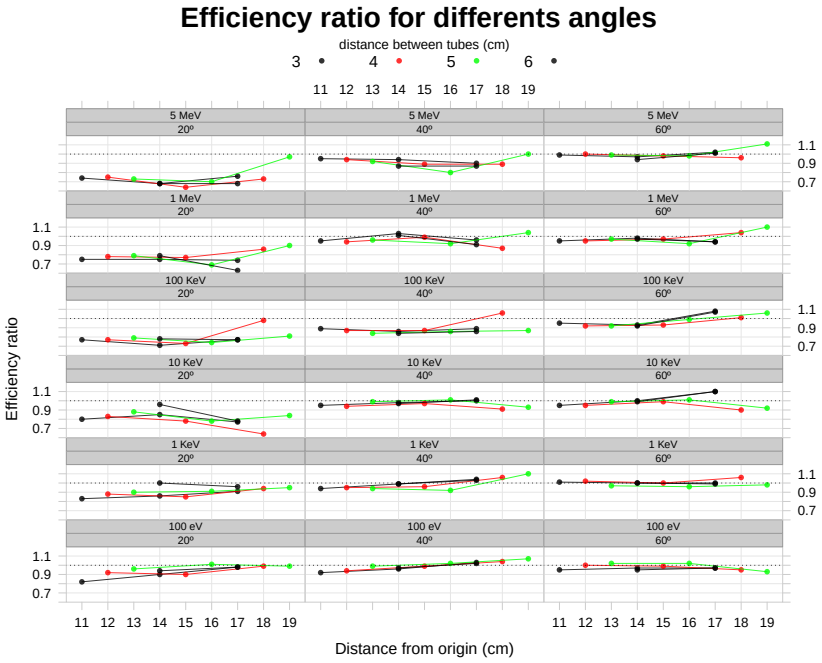

Figure 4.16: *Efficiency ratio (outer tube) for different angles with distances between tubes from 3 to 6 cm and distances to the origin from 11 to 19 cm*

values of parameters to do a more accuracy search with Monte Carlo simulations.

BELEN-20B

In this prototype were available 20 ^{3}He tubes with a pressure of 20 atm. The radius of the beam hole was 5.5 cm. The aim proposed for the application is to obtain maximum efficiency with 2 MeV flat factor as close to 1.0 as possible in the range of energies up to 1 MeV and less than 1.25 in the range up to 2 MeV. There are two files necessary for the entry of OPT, one containing the values of efficiency that gives us results of Monte Carlo simulations of a single tube in the polyethylene matrix at distances between 8 cm and 28 cm from the neutron source.and another with the values of ratio efficiency that gives results of Monte Carlo simulations with two tubes. The first tube is at three distances specified in the efficiency profile for various ranges discussed in the text. The second tube is at distance from is at 4 cm, 7.5 cm, 8.5 cm from the first one.with

tubes		configuration	approach		MCNPX	
#eff	#flat	radius(#tubes)	eff	flat	eff	flat
5	15	8.0(6) 11.0(3) 14.5(8) 17.5(3)	58	1.36	45	1.36
4	16	8.0(4) 11.0(2) 14.0(10) 17.0(4)	45	1.13	37	1.16
3	17	8.0(3) 11.0(1) 14.0(10) 17.0(4) 27.0(2)	36	1.05	31	1.04
2	18	8.0(2) 11.0(2) 14.0(7) 17.0(2) 27.0(7)	28	1.07	23	1.05

Table 4.1: *Configurations and parameters obtained with OPT application employing the 20 tubes of BELEN-20B distributed in two groups of tubes, one to improve efficiency and another to get a flat factor close to 1.*

The table 4.1 shows the results of the configurations distributed in two groups of tubes. The column #ceff are the number of tubes with the OPT call to obtain higher efficiency and #cratio are the number of tubes used to the next OPT call to obtain a ratio as close as possible to 1.0 The result of the run of OPT for a different distributions of tubes in #flat and #eff, is shown in the table 4.1.

In this table *Configuration* column describes the configuration indicating position of the rings (radious from the origin of neutrons) and the number of tubes in this ring, *eff* column gives the efficiency estimated by application, the column *factor* shows flat flat factor estimated by the application and *Monte Carlo* column shows the results for the same configuration by Monte Carlo simulation code, where the variable e corresponds to the efficiency and r is the flat factor. Accepting miscalculated both efficiency and the ratio compared with the Monte Carlo solution, the result gives us configurations that meet the requested specifications and serve as a starting point to find an optimal solution. For example, Figure 4.17 corresponds to the configuration in which 16 tubes are used for best flat factor, in this case the flat factor is somewhat better but the efficiency of the final prototype efficiency is slightly lower. It must be considered that they have not taken into account issues of symmetry in the arrangement of tubes, that would be done in a second step in which we find a more optimal solution by small variations of the tube positions.

BELEN-30

The design goal for the BELEN-30 detector was to achieve maximum efficiency for neutrons of energy less than 2 MeV with 10 tubes of He^3 at

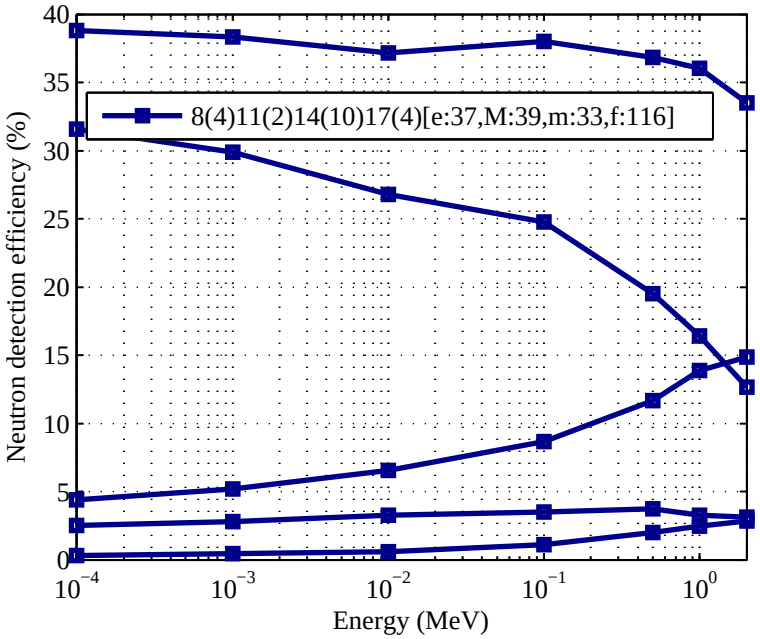

Figure 4.17: *OPT configuration efficiency for BELEN-20*

10 atm and 20 tubes of He^3at 20 atm. The radius of the beam hole was 11.5 cm. The data required for the application with the simulation basis is in three files, one containing the values of efficiency that gives us results of Monte Carlo simulations with a single tube at 20 atm in polyethylene matrix at distances between 14 cm and 28 cm from the neutron source, a second file containing the values of efficiency that gives us results of Monte Carlo simulations with a single tube at 10 atm in polyethylene matrix at distances between 14 cm and 28 cm from the neutron source and another file with the values of ratio efficiency that gives results of Monte Carlo simulations with two tubes. The first tube is at three distances that represents all the ranges of distances between 14 cm and 28 cm. The second tube is at 4,7.5,8.5 cm distances from the first one. With these specifications, OPT runs distributing a group of tubes to obtain higher mean efficiency and another group to obtain a value of flat factor closer to 1.0. The result of the run of OPT for a range of different distributions tubes is shown in the following table 4.2:

In this case, we obtain the configuration with two steps, an initial step in which we seek with 10 tubes the maximum efficiency ("be" column with value 1) and the next step, with 20 tubes, seeks the minimum flat factor ("bf" column value 1). "eff" column and flat column shows the estimated

step	be	bf	#tubes	tubes	eff	flat	MCNPX	
1	1	0	10[10]	14.0(10)				
2	0	1	20[20]	18.0(11)21(9)	46	1.22	37	1.27

Table 4.2: *Configurations and parameters obtained with OPT application employing the 30 tubes of BELEN-30 in two steps, one to improve efficiency and another to get a flat factor close to 1.*

efficiency and "flat" ratio obtained by application, and in the column MCNPX, the results obtained by simulation for the efficiency and flat factor.

The results with this distribution (figure 4.18) are quite similar to those obtained in the prototype that was done to the BELEN-30 that results could be a good starting point to optimize the solution.

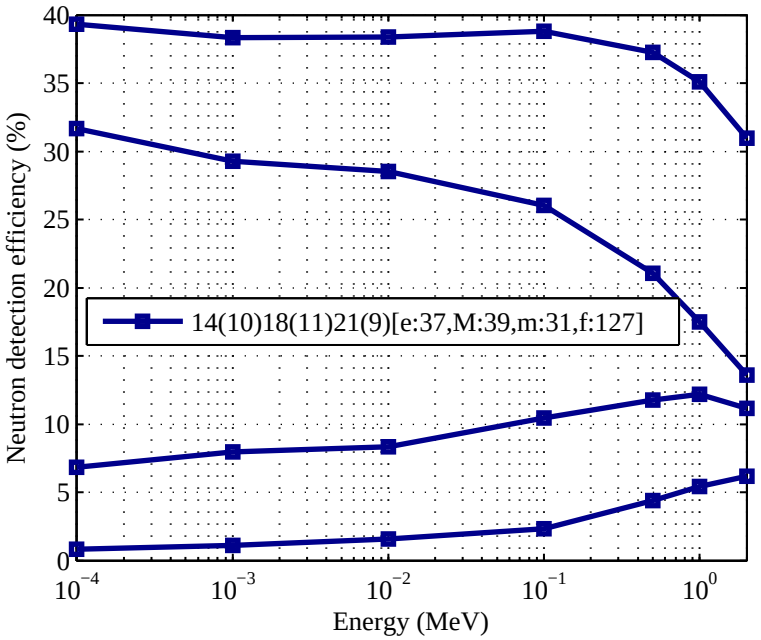

Figure 4.18: *OPT configuration efficiency for BELEN-30*

BELEN-48

The design goal for the BELEN-48 detector is to achieve maximum efficiency for neutrons of energy less than 5 MeV with 40 tubes of He^3 at 8

atm and 8 tubes of He^3at 10 atm. The radius of the beam hole is 5.5 cm. For the OPT call is necessary to pass three files, one file containing the values of efficiency that gives results of Monte Carlo simulations with a single tube at 8 atm in the polyethylene matrix at distances between 8 cm to 28 cm from the neutron source, a second file containing the values of efficiency that gives results of Monte Carlo simulations with a single tube at 10 atm in the polyethylene matrix at distances between 8 cm to 28 cm from the neutron source and another file with the values of ratio efficiency that gives results of Monte Carlo simulations with two tubes. The first tube is at three distances that represents all the ranges of distances between 14 cm and 28 cm. The second tube is at 4.5 cm, 7.5 cm, and 8.5 cm distances from the first one. In the table 4.3 are displayed two solutions directly with the 48 tubes searching for high efficiency and flat factor close to 1 in the first and second adding conditions to the maximization of energy efficiency at 5 MeV.

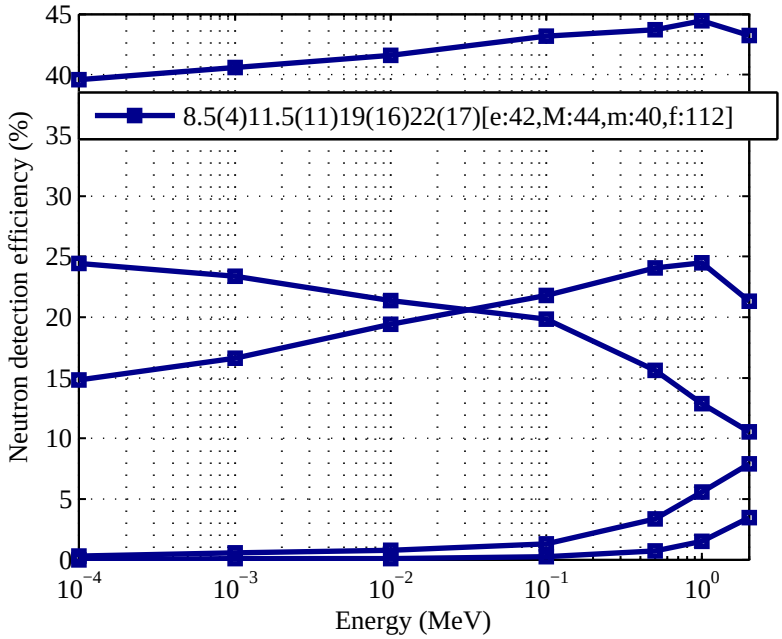

Figure 4.19: *Efficiency for OPT configuration for BELEN-48*

In this case we run OPT twice with different parameters In the first case we seek the maximum efficiency and flat factor close to 1 ("be" columns and "bf" with value 1) and in the second case also seek maximum efficiency for neutron initial energy of 5 MeV. "eff" column and "flat" column show the estimated efficiency and flat ratio obtained by ap-

be	bf	be5	configuration	eff	ratio	MCNPX	
1	1	0	8(2) 11.5(10) 18(9) 21(6) 24(4) 27(17)	38	1.14	34	1.16
1	1	1	8.5(4) 11.5(11) 19(16) 22(17)	46	1.16	43	1.12

Table 4.3: *Configurations and parameters obtained with OPT application employing the 48 tubes of BELEN-48 in two cases. One call to improve efficiency and to get a flat factor close to 1 and the second case also to seek maximum efficiency for neutron initial energy of 5 MeV.*

plication, and in the column MCNPX, the results obtained by simulation for the efficiency and flat factor with the same configuration.

The result of the second row shown in Figure 4.19, is similar to the final configuration for the prototype, however in the prototype the rings have an even number of tubes providing better symmetry to analyze results .

Chapter 5
Calibrations of neutron detector

This chapter shows the results of the BELEN detector calibration, specifically the prototypes BELEN-30 with a ^{252}Cf source at GSI and BELEN48M1 at PTB (the Physikalisch- Technische Bundesanstalt Braunschweig, the german metrology laboratory) .

Calibration tests have to be done for each experimental campaign to assure the correct operation of the detector before starting the measurements. Calibration of the BELEN detector can be performed with isotropic neutron sources such as ^{252}Cf, Am-Be, etc., which produce neutrons in a continuous spectrum as can be seen in figure 5.1 or with known neutron fields produced by some reactions. In this chapter we describe techniques that we have employed to calibrate the neutron detector with a set of reactions that produce neutron monoenergetic sources at PTB.

The PTB is the German National Metrology Institute which major tasks of research and development are the improvement of the national measurement standards, e.g. by exploitation of quantum effects for realizing the SI units, and the precise determination of fundamental constants and material properties. Division 6 "Ionising Radiation" deals with radioactivity as well as photon and neutron metrology and dosimetry. A great variety of well characterised radiation reference fields is available for experiments. PTB took part in international key comparisons for the determination of the fluence of monoenergetic neutrons in the energy range from 144 keV to 14.8 MeV.

5.1 Calibration with ^{252}Cf source

Spontaneous fission ^{252}Cf neutron sources are commonly used to calibrate the detector neutron for efficiency and to test the simulations performance. Due to its availability in macroscopic quantities, ^{252}Cf has been one of the most extensively studied transplutonium isotopes. The majority (96.9%) ^{252}Cf decays are through alpha decay, but due to the nature of encapsulation, these ^{4}He nuclei do not escape the confines of the source. A small (3.092%) but significant proportion of decays via spontaneous

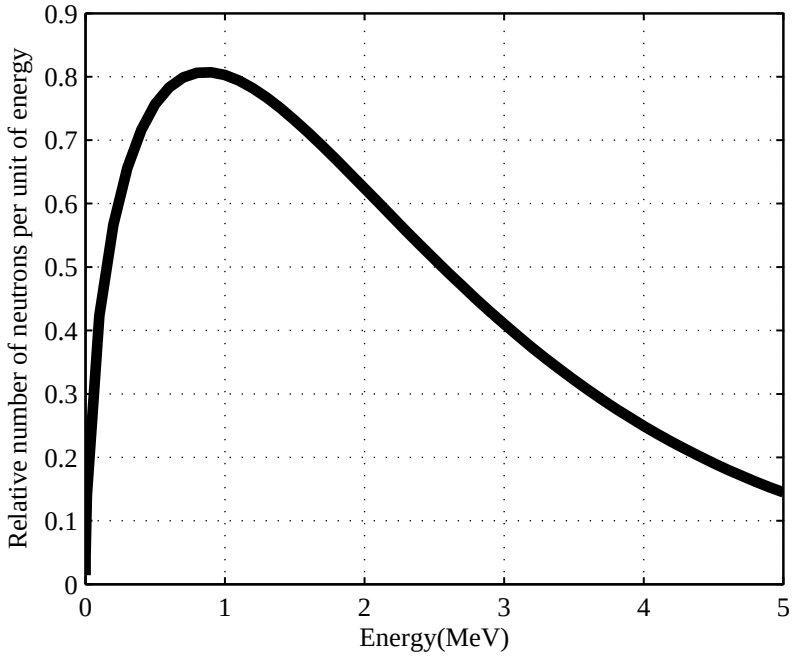

Figure 5.1: *Neutron energy spectrum from ^{252}Cf.*

fission wich produces fission fragments, as well as a neutron yield of 3.768 neutrons/fission (2.31434 10^{12}neutrons/s/g of ^{252}Cf). The neutron energy spectrum is shown in figure 5.1 and have a mean energy of 2.1-2.2 MeV. These neutrons have an energy spectrum which can be modelled as either a Maxwellian or a Watt fission spectrum. In our case we use Watt fission spectrum with the parameters set according to the literature.

For all the ^{252}Cf source, it could be found impurities of ^{249}Cf, ^{251}Cf, that have a negligibly small spontaneous fission branch. Therefore, only the ^{250}Cf and ^{252}Cf isotopes had to be considered. The alpha decay of ^{252}Cf produces ^{248}Cm, with neutron emission branching ratio of 8.39%, but the long half-life of this radioisotope (3.51 years) made its contribution negligible. At the time of the measurement the total activity of the source was due to ^{250}Cf, whose contribution to the neutron activity was less than 1% of neutron emission. In the table 5.1 are detailed the values of the mass and activity of nuclides for the source used for calibration at the GSI and PTB.

The ^{252}Cf calibration source used for calibration measurements had an inital activity of 5 mCi (185 kBq) (1/08/2010) with an active diameter of 3.18 mm. That source is incorporated in ceramic material, and it

Nuclide	Mass % (15/10/2010)	Activity %	Half life (y)
^{249}Cf	9.936	0.1495	350.6
^{250}Cf	30.643	12.266	13.08
^{251}Cf	15.053	0.0877	898
^{252}Cf	44.368	87.497	2.645

Table 5.1: *Composition of ^{252}Cf source at 15/10/2010*

was encapsulated according to the standard capsule design. This model consists on a double-encapsulation of stainless steel (ISO rating: C66545), a schema of the source is shown in figure 5.2.

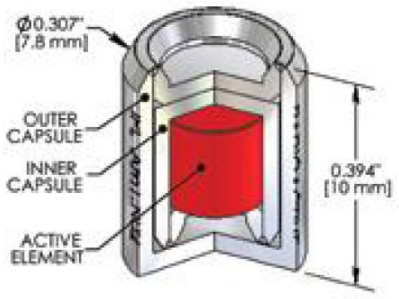

Figure 5.2: *Detail of ^{252}Cf source encapsulation with its dimensions*

The experimental results were compared to those generated by the Monte Carlo simulations code of the BELEN detector. The simulations were performed with all the geometry and materials of the ^{252}Cf neutron source located at the center of the BELEN detector symmetry axis. Details of the experimental and Monte Carlo simulation results are discussed in the next sections.

5.2 Calibration at GSI

The calibration measurements were done at GSI laboratory at October 2011. Calibration measurements was performed with ^{252}Cf calibration source described in section 5.1. The detailed results are shown in the table 5.2

The efficiency result with Monte Carlo simulation of the BELEN-30 neutron detector with the ^{252}Cf source is 33.5±0.2%. At GSI the

GSI results/Group of counters	03/10/11 [%]	Simulation [%]
inner ring	14.6±0.3	14.1±0.1
outer ring	20.3±0.4	19.4±0.1
Total	34.9±0.7	33.5±0.2

Table 5.2: *Experimental and simulated neutron efficiency of BELEN-30 for the ^{252}Cf neutron source at GSI*

experimental efficiency measured was 34.9±0.7%. The experimental and simulated values agree within the margin of uncertainly.

5.3 Calibration at PTB

All the calibration measurements were done at the PTB facility at June 2013. Initially was performed a calibration with the ^{252}Cf source to allow to check only one integrated (mean) efficiency value. And later, using PTB Ion Accelerator Facility (PIAF), was performed a calibration with a set of reactions that produce neutron monoenergetic sources. A scheme of PIAF is shown in figure 5.3. The particles, protons, deuterons and alpha are accelerated by means of a Van de Graaff accelerator with voltages between 0.1 MV and 3.75 MV. An energy-variable cyclotron furnishes ion beams with energies of up to 27 MeV. This facility enables to perform studies also on the neutron angular distribution for each energy and target. Therefore it has been decided to calibrate the BELEN detector with (p,n) and (α,n) reactions on ^{7}Li,^{13}C and ^{51}V producing neutrons with a known (limited) spread in energy, ranging from 0.1 to 5 MeV. The BELEN-48M1 detector with a center hole of 110 mm of diameter was installed at the end of one beam line at the neutron metrology facility with the target holder at the center of the detector as can be seen in figure 5.4. On a parallel beam line it was possible to measure reaction yields and angular distributions with calibrated neutron detectors and then to produce the same neutron flux inside BELEN-48M1, with very similar target and beam conditions. The neutron energy and angular distributions need to be taken into account when comparing the simulated value for each reaction and beam energy to the obtained experimental data.

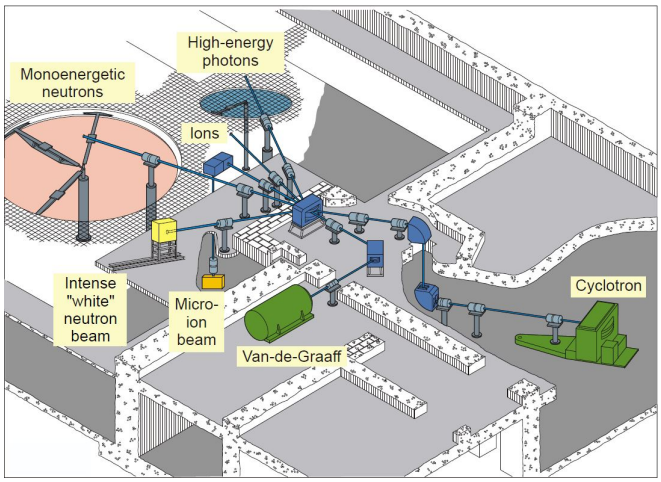

Figure 5.3: *PTB facility*

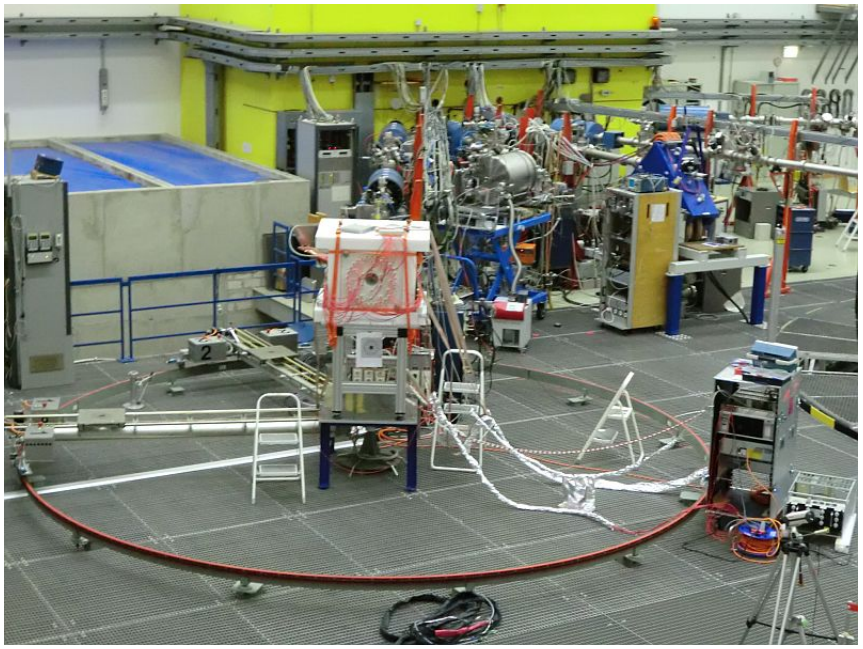

Figure 5.4: *Picture of the PTB facility with the neutron detector BELEN at the center*

5.3.1 Calibration with ^{252}Cf source

Two calibration measurements were performed at the PTB with the 5 mCi (185 kBq) ^{252}Cf calibration source described in section 5.1.

Group of counters	06/21/13 [%]	06/22/13 [%]	Simulation [%]
inner ring	20.4±0.3	19.5±0.3	19.1±0.4
central ring	11±0.2	10.5±0.2	10.9±0.4
outer ring	7.8±0.1	7.7±0.1	7.6±0.6
Total	39.2±0.6	38.1±0.6	37.5±1.3

Table 5.3: *Experimental and simulated neutron efficiency of BELEN-48M1 for the ^{252}Cf neutron source at PTB*

Two experimental efficiency measures were made with the BELEN-48M1 neutron detector, the results were 39.2±0.6% and 38.1±0.6%. The Monte Carlo simulation gives an efficiency of 37.5±1.3%, this is in accordance with the experimental results.

5.3.2 Neutron monoenergetic production at PTB

A neutron source is considered monoenergetic when the energy spectrum consists of a small energy width that is much less than the energy itself. Neutrons at PTB are produced by beams of charged particle that induce binary nuclear reactions, the source of proton and alpha beam is accelerator based. The expression of the neutron yield at the laboratory system angle (θ) is given by equation [41]

$$Y_E(\theta) = \frac{x_i}{ne_0}\left(\frac{N_A}{\mu_i}\right)\frac{\left(\frac{d\sigma}{d\Omega}\right)(E_p,\theta)}{f(E_p,\theta)S(E_p)} \tag{5.1}$$

where x_i is the mass fraction, μ_i is the molecular weight of the target material, denote and $f = dE_n/dE_p$ the kinematic factor. The yield depends on the charged particle beam intensity (charge state n), the differential cross section of the reaction ($d\sigma/d\Omega$) and the specific energy loss in the target material due to stopping power of the projectile ion (proton or alpha) $S = \rho^{-1}(dE_p/dx)$. The yield is usually given in the units of neutrons/(sr.μC.MeV) . There are several codes available for calculating neutron yields of targets with finite thickness [36].

In addition to the neutron yiels, reliable information on the energy and spatial distribution of the neutrons is required. In some cases, different experimental devices are needed to describe the neutron productions in spallation reactions. Usually only neutron emission at an angle of 0° with respect to the charged particle beam is considered. Placing the sample at 0° the neutron yield is usually forward peaked and the neutrons emitted at 0° have the highest energy. The angular dependence of both the neutron energy and the neutron yield, is comparatively small. For this reason monoenergetic neutron sources are usually compared by their 0° yield.

The neutron flux produced in spallation reactions depends strongly on the projectile and target combination. As a general rule, the heavier the target nucleus the larger the neutron excess and the neutron yield. However, the radio-toxicity induced in the spallation target could be drastically reduced by using lighter targets. Therefore, a target may only be as thick as the required neutron energy width allows. For a given target thickness there will be the more nuclear interactions the lower the electronic stopping cross section is compared to the nuclear cross section. The stopping power define a measure of the effect of a target on the kinetic of a charged particle passing through it. For hydrogen projectiles, the nuclear stopping power is very small for all energies used in this experiment.

Produced neutrons are also attenuated when going through the target material. This attenuation depends on the emission angle and material thickness that the neutrons have to cross. At around 90°, neutrons go through a significant thickness of material: this gives a reduced fluence rate. At backward angles, neutrons have to go through target surrounding materials. This results in a transmission depending on the material used, for example, if the target holder is made of steel, the absorption resonance of around 24 keV must be taken into account.

5.3.3 Measuraments and calibration method

The PTB accelerate a beam of particles impinging onto targets with diferent thickness, located at the center of the BELEN symmetry axis. An small-scale electrostatic accelerator is used to provide the ion beams. The reaction should have sufficient yield to produce enough neutrons with thin targets and at moderate beam currents to do not damage the target. The beam must be well centered because any variation of the ion beam current that impacts on the target change the neutron emission and thus the fluence rate. The fluence rate variation in time for the beam is therefore

monitored using a current integrator or monitor. The current integrator measures the current deposited on the target (charge Q).

The BELEN efficiency was determined as the ratio of the number of detected neutrons to the number of neutrons N_n produced in the reaction. The number of counts in the detector must be corrected by detector dead time. The influence of background is removed by background measurement. To develop a simulation and a verification of the experimental data, it is necessary to have a precise description of the spectrum of neutrons produced by the reaction.

Reaction	$E_{p/\alpha}$ keV	$E_{n,av}$ keV	E_n max-min
$^{51}V(p,n)^{51}Cr$	1800	225	200-250 keV
	2140	552	510-590 keV
	2270	677	630-730 keV
$^{13}C(p,n)^{13}N$	4450	1023	0.77-1.36 MeV
$^{13}C(\alpha,n)^{16}O$	1130	2827	2.5-3.2 MeV
	3300	4383	3.6-5.3 MeV

Table 5.4: *Reactions and their neutron energy for the diferents beam energies*

The following sections describe in more detail the reactions used in the calibration at PTB.

5.3.3.1 Reaction $^{51}V(p,n)^{51}Cr$

The $^{51}V(p,n)^{51}Cr$ reaction has been well studied in the proton energy range used in this experiment [46] . Angular distribution has been mesured and found to be quasi-isotropic. This reaction is better than other to make a monoenergetic source of neutrons because the slow variation of intensity and energy with angle and also the target is easy to be obtained [10]. There is only one isotope of natural vanadium, and thin targets of the metal are rather readily prepared by evaporation. Three different targets were used and irradiated with three beam energies as can be seen in table 5.5.

5.3.3.2 Reaction $^{13}C\ (p,n)^{13}N$

Due to its extraordinary stability and low-neutron production cross section, especially under proton irradiation, natural carbon (consisting of

98.89 % ^{12}C and 1.11 % ^{13}C) is an excellent material for target backings, beam-dumps and collimators for neutron producing reactions in cyclotrons at high beam intensities. Based on these characteristics of carbon we used ^{13}C, as a useful neutron producing target. The target consisted of a ^{13}C layer of 0.480 MG/Cm^2.

5.3.3.3 Reaction ^{13}C (α,n)^{16}O

The target consisted of a ^{13}C layer of 0.5 MG/Cm^2on a aluminium backing. The purity of this target was bit stated but the ^{12}C content was certainly low enough not to introduce serious systematic errors in the absolute yield measurements. Yields from the reaction have been studied previously for various ranges of particle energy extending up to 5.2 Mev. In addition, angular distribution measurements similar to the present experiment have been published [42]. For this calibration three different targets were used and irradiated with three beam energies

5.3.4 Simulation results

A code has been developed to generate the spectrum of the reactions, using data from the differential cross section (obtained in different papers [6, 10, 11, 21, 36, 42, 46]) and the computed results of the stopping power from the SRIM code [48]. However, due to uncertainty in some data used in the code, it is much more precise to use the yields obtained in a later experiment at PTB. In this experiment was calculated the yield at different angles for the reactions ^{51}V(p,n)^{51}Cr, ^{13}C(p,n)^{13}N and ^{13}C(α,n)^{16}O. The spectrum obtained is also the basis to define the neutron source in the simulation. To calculate the total number of neutrons produced by the reaction, the spectrum has been fitted with Legendre polynomials and then integrated over the whole solid angle following the equation 5.2:.

$$N_n = 2\pi Q \int_0^{\pi} \frac{dY_n}{d\Omega}(\theta) d(cos(\theta)) \tag{5.2}$$

where $\frac{dY_n}{d\Omega}(\theta)$ represents the fit function that fits the yield data obtained in a posterior experiment. In the case of ^{13}C(p,n)^{13}N due to the limited data we available, we evaluate directly the integral as the sum of areas corresponding to those values.

For the nuclear reaction with the ^{51}V(p,n)^{51}Cr a better method to calculate neutrons is counting the gammas emited by ^{51}Cr decay, the

number is related with the number of neutrons produced in each reaction. To calculate the neutron production of the reaction is used a counting method. The number of ^{51}Cr produced by proton irradiation is equal to the number of neutrons emitted. Therefore, if we mesure the number of ^{51}Cr decays by the emision of gamma rays at 320 keV after irradiation we have the number of neutrons emitted. This is only possible because its long half-life of 27 days. The activity of the target was measured for several hours but to reduce the importance of the decay losses this time was short compared to the ^{51}Cr half-life. The number of neutrons, N_n produced can then be calculated with:

$$N_n = \frac{C_\gamma}{\lambda T \varepsilon} \tag{5.3}$$

where C_γ are the counts of 320 keV gamma, λ is the decay constant of ^{51}Cr, T is the measuring time of the counting and ε is the efficiency of the gamma detector. This number was corrected for background.

Energy keV	Reaction (p or α energy in keV)	Efficiency (%) Simulation	Integration	Activation
225	^{51}V(p,n)^{51}Cr (1800)	38.1	30.6±1.4	**33.6±1.2**
552	^{51}V(p,n)^{51}Cr (2140)	38.4	**37.0±1.0**	34.3±1.2
677	^{51}V(p,n)^{51}Cr (2270)	38.6	33.1±0.6	**33.0±1.1**
1023	^{13}C(p,n)^{13}N (4450)	38.3	**34.5±1.0**	
2827	^{13}C(α,n)^{16}O (1054)	38.5	**38.4±0.6**	
4383	^{13}C(α,n)^{16}O (3350)	36.6	**39.3±0.7**	

Table 5.5: *List of the nuclear reactions studied, with their mean neutron energy production, the efficiency obtained by simulation and by experimental data*

The results for the efficiency are detailed in table 5.5. To calculate the total number of neutrons produced by the reaction, we integrate the spectrum of the neutron yield fitted with Legendre polynomials using the equation 5.2. In the case of the reaction ^{13}C(p,n)^{13}N, due to the limited data available we evaluate directly the integral with the sum of the values instead of using Legendre polynomials . The values of efficiency are listed in the table at the column entitled Integration. As has been explained before, for the nuclear reaction with the ^{51}V(p,n)^{51}Cr a more direct method to calculate neutrons is counting the gammas emited by ^{51}Cr decay, this result corresponds to the column of the table indicated by Activation.

Energy	Ratio 2/1		Ratio 3/1	
keV	Sim	Exp	Sim	Exp
144	0.144	0.148	0.023	0.025
225	0.227	0.225	0.051	0.051
552	0.345	0.345	0.125	0.121
677	0.381	0.383	0.154	0.150
1023	0.435	0.457	0.217	0.226
2827	0.740	0.705	0.615	0.611
4383	0.861	0.865	0.863	0.858

Table 5.6: *Comparasion of mean neutron energy and results of the ratio for the second ring divided by first one and the ratio of the third ring divided by first one*

As can be seen in the table 5.5 and in the figure 5.5 the results do not match the expected, even there is a discrepancy between the two methods used to find the total number of neutrons. Nor is there a pattern that defines the behavior of the experimental results respect to simulations. To add more information to the results, we calculated the ratio between the neutrons mesured in the three rings of counters in BELEN . The table 5.6 lists the ratios between the different rings for the simulation and the experimental value. We can see that in some cases the ratio is almost identical and it may mean that BELEN is detecting neutrons of similar energy and it appears that the total number of produced neutrons in the reactions is overestimated in the simulations.

5.4 Conclusions

BELEN characterization by ^{252}Cf calibration source gives us a good coincidence with the simulations. Both in the case of BELEN-30 and BELEN48M1 seems to support the results of efficiency obtained through simulations for the BELEN detector. However in the case of monoenergetic neutron reactions the result is not conclusive. The data do not conform with the simulation for all energies. It is possible that this is product of the uncertainty in the experimental data obtained, in the description of the reactions or the difficulty of measurement. To ensure that adjustment is more accurate would be interesting to do the calibration with well known reactions.

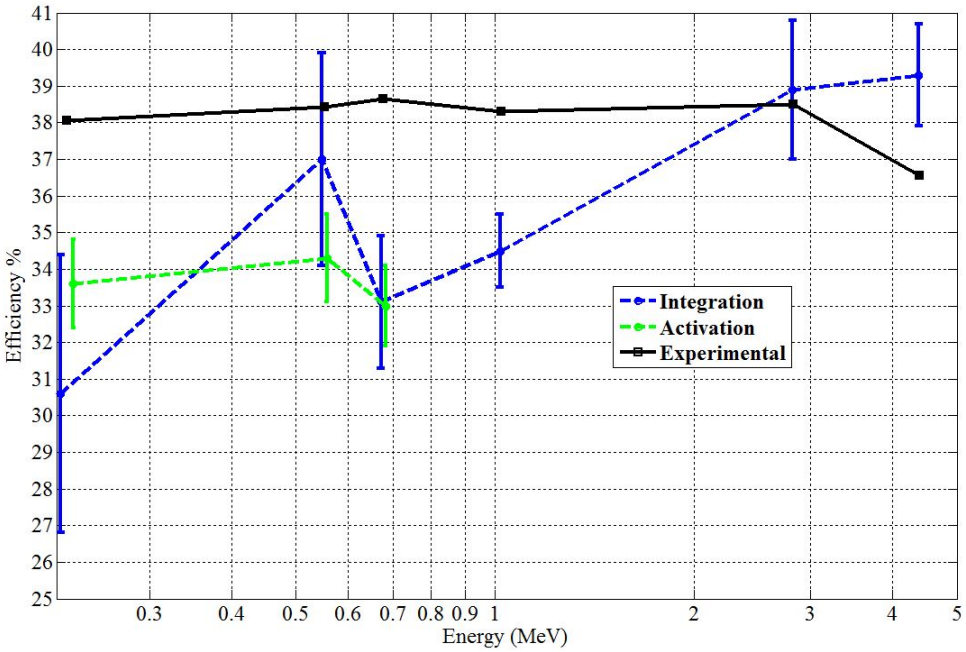

Figure 5.5: *A comparison of the efficiency obtained by Monte-Carlo simulation and the experimental efficiency*

Chapter 6
Conclusions

In this thesis we have studied the main elements and configuration design of a 4π moderated neutron detector. The objective is to develop a device (BELEN) within the DESPEC collaboration for experiments at the future FAIR facility. Different prototypes of BELEN have been employed at several installations for the study of β-delayed neutron emitters. The aim is to obtain a configuration to get the maximum efficiency while maintaining the flat response of the neutron detector along the expected energy range for the neutron.We have found the optimal configurations for BELEN-20B, BELEN-30 prototypes and for the DESPEC candidates BELEN-48 (AIDA), BELEN-48M1 and BELEN-48M2. In order to choose the neutron detector configuration we have developed a methodology for easy finding the best configurations depending on the initial requeriments. This methodology has led us to develop an application to facilitate both the creation of the script to execute simulations, and the subsequent analysis of the simulation results for each configuration. The objectives of the applications are to reduce the number of initial simulations needed and establish a methodology to obtain a configuration near to the optimal. The results of the application for some of the prototypes are close to optimal but it is always necessary to make subsequent simulations by varying the parameters slightly to get the best result.

To characterize the BELEN detector prototypes, we have compared the experimental results obtained in different measurements. For the BELEN-20B the measuraments have been performed at the JYFL facilitity in Jyväscylä (Finland) with fission products which are delayed-neutron precursors ^{94}Rb,^{88}Br,^{95}Rb,^{137}I with well known properties of neutron production. For the characterization of the BELEN-30 it was used a ^{252}Cf neutron source at GSI laboratory, where the BELEN detector join in an experiment using the FRS (Fragment Separator) facility. In both cases the data obtained was in concordance with the result of the simulation.

The BELEN-48 efficiency was mesured at PTB with a^{252}Cf neutron source and with ^{51}V(p,n)^{51}Cr, ^{13}C(p,n)^{13}N and ^{13}C(α,n)^{16}O reactions. The nuclear reactions take place on targets located at the center of the

BELEN symmetry axis. In a later experiment it was calculated the neutron yield at different angles for those reactions. The results obtained with the ^{252}Cf neutron source was according to the simulations. For some nuclear reactions there were some discrepancies with the expected values. The reason for the discrepancy is being studied to improve future calibrations.

Finally, we proposed a configuration for the future experimental campaigns to measure β-delayed multiple neutron emission properties of a large amount of very neutron-rich nuclei at the RIKEN Nishina Center. This detector called BRIKEN (Beta-delayed neutron measurements at RIKEN) will consist of 174 ^{3}He tubes (from UPC+GSI+ORNL+RIKEN) and is expected to enhance greatly the understanding of β-strength distribution for neutron-rich nuclei, and provide an essential piece of information for r-process model calculations.

Bibliography

[1] Nero manual. Technical report.

[2] MCNPX users manual version 2.5.0. Technical report, Los Alamos National Laboratory, 2005.

[3] Physics reference manual Geant4 10.1. Technical report, 2014.

[4] D Abriola, Balraj Singh, and I Dillmann. Beta delayed neutron emission evaluation. 2011.

[5] S. Agostinelli, J. Allison, K. Amako, J. Apostolakis, H. Araujo, P. Arce, M. Asai, D. Axen, S. Banerjee, G. Barrand, F. Behner, L. Bellagamba, J. Boudreau, L. Broglia, A. Brunengo, H. Burkhardt, S. Chauvie, J. Chuma, R. Chytracek, G. Cooperman, G. Cosmo, P. Degtyarenko, A. Dell'Acqua, G. Depaola, D. Dietrich, R. Enami, A. Feliciello, C. Ferguson, H. Fesefeldt, G. Folger, F. Foppiano, A. Forti, S. Garelli, S. Giani, R. Giannitrapani, D. Gibin, J.J. Gomez Cadenas, I. GonzÃ¡lez, G. Gracia Abril, G. Greeniaus, W. Greiner, V. Grichine, A. Grossheim, S. Guatelli, P. Gumplinger, R. Hamatsu, K. Hashimoto, H. Hasui, A. Heikkinen, A. Howard, V. Ivanchenko, A. Johnson, F.W. Jones, J. Kallenbach, N. Kanaya, M. Kawabata, Y. Kawabata, M. Kawaguti, S. Kelner, P. Kent, A. Kimura, T. Kodama, R. Kokoulin, M. Kossov, H. Kurashige, E. Lamanna, T. LampÃ©n, V. Lara, V. Lefebure, F. Lei, M. Liendl, W. Lockman, F. Longo, S. Magni, M. Maire, E. Medernach, K. Minamimoto, P. Mora de Freitas, Y. Morita, K. Murakami, M. Nagamatu, R. Nartallo, P. Nieminen, T. Nishimura, K. Ohtsubo, M. Okamura, S. O'Neale, Y. Oohata, K. Paech, J. Perl, A. Pfeiffer, M.G. Pia, F. Ranjard, A. Rybin, S. Sadilov, E. Di Salvo, G. Santin, T. Sasaki, N. Savvas, Y. Sawada, S. Scherer, S. Sei, V. Sirotenko, D. Smith, N. Starkov, H. Stoecker, J. Sulkimo, M. Takahata, S. Tanaka, E. Tcherniaev, E. Safai Tehrani, M. Tropeano, P. Truscott, H. Uno, L. Urban, P. Urban, M. Verderi, A. Walkden, W. Wander, H. Weber, J.P. Wellisch, T. Wenaus, D.C. Williams, D. Wright, T. Yamada,

H. Yoshida, and D. Zschiesche. "Geant4 a simulation toolkit ". *Nuclear Instruments and Methods in Physics Research Section A: Accelerators, Spectrometers, Detectors and Associated Equipment*, 506(3):250 – 303, 2003.

[6] R. L. Becker and H. H. Barschall. Total cross sections of light elements for α, n neutrons. *Phys. Rev. 102*, 1384, 1956.

[7] I. N. Borzov. Beta-decay rates. *Nuclear Physics A*, 777:645–675, October 2006.

[8] R. Caballero-Folch. *First measurement of beta-decay half-lives and neutron emission probabilities in several isotopes beyond N=126.* PhD thesis, 2015.

[9] R. Caballero-Folch, C. Domingo-Pardo, G. Cortés, J.L. Taín, J. Agramunt, A. Algora, F. Ameil, Y. Ayyad, J. Benlliure, M. Bowry, F. Calvi no, D. Cano-Ott, T. Davinson, I. Dillmann, A. Estrade, A. Evdokimov, T. Faestermann, F. Farinon, D. Galaviz, A. García-Ríos, H. Geissel, W. Gelletly, and R. Gernh˙ Beta-decay and beta-delayed neutron emission measurements at GSI-FRS beyond, for r-process nucleosynthesis. *Nuclear Data Sheets*, 120:81 – 83, 2014.

[10] G. Deconninck and J. Royen. La reaction ^{51}V(p,n) ^{51}Cr comme source de neutrons monoenergetiques. *Nuclear Instruments and Methods*, 75:266–270, 1969.

[11] M. Drosg. Monoenergetic neutron production by two-body reactions in the energy range from 0.0001 to 500 MeV (overview).

[12] Farouqi et al. Charged-particle and neutron-capture processes in the high-entropy wind of the core-collapse supernovae. *Charged-particle and neutron-capture processes in the high-entropy wind of the core-collapse supernovae*, 712, 2010.

[13] G. Lorusso et al. Nero the neutron emission ratio observer. In *International Symposium on Nuclear Astrophysics, Nuclei in the Cosmos IX*, page 243, Cern,Geneva,Switzerland, June 2006.

[14] J. Pereira et al. The neutron long counter nero for studies of beta-delayed neutron emission in the r-process. *Nucl. Instr. Meth. A*, 618, 2010.

[15] Kratz et al. Beta-minus strength function phenomena of exotic nuclei: a critical examination of the signature of nuclear model predictions. *Beta-minus strength function phenomena of exotic nuclei: a critical examination of the signature of nuclear model predictions*, 417, 1984.

[16] F. Calviño and G. Cortés and A. Riego and R. Caballero-Folch and C. Pretel and Ll. Batet and A. Torner and A. Poch, M.B. Gómez-Hornillos and V. Gorlychev. TDR beta-delayed neutron detector. Technical report, Universitat Politècnica de Catalunya, Barcelona, Spain, 2014.

[17] M. B. Gómez Hornillos et al. First measurements with the BEta deLayEd neutron detector (BELEN-20) at JYFLTRAP. *J. Phys. Conf. Ser.*, 312:052008, 2011.

[18] V. Gorlychev. *"Design of a 4Pi neutron detector for beta-delay neutron detection experiments."*. PhD thesis, 2014.

[19] R. Grzywacza, K.P. Rykaczewskib, C.J. Grossb, M. Madurgaa, K. Miernikb, D.T. Millera, S.V. Paulauskasa, S.W. Padgetta C. Rascod, M. Wolinska-Cichockab, and E.F. Zganjard. Hybrid-3HEN new detector for gammas and neutron. Technical report, 2013.

[20] A. O. Hanson and J. L. McKibben. A neutron detector having uniform sensitivity from 10 KeV to 3 MeV. *Phys. Rev.*, 72:673–677, Oct 1947.

[21] K.K. Harris, H.A. Grench, R.G. Johnson, F.J. Vaughn, and Lockheed Palo Alto Research Lab. *The V51(p, N)Cr51 Reaction as a Neutron Source of Known Intensity*. Defense Technical Information Center, 1964.

[22] Clemens Herlitzius. *Improvement of the Neutron Emission Ratio Observer by an Active Cosmic Ray Shield*. PhD thesis, 2008.

[23] C. Hinke. *Spectroscopy of the doubly magic nucleus 100Sn and its decay*. PhD thesis, 2010.

[24] P. T. Hosmer, H. Schatz, A. Aprahamian, O. Arndt, R. R. C. Clement, A. Estrade, K.-L. Kratz, S. N. Liddick, P. F. Mantica, W. F. Mueller, F. Montes, A. C. Morton, M. Ouellette, E. Pellegrini, B. Pfeiffer, P. Reeder, P. Santi, M. Steiner, A. Stolz, B. E. Tomlin,

W. B. Walters, and A. Wöhr. Half-life of the doubly magic r-process nucleus ^{78}Ni. *Phys. Rev. Lett.*, 94:112501, Mar 2005.

[25] https://people.nscl.msu.edu/ nero/. Neutron emission ratio observer nero.

[26] https//www.gsi.de. Gsi helmholtzzentrum für schwerionenforschung.

[27] https//www.ptb.de. Ptb the national metrology institute of germany.

[28] https://www.wiki.ed.ac.uk/display/BRIKEN/Home. Briken.

[29] http://www2.ph.ed.ac.uk/ td/DSSD/. AIDA.

[30] http://www.fair center.eu/. An international facility for antiproton and ion research.

[31] http://www.nishina.riken.jp/RIBF/BigRIPS/overview.html. Riken.

[32] J. Agramunt and J.L. Tain and M.B. Gómez-Hornillos and A.R. Garcia and F. Albiol and A. Algora and R. Caballero-Folch and F. Calviño and D. Cano-Ott and G. Cortés and C. Domingo-Pardo and T. Eronen and W. Gelletly and D. Gorelov and V. Gorlychev and H. Hakala and A. Jokinen and M.D. Jordan and A. Kankainen and V. Kolhinen and L. Kucuk and T. Martinez and P.J.R. Mason and I. Moore and H. Penttilä and Zs. Podolyák and C. Pretel and M. Reponen and A. Riego and J. Rissanen and B. Rubio and A. Saastamoinen and A. Tarifeño-Saldivia and E. Valencia. Characterization of a neutron-beta counting system with beta-delayed neutron emitters. *Nuclear Instruments and Methods in Physics Research Section A: Accelerators, Spectrometers, Detectors and Associated Equipment*, 807:69 – 78, 2016.

[33] Doug Wrigh Jerome M. Verbeke, Chris Hagmann. Simulation of neutron and gamma ray emission from fission. Technical report, 2009.

[34] Glenn F Knoll. *Radiation detection and measurement*. Wiley, New York, NY, 1979.

[35] K.-L. Kratz, J.-P. Bitouzet, F.-K. Thielemann, P. Moeller, and B. Pfeiffer. Isotopic r-process abundances and nuclear structure far from stability - Implications for the r-process mechanism. *Astrophysical Journal*, 403:216–238, January 1993.

[36] Evert Birgersand Göran Lövestam. Neusdesc neutron source description software manual. Technical report, 2009.

[37] L Mathieu, O Serot, T Materna, A Bail, U Köster, H Faust, O Litaize, E Dupont, C Jouanne, A Letourneau, and S Panebianco. New neutron long-counter for delayed neutron investigations with the lohengrin fission fragment separator. *Journal of Instrumentation*, 7(08):P08029, 2012.

[38] T. Mehren, B. Pfeiffer, S. Schoedder, K.-L. Kratz, M. Huhta, P. Dendooven, A. Honkanen, G. Lhersonneau, M. Oinonen, J.-M. Parmonen, H. Penttilä, A. Popov, V. Rubchenya, and J. Äystö. Beta-decay half-lives and neutron-emission probabilities of very neutron-rich Y to Tc isotopes. *Phys. Rev. Lett.*, 77:458–461, Jul 1996.

[39] E. Mendoza, D. Cano-Ott, T. Koi, and C. Guerrero. New Standard Evaluated Neutron Cross Section Libraries for the Geant4 Code and First Verification. *IEEE Transactions on Nuclear Science*, 61:2357–2364, August 2014.

[40] Peter Möller, Bernd Pfeiffer, and Karl-Ludwig Kratz. New calculations of gross β-decay properties for astrophysical applications: Speeding-up the classical r process. *Phys. Rev. C*, 67:055802, May 2003.

[41] Ralf Nolte and David J Thomas. Monoenergetic fast neutron reference fields: I. neutron production. *Metrologia*, 48(6):S263, 2011.

[42] J. D. Clement R. B. Watlton and F. Boreli. Interaction of neutrons with oxygen and a study of the 13C(alpha, n)16O reaction. 1957.

[43] R. Caballero-Folch and C. Domingo-Pardo and J. L. Taín and G. Cortés and J. Agramunt and A. Algora and F. Ameil and Y. Ayyad and J. Benlliure and M. Bowry and F. Calviño and D. Cano-Ott and T. Davinson and I. Dillmann and A. Estrade and A. Evdokimov and T. Faestermann and F. Farinon and D. Galaviz and A. García-Rios and H. Geissel and W. Gelletly and R. Gernhauser and M. B. Gómez-Hornillos and C. Guerrero and M. Heil and C. Hinke and R. Knöbel and I. Kojouharov and J. Kurcewicz and N. Kurz and Y. Litvinov and L. Maier and J. Marganiec and M. Marta and T. Martínez and F. Montes and I. Mukha and D. R. Napoli and C. Nociforo and C. Paradela and S. Pietri and Zs. Podolyák and A.

Prochazka and S. Rice and A. Riego and B. Rubio and H. Schaffner and C. Scheidenberger and K. Smith and E. Sokol and K. Steiger, and B. Sun and M. Takechi and D. Testov and H. Weick and E. Wilson and J. S. Winfield and R. Wood and P. Woods and A. Yeremin. Beta delayed neutron emission measurements around the third r process abundance peak. volume 1541, pages 137–139, 2013.

[44] P.L. Reeder, R.A. Warner, R.L. Gill, and A. Piotrowski. *Pn measurements at TRISTAN by a beta coincidence technique.* Aug 1986.

[45] Rykaczewski and S. Liddick and R. A. Lillie and M. Saltmarsh and J. C. Batchelder and C. R. Bingham and R. K. Grzywacz and J. A. Winger and E. F. Zganjar. Proposal for a new neutron detector high efficiency neutron counter for studies of beta-delayed neutron emission(3HEN). Technical report, 2005.

[46] S. S. Kerekatte S. Kailas, S. K. Gupta and C. V. Fernandes. 51V(p,n)51Cr reaction from ep 1.9 to 4.5 MeV. *Pramana - Journal of Physics*, 24, 1985.

[47] K. Steiger. *Diploma thesis.* PhD thesis, 2009.

[48] J. F. Ziegler and J. P. Biersack. SRIM The stopping and range of ions in solids. Technical report, 2009.